[illegible]

Control No.

[illegible]
CPB C3-[illegible]-62

FINAL REPORT

DETERMINATION OF LOW-TEMPERATURE FATIGUE PROPERTIES OF STRUCTURAL METAL ALLOYS

1 April 1962 thru 30 September 1964

October 1964

prepared for:

NATIONAL AERONAUTICS AND SPACE ADMINISTRATION
GEORGE C. MARSHALL SPACE FLIGHT CENTER
HUNTSVILLE, ALABAMA

prepared by:

MARTIN COMPANY
DENVER, COLORADO

N65 13142 (ACCESSION NUMBER)
165 (PAGES)
CR 5-9839 (NASA CR OR TMX OR AD NUMBER)
(THRU)
1 (CODE)
12 (CATEGORY)
FACILITY FORM 602

GPO PRICE $
OTS PRICE(S) $
Hard copy (HC) [illegible]
Microfiche (MF) [illegible]

Martin-CR-64-74

Copy No. 13

Contract NAS8-2631

Control No.
TP2-85223 (IF)
CPB C2-1053-62

FINAL REPORT
DETERMINATION OF LOW-TEMPERATURE FATIGUE
PROPERTIES OF STRUCTURAL METAL ALLOYS
1 APRIL 1962 THRU 30 SEPTEMBER 1964

October 1964

Authors

F. R. Schwartzberg
T. F. Kieter
R. D. Keys

Approved

W. H. Clohessy
Director of Research and Development

MARTIN COMPANY
Denver, Colorado
Aerospace Division of Martin-Marietta Corporation

FOREWORD

This report was prepared by Ma[illegible]rietta Corporation under Contract NAS8-2631, Determination o[illegible] -Temperature Fatigue Properties of Structural Metal Alloys, Final Report, for the George C. Marshall Space Flight Center of the National Aeronautics and Space Administration. The work was administered under the technical direction of the Propulsion and Vehicle Engineering Laboratory, Materials Division of the George C. Marshall Space Flight Center with W. B. McPherson acting as project manager.

CONTENTS

		Page
Foreword		ii
Contents		iii
Abstract		xii and xiii
I.	Introduction	1
II.	Materials	4
III.	Specimens	9
IV.	Test Apparatus and Facilities	14
	A. Cryostat	14
	B. Alignment and Assembly	17
	C. Automation	20
	D. Facility	[illegible]
	E. Performance	[illegible]
V.	Test Procedure	30
	A. Tension	31
	B. Fatigue	30
VI.	Experimental Results	32
	A. Tension Tests	32
	B. Fatigue Tests	32
VII.	Discussion of Results	5
	A. Aluminum Alloys	5
	B. Titanium Alloys	6
	C. Stainless Steel	[illegible]

Appendix A -- Cryostat Drawings . . . . . A-1 thru A-9

Appendix B -- Tensile Data . . . . . B-1 thru B-11

Appendix C -- Fatigue Data . . . . . C-1 thru C-29

Distribution

Figures

1 Specifications for Tensile Specimen 10

2 Specifications for Unnotched and Welded Fatigue Specimen 11

3 Specifications for Notched Fatigue Specimen . . . 12

4 Effect of Misalignment on the Applied Axial Load of 5456-H343 Aluminum Alloy at -423°F 13

5 SF 10U Fatigue-Testing Machine 15

6 Cutaway View of Cryostat Assembly Mounted in Fatigue-Testing Machine 16

7 Cryostat Components before Assembly 18

8 Liquid Hydrogen Cryostat Lid Assembly 19

9 View of Cryostat and Mounting Hardware 21

10 Frames from High-Speed Motion Pictures of Misaligned 7075-T6 Aluminum Alloy Fatigue Test . . . 22

11 Frames from High-Speed Motion Picture of Properly Aligned 7075-T6 Aluminum Alloy Fatigue Test . . . 23

12 Liquid Nitrogen Fill Controller 25

13 Liquid Hydrogen Fill Controller 25

14 Schematic Diagram of Liquid Hydrogen Flow System 26

15 Liquid Hydrogen Fatigue-Testing Facility 28

16 Liquid Nitrogen Fatigue-Testing Facility 29

17 Tensile Properties of 2014-T6 Aluminum Alloy at Cryogenic Temperatures 33

18 Tensile Properties of 2219-T87 Aluminum Alloy at Cryogenic Temperatures 34

19 Tensile Properties of 2219-T62 Aluminum Alloy at Cryogenic Temperatures 35

20 Tensile Properties of 7039-T6 Aluminum Alloy at Cryogenic Temperatures 36

21 Tensile Properties of 5456-H343 Aluminum Alloy at Cryogenic Temperatures 37

22 Tensile Properties of 7075-T6 Aluminum Alloy at Cryogenic Temperatures 38

23 Tensile Properties of 2020-T6 Aluminum Alloy at Cryogenic Temperatures 39

24 Tensile Properties of 5Al-2.5Sn Titanium Alloy at Cryogenic Temperatures 40

25 Tensile Properties of 6Al-4V Titanium Alloy at Cryogenic Temperatures 41

26 Tensile Properties of 13V-11Cr-3Al Titanium Alloy at Cryogenic Temperatures 42

27 Tensile Properties of 321 Stainless Steel Alloy at Cryogenic Temperatures 43

28 Fatigue Properties of Unnotched 2014-T6 Aluminum Alloy 44

29 Fatigue Properties of Notched 2014-T6 Aluminum Alloy 45

30 Fatigue Properties of Welded 2014-T6 Aluminum Alloy 46

31 Fatigue Properties of Unnotched 2219-T62 Aluminum Alloy 47

32 Fatigue Properties of Notched 2219-T87 Aluminum Alloy 48

33 Fatigue Properties of Welded 2219-T87 Aluminum Alloy 49

34 Fatigue Properties of Unnotched 2219-T62 Aluminum Alloy 50

35 Fatigue Properties of Notched 2219-T62 Aluminum Alloy 51

36 Fatigue Properties of Welded 2219-T62 Aluminum Alloy 52

37 Fatigue Properties of Unnotched 7039-T6 Aluminum Alloy 53

38 Fatigue Properties of Notched 7039-T6 Aluminum Alloy 54

39 Fatigue Properties of Welded 7039-T6 Aluminum Alloy 55

40 Fatigue Properties of Unnotched 5456-H343 Aluminum Alloy 56

41 Fatigue Properties of Notched 5456-H343 Aluminum Alloy 57

42 Fatigue Properties of Welded 5456-H343 Aluminum Alloy 58

43 Fatigue Properties of Unnotched 7075-T6 Aluminum Alloy 59

44 Fatigue Properties of Notched 7075-T6 Aluminum Alloy 60

45 Fatigue Properties of Unnotched 2219-T6 Aluminum Alloy 61

46 Fatigue Properties of Unnotched 5Al-2.5Sn (Annealed) Titanium Alloy . . . . . [illegible]

47 Fatigue Properties of Notched 5Al-2.5Sn (Annealed) Titanium Alloy . . . . . [illegible]

48 Fatigue Properties of Welded 5Al-2.5Sn (Annealed) Titanium Alloy . . . . . [illegible]

49 Fatigue Properties of Unnotched 6Al-4V (Solution Treated and Aged) Titanium Alloy 65

50 Fatigue Properties of Notched 6Al-4V (Solution Treated and Aged) Titanium Alloy 66

51 Fatigue Properties of Welded 6Al-4V (Solution Treated and Aged) Titanium Alloy 67

52 Fatigue Properties of Unnotched 13V-11Cr-3Al (Solution Treated and Aged) Titanium Alloy 68

53 Fatigue Properties of Welded 13V-11Cr-3Al (Solution Treated and Aged) Titanium Alloy 69

54 Fatigue Properties of Unnotched 321 (Annealed) Stainless Steel 70

55 Fatigue Properties of Notched 321 (Annealed) Stainless Steel 71

56 Fatigue Properties of Welded 321 (Annealed) Stainless Steel 72

57 Modulus of Elasticity of Aluminum Alloys at Cryogenic Temperatures 75

58 Comparison of Fatigue Properties for Aluminum Alloys 84

59 Effect of Stress Ratio on the Fatigue Properties of Two Aluminum Alloys at -423°F . . . . . 8[illegible]

60 Effect of Interstitial Content on the Unnotched Tensile Strength of 5Al-2.5Sn Titanium Alloy . . . 88

61 Variation of Elasticity of Three Titanium Alloys at Cryogenic Temperatures . . . [illegible]

62 Comparison of Fatigue Properties for Titanium Alloys . . . [illegible]

A-1 Fatigue Cryostat Assembly . . . A-1

A-2 Cryostat Base Stem . . . A-2

A-3 Cryostat Top Stem . . . A-3

A-4 Lower Retainer Plate and Wave Block . . . A-4

A-5 Upper Retainer Plate and Wedge Block . . . A-5

A-6 Grip Block Half, Assembly Rough Blank, and Assembly . . . A-6

A-7 Vacuum Fitting-Cryostat Stem . . . A-9

Table

1 List of Materials Selected for Experimental Program . . . 5

2 Details of Welding Procedure for Aluminum Alloys . . . 6

3 Details of Welding Procedure for Titanium Alloys . . . 6

4 Chemical Analyses of Titanium Alloy Sheet, Wire, and Weld Bead . . . 8

5 Comparison of Fatigue Properties for Aluminum Alloys . . . 82

6 Comparison of Fatigue Properties for Titanium Alloys . . . 93

B-1 Tensile Properties of 2014-T6 Aluminum Alloy at Cryogenic Temperatures . . . B-1

B-2 Tensile Properties of 2219-T87 Aluminum Alloy at Cryogenic Temperatures B-2

B-3 Tensile Properties of 2219-T62 Aluminum Alloy at Cryogenic Temperatures B-3

B-4 Tensile Properties of 7039-T6 Aluminum Alloy at Cryogenic Temperatures B-4

B-5 Tensile Properties of 5456-H343 Aluminum Alloy at Cryogenic Temperatures B-5

B-6 Tensile Properties of 7075-T6 Aluminum Alloy at Cryogenic Temperatures B-6

B-7 Tensile Properties of 2020-T6 Aluminum Alloy at Cryogenic Temperatures B-7

B-8 Tensile Properties of 5Al-2.5Sn Titanium Alloy at Cryogenic Temperatures B-8

B-9 Tensile Properties of Solution Treated and Aged 6Al-4V Titanium Alloy at Cryogenic Temperatures . B-9

B-10 Tensile Properties of Solution Treated and Aged 13V-11Cr-3Al Titanium Alloy at Cryogenic Temperatures B-10

B-11 Tensile Properties of 321 Stainless Steel Alloy at Cryogenic Temperatures B-11

C-1 Fatigue Properties of Parent Metal 2014-T6 Aluminum Alloy C-1

C-2 Fatigue Properties of Notched 2014-T6 Aluminum Alloy C-2

C-3 Fatigue Properties of Welded 2014-T6 Aluminum Alloy C-3

C-4 Fatigue Properties of Parent Metal 2219-T87 Aluminum Alloy C-4

C-5 Fatigue Properties of Notched 2219-T87 Aluminum Alloy C-5

C-6 Fatigue Properties of Welded 2219-T87 Aluminum Alloy C-6

C-7 Fatigue Properties of Parent Metal 2219-T62 Aluminum Alloy C-7

C-8 Fatigue Properties of Notched 2219-T62 Aluminum Alloy C-8

C-9 Fatigue Properties of Welded 2219-T62 Aluminum Alloy C-9

C-10 Fatigue Properties of Parent Metal 7039-T6 Aluminum Alloy C-10

C-11 Fatigue Properties of Notched 7039-T6 Aluminum Alloy C-11

C-12 Fatigue Properties of Welded 7039-T6 Aluminum Alloy C-12

C-13 Fatigue Properties of Parent Metal 5456-H343 Aluminum Alloy C-13

C-14 Fatigue Properties of Notched 5456-H343 Aluminum Alloy C-14

C-15 Fatigue Properties of Welded 5456-H343 Aluminum Alloy C-15

C-16 Fatigue Properties of Parent Metal 7075-T6 Aluminum Alloy C-16

C-17 Fatigue Properties of Notched 7075-T6 Aluminum Alloy C-17

C-18 Fatigue Properties of Parent Metal 2020-T6 Aluminum Alloy C-18

C-19 Fatigue Properties of Annealed Parent Metal 5Al-2.5Sn Titanium Alloy C-19

C-20 Fatigue Properties of Notched 5Al-2.5Sn Titanium Alloy C-20

C-21 Fatigue Properties of Annealed [illegible] 5Al-2.5Sn Titanium Alloy C-21

C-22 Fatigue Properties of Solution Treated and Aged Parent Metal 6Al-4V Titanium Alloy C-22

C-23 Fatigue Properties of Notched 6Al-4V Titanium Alloy C-23

C-24 Fatigue Properties of Solution Treated and Aged Welded 6Al-4V Titanium Alloy C-24

C-25 Fatigue Properties of Solution Treated and Aged Parent Metal 13V-11Cr-3Al Titanium Alloy C-25

C-26 Fatigue Properties of Welded 13V-11Cr-3Al Titanium Alloy C-26

C-27 Fatigue Properties of Parent Metal AISI 321 Stainless Steel C-27

C-28 Fatigue Properties of Notched AISI 321 Stainless Steel C-28

C-29 Fatigue Properties of Welded AISI 321 Stainless Steel C-29

ABSTRACT

The results of two year's effort on this program are presented in this final report.

Two cryogenic fatigue-testing systems were constructed: one for operation at -320°F, one for -423°F testing. Cryostats were designed to permit fully reversed stressing of sheet materials under axial load conditions. A cryostat design incorporating a vacuum-insulated, double-walled, stainless steel container with a tubular loading stem passing through its central axis was used. The cryostat mounts on the reciprocating platen of the test machine and moves with it while the lid and associated lines and instrumentation remain fixed. The equipment techniques developed have demonstrated that by careful alignment, fatigue tests of axial-loaded, flat sheet materials can be effectively accomplished with fully reversed stresses. The apparatus has performed satisfactorily for almost two years despite severe environmental conditions.

Various aluminum, stainless steel, and titanium sheet alloys (0.100-in. nominal thickness) listed below were evaluated in the parent metal, notched, and, where applicable, welded conditions:

Aluminum	Stainless Steel	Titanium
2014-T6	321	Ti-5Al-2.5Sn
2219-T87		Ti-6Al-4V
2219-T62		Ti-13V-11Cr-3Al
7039-T6		
5456-H343		
7075-T6		
2020-T6		

Properties were determined at 70, -320, and -423°F for fatigue life in the 10^3 to 10^7 cycle range.

The weldable aluminum alloys all showed satisfactory fatigue behavior at cryogenic temperatures. The two nonweldable alloys, 7075-T6 and 2020-T6, are less desirable for cryogenic service.

The Ti-5Al-2.5Sn and Ti-6Al-4V titanium alloys exhibited very good fatigue resistance. Ti-13V-11Cr-3Al faired rather poorly below room temperature.

The 321 stainless steel showed satisfactory fatigue properties.

I. INTRODUCTION

Selection of the proper materials for booster and space vehicle systems that use cryogenic propellants is a challenge because of the behavior of structural materials at low temperatures. Routine mechanical properties, such as tensile and compressive strength, modulus of elasticity, and ductility are usually determined to assess the behavior of a candidate material. Behavior under stress concentration and cyclic loading conditions must also be studied to evaluate adequately a potential material.

Cryogenic literature reveals some data on the routine properties, but there is a significant lack of reliable information on fatigue or cyclic loading. Cryogenic fatigue data on welded material are virtually nonexistent. The experimental program presented in this report was prepared to fill this obvious requirement for sound engineering data.

Fatigue tests can best be described by the method used to apply loads. Repeated loading to both a constant-stress amplitude and a constant-strain amplitude are used. With the first method, direct axial loading is employed, and, with the second, bending techniques, either plane or rotational, are used. For axial testing, the entire cross section is uniformly loaded. Stress is determined by load/area. In bending, the stress varies throughout the cross section of the test specimen, from a maximum at the outer fiber through zero at the neutral axis, to a maximum negative value at the opposite outer surface. With this technique, stress must be obtained by calculating from the moment formula $S = (Mc)/I$.

Although these bending tests have been the most popular fatigue techniques in the past, they are being replaced by the axial-loading method because of certain disadvantages in using bending fatigue.

As shown by the formula, bending stress is calculated with the bending moment and section modulus. The bending moment, M, is a function of the modulus of elasticity of the test material. Accuracy of the stress calculation is therefore directly proportional to the accuracy of the modulus value. Although moduli of common engineering materials at room temperature are known, there is little information in the literature on values at cryogenic temperatures.

The endurance limit obtained by bending techniques may be as great as 30% higher than values obtained by axial loading. Although the reasons for this are not fully understood, certain state-of-stress theories have been proposed. One explanation is the possible development of favorable transverse stresses in the elongated or compressed surface layers and an outer-layer resistance to deformation caused by the underlying material during bending load tests.

Another shortcoming of the bending technique is that when plastic yielding occurs, stresses in the member cannot be readily calculated. Even in tests performed in the elastic range, minute localized plastic deformation may change the outer fiber stress.

There is a greater chance of failure from minor surface defects in bending than in axial loading. These defects may also create larger scatter with a limited number of specimens.

In calculating stress, the simple moment formula can be used only on specimens free from holes, grooves, and outline or surface discontinuities, such as weld beads. Therefore, to evaluate the bending fatigue of welded specimens, it would be more desirable to machine the weld bead flush. However, this would detract from the validity of the joint information since it eliminates stress concentrations.

This method was selected for this program because of the superiority of the axial-loading technique and its ability to simulate anticipated structural loads. The axial-loading machines employ a rotating mass to apply a controlled dynamic load sinusoidally about a static-load level.

Tension/compression tests of sheet materials under axial loading are not often performed since these tests are normally restricted to bar materials. Fortunately, the sheet gage selected by NASA presented the opportunity to attempt complete reversal of stresses without having to resort to the bending technique. The success of such an approach depends on the flatness of the sheet products available. The aluminum alloys and stainless steel used for this research were sufficiently flat to permit fully reversed stressing. Unfortunately, the heat-treated titanium sheet materials were rather warped and could not be tested safely under compressive loads. Tension/tension loads were therefore used for both the annealed and heat-treated titanium alloys.

[illegible]

Testing at liquid hydrogen temperature was [illegible] Denver Laboratories. All equipment was designed and [illegible] at this location. Evaluation of fatigue properties at 70 and -320°F was conducted at the [illegible] Laboratories.

II. MATERIALS

Materials selected for evaluation in this program are those that are being considered for structural service at cryogenic temperatures. Several of the materials selected by NASA were mutually recognized as exhibiting poor behavior at these temperatures. However, they were retained to show the comparison between various compositions.

Material condition was selected to give the high strength levels normally considered for airborne construction. The following specimen test conditions were used for this program:

1) Unnotched;

2) Notched;

3) Welded.

The materials selected for evaluation are listed in Table 1. Several materials were not subjected to all three test conditions. The exceptions were:

1) 7075-T6 aluminum - Unnotched and notched only;

2) 2020-T6 aluminum - Unnotched only;

3) 13V-11Cr-3Al titanium - Unnotched and welded only.

The alpha (Ti-5Al-2.5Sn) and alpha-beta (Ti-6Al-4V) alloys were purchased as extra-low interstitial grade to assure maximum toughness at cryogenic temperatures. No attempt was made to procure low interstitial beta (Ti-13V-11Cr-3Al) alloy because of its well-known brittle behavior, independent of impurities, below -100°F. Insufficient material remained from first-year work on unnotched and welded behavior to permit additional notch testing from a single heat. Additional material was procured to match chemistry to the initial heat as closely as possible.

Table 1 List of Materials Selected for Experimental Program

Alloy Base	Designation	Temper	Nominal Thickness (in.)	Producer	Heat Number
Aluminum	2014	-T6	0.100	Reynolds	--
Aluminum	2219	-T87	0.100	Alcoa	--
Aluminum	[illegible]9	-T[illegible]2	0.100	Alcoa	--
Aluminum	7039	-T6	0.125	Kaiser	--
Aluminum	5456	-H343	[illegible]	Alcoa	--
Aluminum	7075	-T6	0.100	Reynolds	--
Aluminum	2020	-T6	[illegible]	[illegible]	--
Titanium	Ti-5Al-2.5Sn	Annealed	0.100	Titanium Metals Corporation	D-3272† D-3646‡
Titanium	Ti-6Al-4V	Solution-Treated and Aged (1660°F/ 5 min, WQ; 1000°F/ 4 hr, AC)	[illegible]	Titanium Metals Corporation	D-2488† D-5599*
Titanium	Ti-13V-11Cr-3Al	Solution-Treated and Aged (1450°F/ 20 min, AC; 900°F/ 24 hr AC)	0.100	Titanium Metals	D-1639†
Stainless Steel	321	Annealed	0.090	Republic	3342058

*Material supplied by National Aeronautics and Space Administration.
†Material used for unnotched and welded specimens.
‡Material used for notched specimens.

Aluminum and titanium alloys were welded with the tungsten inert gas (TIG) process and automatic welding heads. Tables 2 and 3 list details of the procedure used for each material.

Table 2 Details of Welding Procedure for Aluminum Alloys

Alloy	Filler Wire	Wire Diameter (in.)	Voltage (v)	Current (amp)	Speed (in./min)
2014-T6	2319	3/32	11	160	12
2219-T87	2319	3/32	11	170	12
2219-T62	2319	3/32	11	170	12
7039-T6	5083	3/32	10	200	10
5456-H343	5556	3/32	11	170	11

Note: TIG-welded with Airco D head; argon protective gas; ac.

Table 3 Details of Welding Procedure for Titanium Alloys

Alloy	Wire Diameter (in.)	Voltage (v)	Current (amp)	Speed (in./min)
Ti-5Al-2.5Sn	0.030	10.5	215	13
Ti-6Al-4V	0.030	11	215	13
Ti-13V-11Cr-3Al	0.045	11	215	13

Note: TIG-welded with Airco D head and 300A. P&H power supply; dc, straight polarity; helium-argon back-up and trailing gas protection; parent-metal filler wire.

All weld panels were radiographically inspected. The aluminum panels exceeded the Class II requirements of MSFC Drawing 10509310. Weld quality approximated the requirements displayed in the NASA specifications for Class I welds. Similarly, the titanium alloys were of high quality. Very minor porosity was noted in several areas of the Ti-13V-11Cr-3Al.

Particular emphasis was placed on procurement of low-interstitial titanium sheet and welding wire and on prevention of contamination during welding to maintain low interstitial content. Interstitial analyses reported in the test certification provided by vendors for the sheet and wire were confirmed by vacuum fusion analyses for oxygen, nitrogen, and hydrogen performed by Titanium Metals Corporation of America on the sheet metal, welding wire, and weld beads. These results, listed in Table 4, show excellent agreement between the certification and the check analyses. The low levels of oxygen and nitrogen in the weld beads are proof of satisfactory inert gas protection during the welding process.

Table 4 Chemical Analyses of Titanium Alloy Sheet, Wire, and Weld Bead

Material	Weight Composition (%)*									
	Heat Number	Al	V	Sn	Cr	Fe	C	O	N	H
Ti-5Al-2.5Sn Parent Metal	D-3272†	5.1	--	2.5	--	0.08	0.022	0.06 (0.07)	0.014 (0.016)	0.017 (0.013)
Ti-5Al-2.5Sn Parent Metal	D-3646‡	5.2	--	2.4	--	0.12	0.022	0.08	0.013	0.006
Ti-5Al-2.5Sn Welding Wire	3930563	5.5	--	2.5	--	0.20	0.033	0.10 (0.07)	0.012 (0.118)	0.005 (0.003)
Ti-5Al-2.5Sn Weld Bead	--	--	--	--	--	--	--	(0.07)	(0.020)	(0.007)
Ti-6Al-4V Parent Metal	D-2488†	6.0	4.1	--	--	0.09	0.019	0.09 (0.12)	0.016 (0.020)	0.006 (0.006)
Ti-6Al-4V Parent Metal	D-5599‡	6.1	4.0	--	--	0.09	0.21	0.11	0.017	0.012
Ti-6Al-4V Weld Bead	--	--	--	--	--	--	--	(0.12)	(0.017)	(0.007)
Ti-13V-11Cr-3Al Parent Metal	D-1639†	3.1	13.4	--	11.4	0.17	0.027	0.14	0.027	0.008

*Analyses from vendor's certification of test; values in parentheses are checks performed by Titanium Metals Corporation of America.
†Material for unnotched and welded specimens.
‡Material for notched specimens.

III. [illegible]

Tensile specimens were machined to specifications shown in Fig. 1 and designed specifically for use with the multiple-linkage system described by Keys (Ref 1).

Unnotched and welded fatigue specimens were machined according to the sketch in Fig. 2. Aluminum specimens were machined to 0.375-in. gage width A dimension, and titanium material to a gage width of 0.200 in. In contrast to the usual fatigue specimen shapes, the specimen design incorporates a straight-column test-gage section. A constant-width test section was selected to permit proper evaluation of weld bead and heat-affected zone in a short column length.

Notched specimens were machined according to specifications given in Fig. 3. A notch depth of 33% was used. Notch specimens were initially machined with an elastic stress concentration factor (K_t) of 7.4. Preliminary testing of 2014-T6 aluminum alloy specimens containing this notch acuity showed severe degradation of strength properties compared with the unnotched material. After discussion with the NASA project engineer, W. B. McPherson, and H. Grover of Battelle Memorial Institute, it was decided to use a milder notch ($K_t = 3.5$) for additional testing. Specimens already machined with the sharp notch were reworked to provide the milder notch.

Column analysis of the unnotched specimen configuration revealed that the specimen exhibited a high margin of safety from column buckling if properly aligned. An additional analysis was performed to show the relationship between the degree of misalignment and applied axial loads for various alloys. Figure 4 shows this relationship for a typical aluminum alloy composition (5456-H343) at -423°F. As shown in the diagram, to permit axial loads in the 1500- to 2000-lb range, alignment must be maintained at better than 0.001 in.

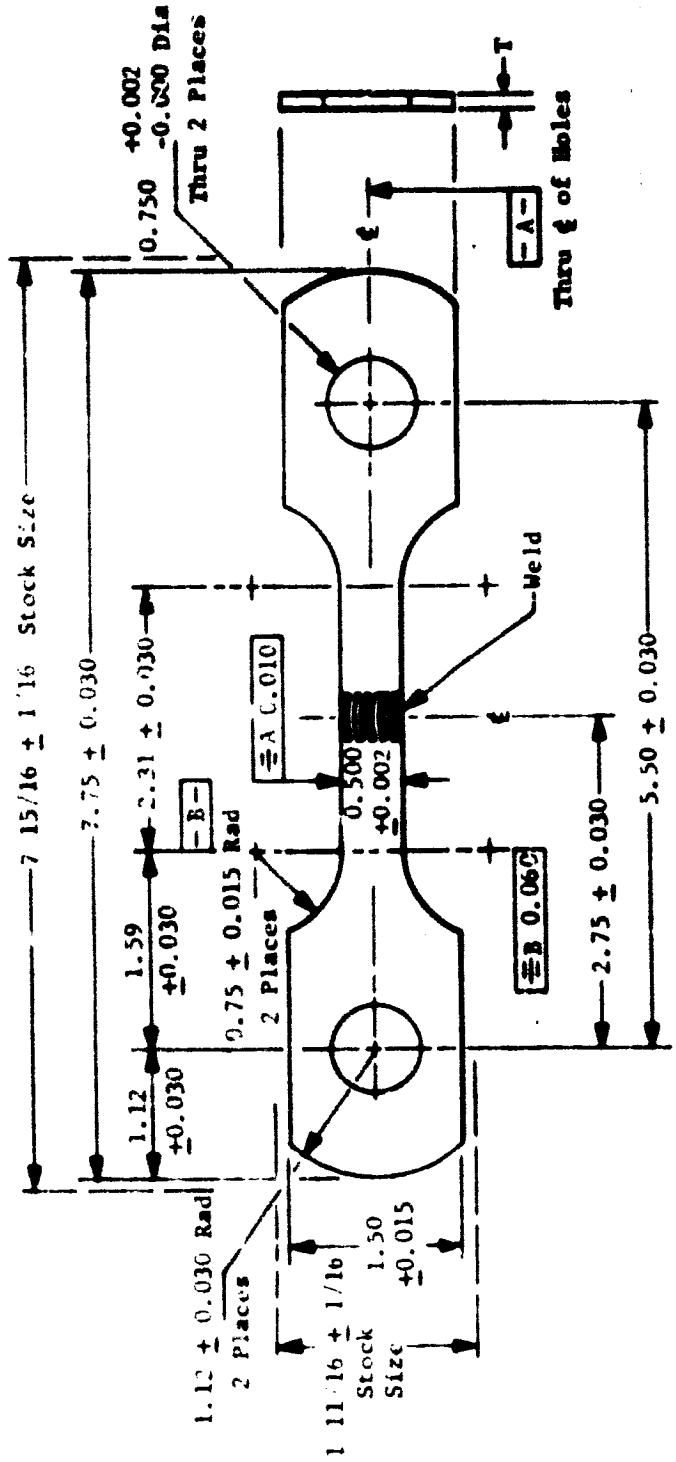

Fig. 1 Specifications for Tensile Specimen

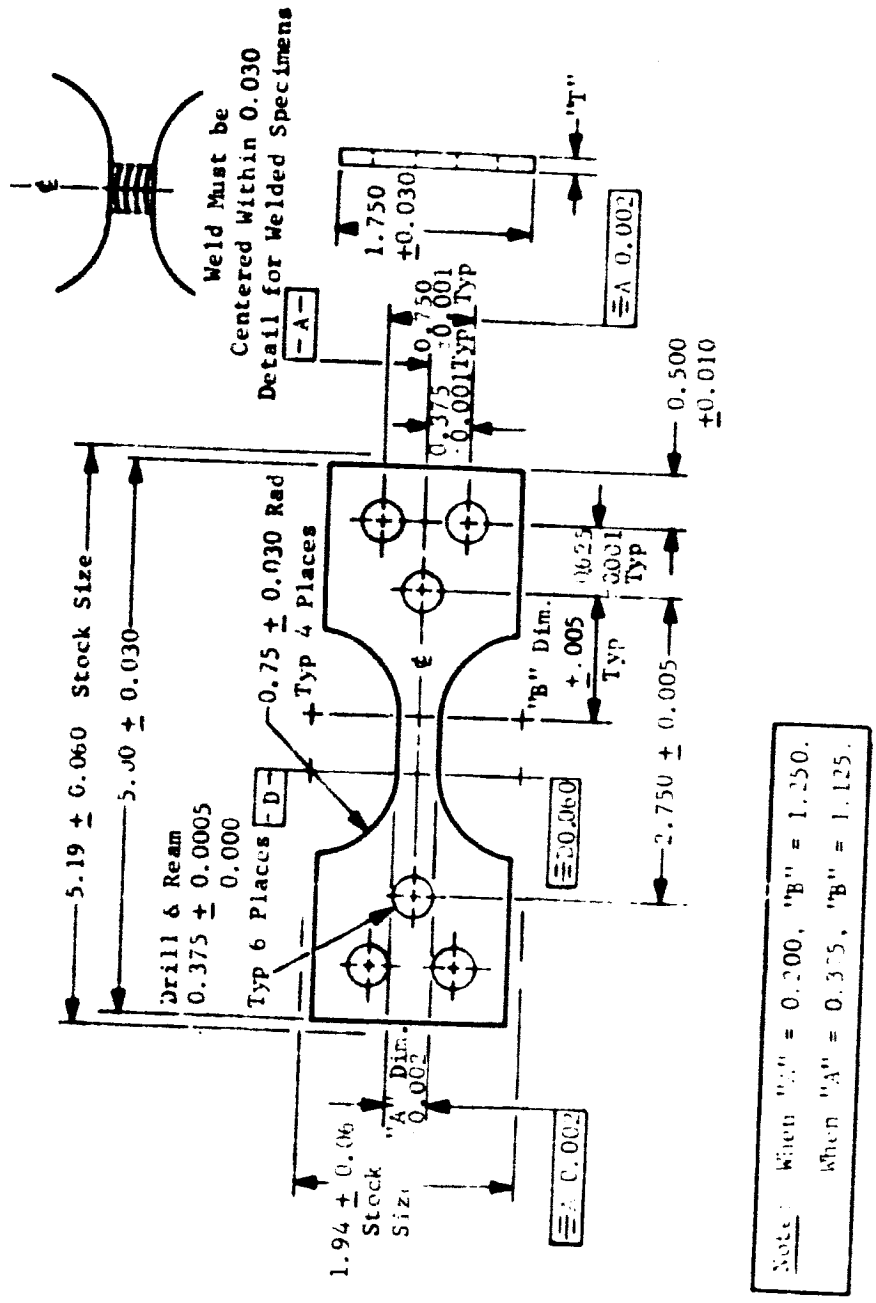

Note: When "A" = 0.200, "B" = 1.250.
When "A" = 0.375, "B" = 1.125.

Figure 2. Specimen Details for Unnotched and Welded Fatigue Specimen

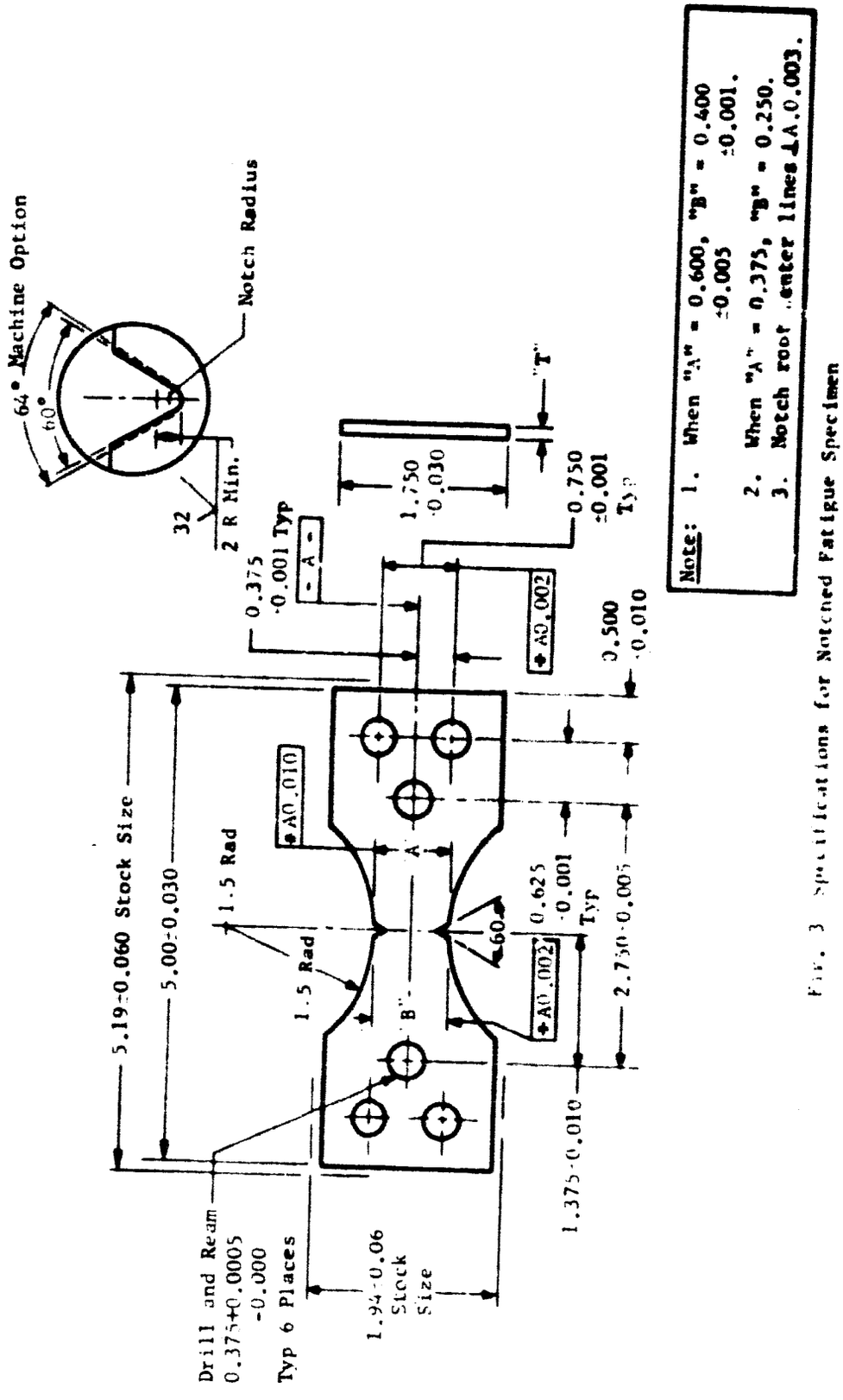

Fig. 3 Specifications for Notched Fatigue Specimen

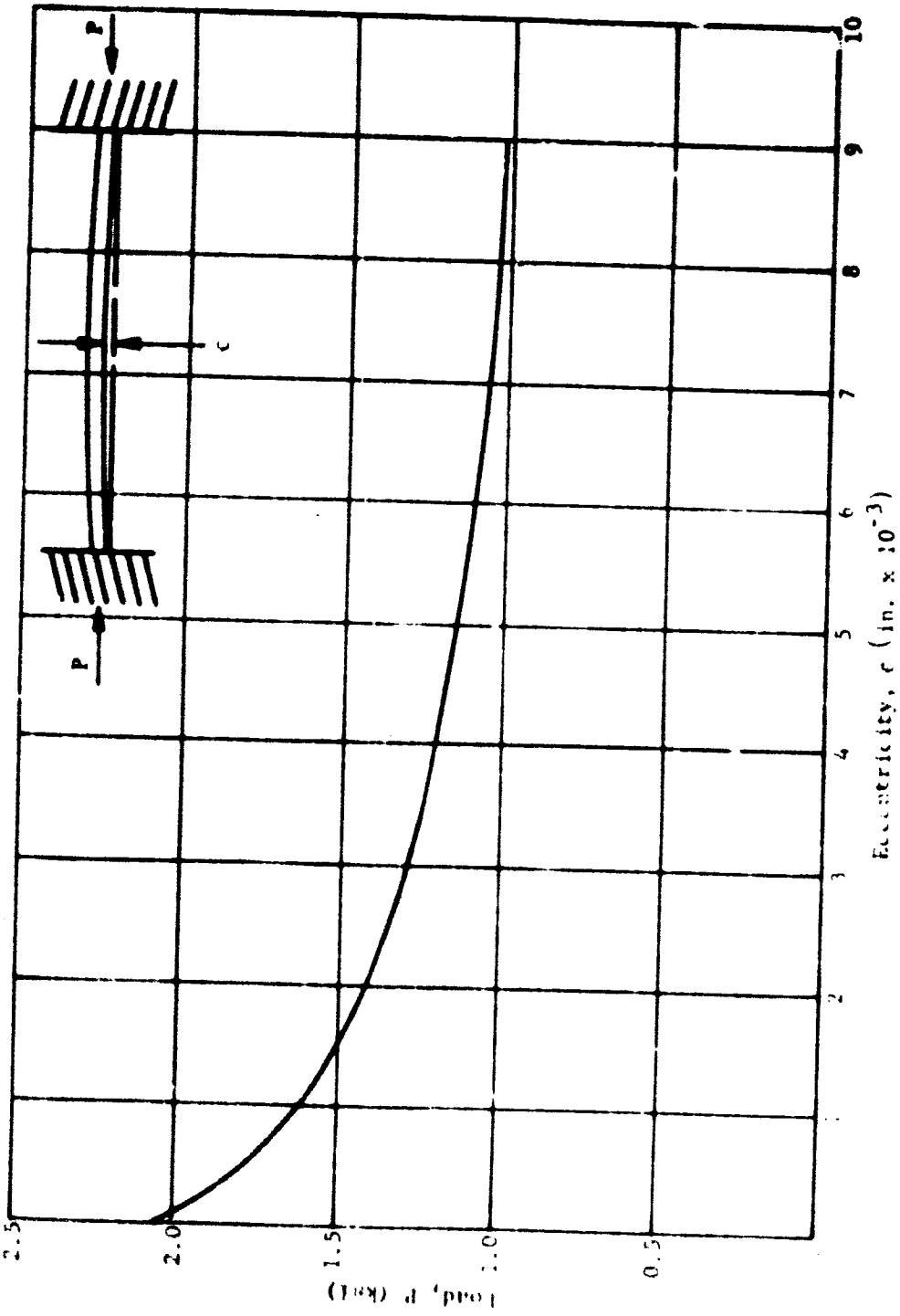

Effect of Eccentric Displacement on the Applied Axial Load of 5456-H343 Aluminum Alloy at -423°F

IV. [illegible]

The fatigue-test apparatus (Fig. 5) was designed for use with Sonntag SF 10 U fatigue-testing machines. These machines have a reciprocating platen located in the center of the test bed. Load is applied between this platen and the head frame anchored to the test bed. Such machines have a capacity of 5000-lb dynamic load and ±5000-lb static load. The test apparatus was designed to match this capacity.

The principal requirements for this system were:

1) Ability to operate at -320 and -423°F;

2) Good thermal efficiency;

3) Ease of specimen change;

4) Precise alignment;

5) Assumation of temperature-control system.

A. CRYOSTAT

A test cryostat was designed based on the described requirements. (See Appendix A for detailed drawings of the components.) Figure 6 shows a cutaway view of the liquid hydrogen cryostat assembly mounted in the test machine. The design incorporates a vacuum-insulated, double-walled, stainless steel container with a tubular loading stem that passes through its central axis. Another tubular loading stem passes through the cryostat lid. The test specimen is gripped between these two stems. The cryostat mounts on the reciprocating platen of the test machine and moves with the platen while the lid, with the liquid supply line, vent line, and instrumentation support attached, remains fixed to the machine head frame. By using this system, the test cryostat would have to withstand long-term forces of approximately 2 g and, after fracture of the test specimen, forces exceeding 36-g accelerations, as well as impact from the broken ends of the specimen hammering together.

Fig. 5 SF 10U Fatigue-Testing Machine

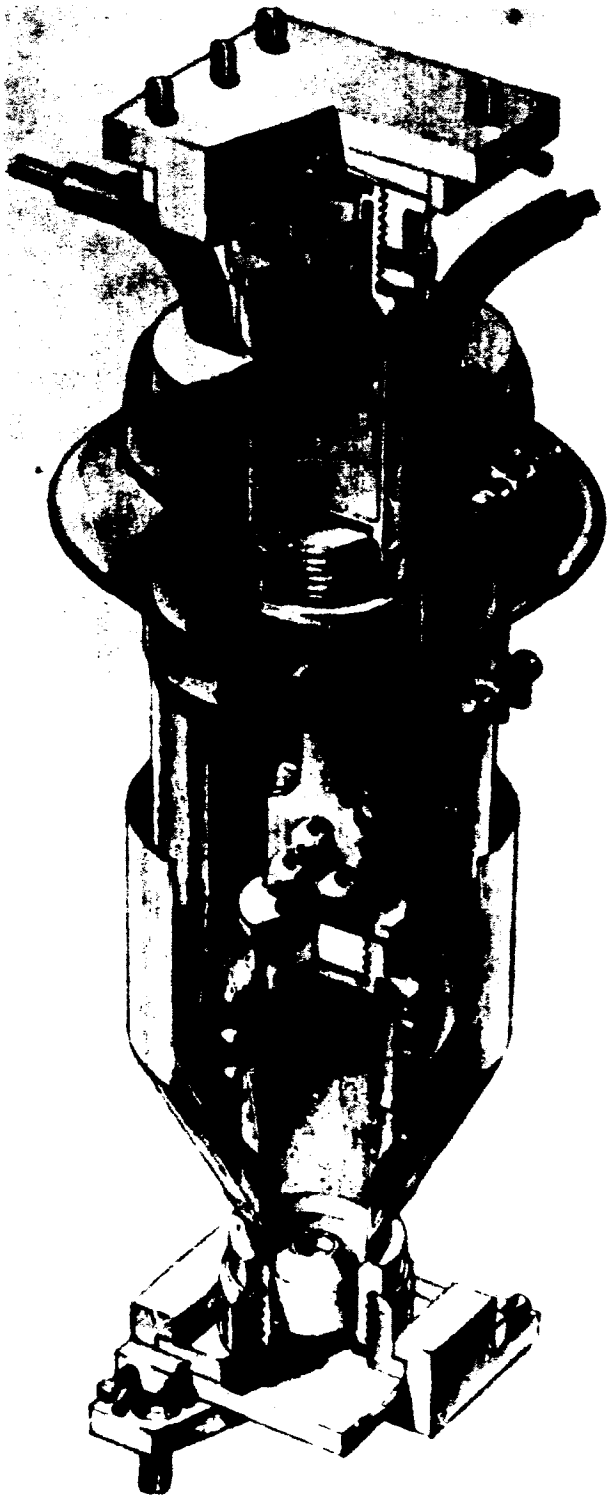

Fig. 6 Cutaway View of Cryostat Assembly Mounted in Fatigue-Testing Machine

The tubular loading stems were machined to a diameter of approximately 2 in. and a wall thickness of 0.070 in. The ends were threaded to receive the specimen grips and anchor into base blocks. Richards-type vacuum valves were recessed into the stem bases to avoid accidental damage and freezeout during test. The double-walled body was made by welding cylindrical sections to spun dome pieces that were, in turn, welded to small flanges on the stems. An unusual feature of the cryostats was the use of ready-formed, stainless steel, spun domes. These domes were cookingware items (soup tureens and flour scoops) purchased from a local restaurant supply store. Figure 7 shows the cryostat components before assembly.

The liquid hydrogen cryostat lid was made so that a vacuum-insulated liquid-fill line, and a vent line with a concentric liquid dump line within it, were welded into the lid unit. The dump line served as a support for the liquid-level sensor elements. The seal between the lid and the cryostat was a conductive neoprene bellows. An O-ring was used to seal the lid against the upper stem. Figure 8 shows the lid assembly.

All cryogenic structural parts were made from 300 series stainless steels. Two cryostats were constructed: one for use at -423°F and one for -320°F. The two units were identical except for the absence of liquid nitrogen cooling of the lower stem in the nitrogen cryostat and a less-sophisticated lid assembly for nitrogen service.

B. ALIGNMENT AND ASSEMBLY

Since test alignment was critical, specimens were designed to align themselves axially by three close-tolerance fastener holes in each end. Lateral alignment was provided by confining the specimen between polished guide shoulders extending well into the fillet sections. Allowance was made in the design of the grip slots for up to 0.005-in. variation in specimen thickness. The grips were made by furnace-brazing premachined grip halves and then finish-machining the assembly for precise alignment. The bases of the grips are threaded for ease of installation in the loading stems. A slotted alignment shoulder permits the grip to be wrench-tightened.

Fig. 7 Cryostat Components before Assembly

Fig. 5 Liquid Hydrogen Cryostat Lid Assembly

A thermal locking action was used to obtain tight joints within the grips. When aluminum specimens are used, they contract tightly against the steel-mounted fastener pins, producing locking. Conversely, with titanium specimens, the grips contract to tighten the bolt group against the specimen. A thermal lock is also achieved by using titanium washers between the threaded grip bases and the loading stems.

The loaded cryostat assembly inserts into the fatigue-testing machine by a unique mounting system that provides rapid installation and precise alignment. This mounting system uses tee-slotted retainer plates fixed to the test machine heads; matched tee-shaped blocks, tapped out to accept the loading stems, are mounted on the cryostat assembly. When these blocks are inserted in the retainer plates, they provide a precise fit of the entire assembly. The mounting system is locked with paired wedge plates located inside the retainer plates. Figure 9 shows the retainer plate (A), tee-block (B), and wedge plates (C). Alignment of each component of the system is necessary for testing of sheet materials, and each component must be installed in its indexed position for each test. The tee blocks and their retainers were hand-fitted for precise alignment. The entire system was also given a final precise alignment after assembly with a strain-gage alignment cell. Alignment was achieved by adjusting the head frame and retainer plates.

To illustrate the effect of column alignment, high-speed motion pictures were made of both an aligned and an intentionally misaligned (7075-T6 aluminum alloy) specimen tested at 70°F. Figure 10 shows the effect of misalignment. Column buckling is clearly shown under compressive load. (This column buckling is shown to cause failure.) A properly aligned 7075-T6 specimen was tested at three stress levels (20,000, 63,000, and 75,000 psi). This latter stress level was above the yield strength for this material. Figure 11 shows no evidence of column buckling under compressive loads. Failure occurred in the tension portion of the cycle.

C. AUTOMATION

Systems used for both -320 and -423°F operation were constructed so that testing could be performed automatically, with only periodic monitoring needed. Automatic level sensor/fill controllers were constructed for each system.

Fig. 9 View of Cryostat and Mounting Hardware

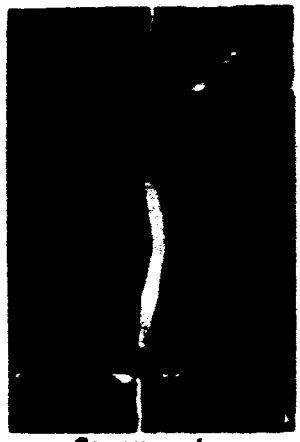

Compression

Tension

Compression

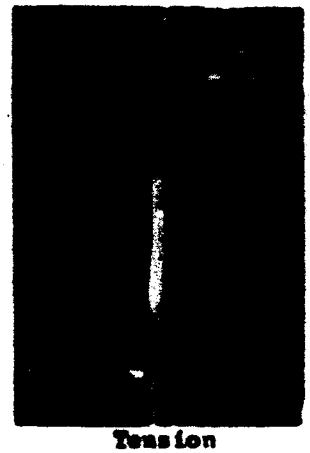

Tension

(a) Views before Failure (two complete cycles)

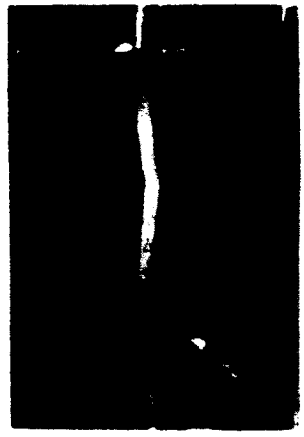

(b) Views at Failure (adjacent frames)

Fig. 10 Frames from High-Speed Motion Pictures of Misaligned 7075-T6 Aluminum Alloy Fatigue Test

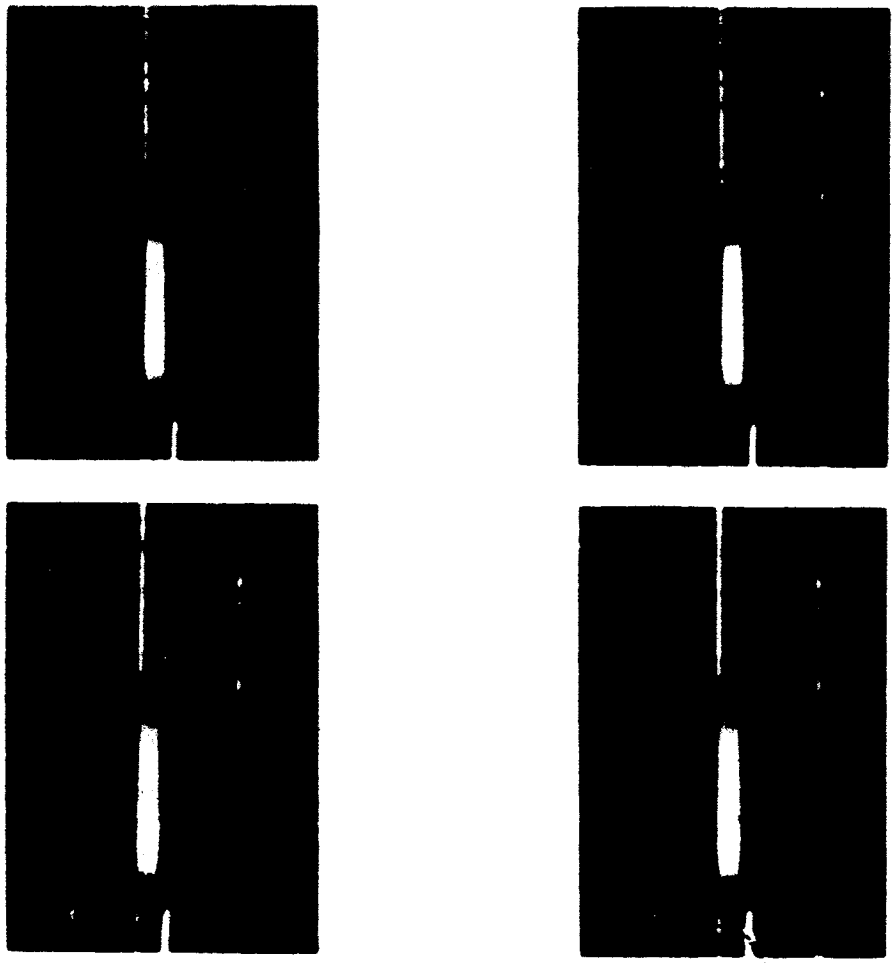

(a) Views before Failure (alternate frames)

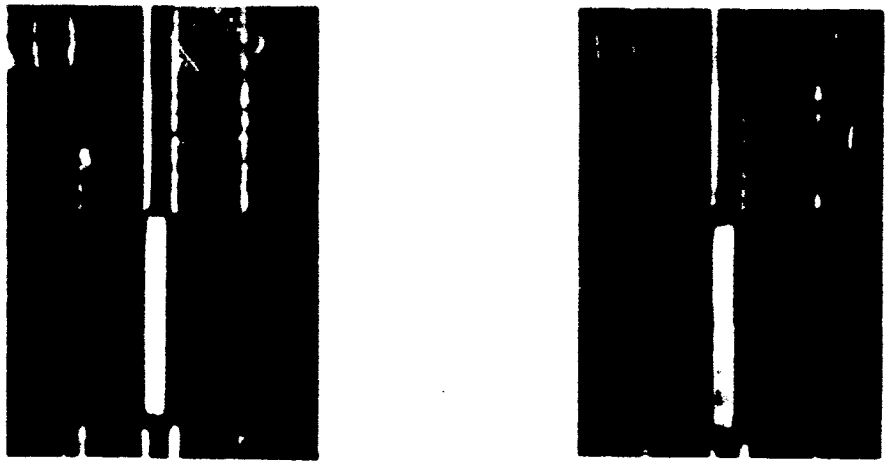

(b) Views at Failure (adjacent frames)

Fig. 11 Frames from High-Speed Motion Picture of Aligned 7075-T6 Aluminum Alloy Fatigue Test

During the first year's work, a Martin-developed circuit was used that incorporates a small diameter platinum wire (0.0005-in.) approximately 3/8-in. long as the sensing element. A sharp resistance change of the heated platinum wire occurs as the element is cycled from the liquid to the vapor phases. A transistorized relay-control circuit is used to detect the resistance changes of the wire. Point sensors located approximately 2 in. apart in the cryostat are used to maintain liquid level between the sensors. Fill is automatic through a solenoid-operated valve that permits liquid fill until the upper sensor is immersed. Fill is then discontinued until the lower sensor becomes exposed because of boil-off. The fill process is then repeated. Figures 12 and 13 show the liquid nitrogen and liquid hydrogen controllers, respectively.

Frequent failures encountered in the platinum wire necessitated a change to thermistor sensing elements during the second year's effort. For safety, a thermistor in the lid of the liquid hydrogen cryostat serves as an overfill sensor. In case of overfill, the fill valve closes, and the fatigue machine is stopped. This action also occurs if the facility power fails.

For additional safety, the control panel includes remote controls to start and stop the fatigue machine. Therefore, it is unnecessary for the operator to enter the test cell after the cryostat is installed in the fatigue machine. An intercom system provides audible monitoring of the test, both in the control room and at various laboratory locations.

A schematic diagram for the liquid hydrogen flow system is shown in Fig. 14. A self-pressurizing, 1000-ℓ mobile storage Dewar is used to provide liquid hydrogen. Fill is controlled by a Martin-designed and -constructed cryogenic valve operated by a solenoid-gas actuator combination. All liquid transfer lines are vacuum-insulated. Nitrogen and helium gas are supplied to the system to sweep-purge the cryostat, fill line, and vent system. The entire system is normally purged for 5 minutes before filling. The vent system has been designed to permit hydrogen testing under all weather conditions. The necessity for this approach results from a potential gradient to ground that is developed through the atmosphere during certain weather conditions. This potential is often sufficient to ignite a hydrogen-oxygen mixture at the vent stack outlet. The vent system includes a water valve to preclude ignition back to the cryostat and possible explosion. The water valve consists of a 30-gal. drum containing a bell jar. The inlet to the bell jar is below liquid level; the outlet above. A goose-neck trap is used to prevent water from backing into the vent.

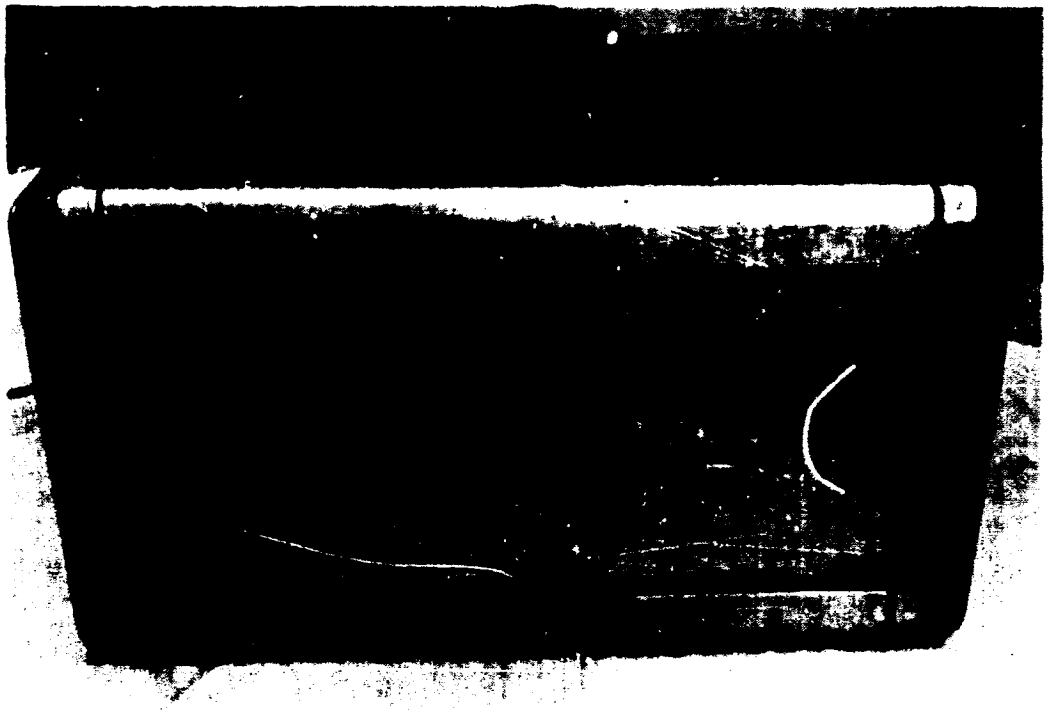

Fig. 12 Liquid Nitrogen Fill Controller

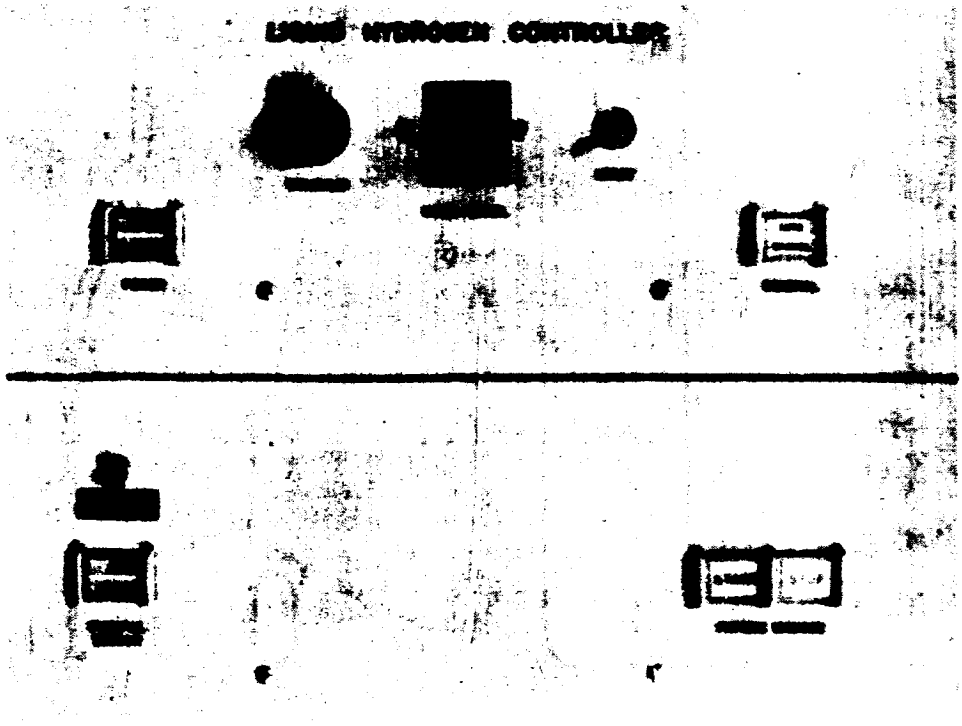

Fig. 13 Liquid Hydrogen Fill Controller

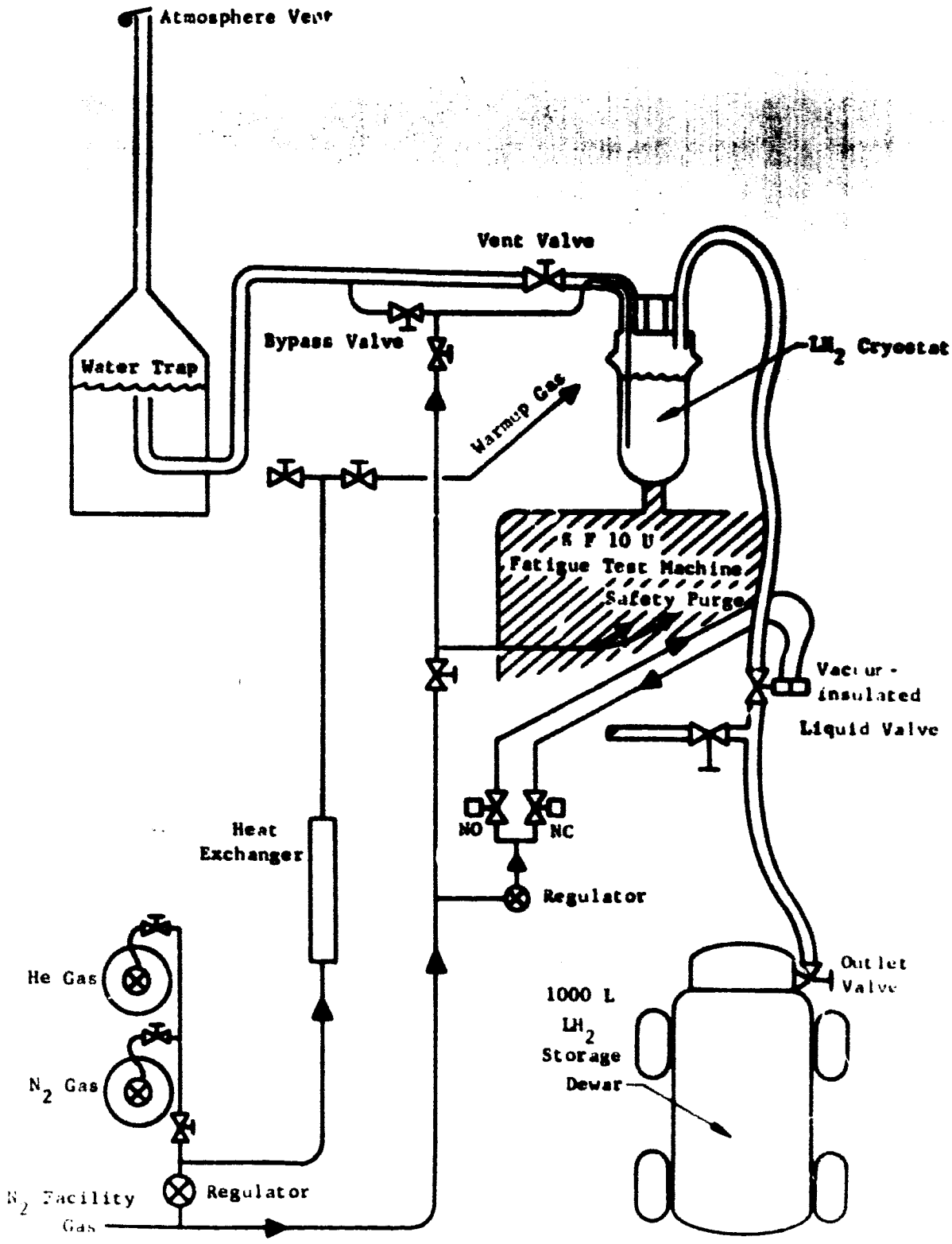

Fig. 14 Schematic Diagram of Liquid Hydrogen Flow System

D. FACILITY

It was necessary to move an SF 10 U fatigue-testing machine from the Denver Materials Engineering Laboratory to the Denver Hydrogen Research Laboratory to perform the liquid hydrogen handling and testing in a safe location. A test cell was constructed for this machine. A 12x14-ft concrete slab base and a blowout-type test room were prepared, the latter adjoining the existing tensile test cell. It is constructed of welded steel, with a heavy plate blast wall separating the two cells and a similar blast wall between the cell and Dewar parking area. The remaining two sides are covered with fiberglas attached to the frames with screws so that the wall can readily blow out in the event of an explosion. A sketch (a) and a photograph (b) of the liquid hydrogen fatigue-testing facility are shown in Fig. 15. The liquid nitrogen facility is shown in Fig. 16.

E. PERFORMANCE

Thermal performance of the cryostat and system has been very satisfactory. Original calculations indicated a liquid hydrogen boiloff rate of 3.5 per test hour for the cryostat alone, with a liquid nitrogen-filled outer jacket to minimize hydrogen loss. In actual practice, the liquid nitrogen fill was discontinued since the total system boiloff of the cryostat, 7 ft of transfer line, six coupling joints, a liquid shutoff valve, and a storage Dewar outlet system averaged only 7 ℓ/hr.

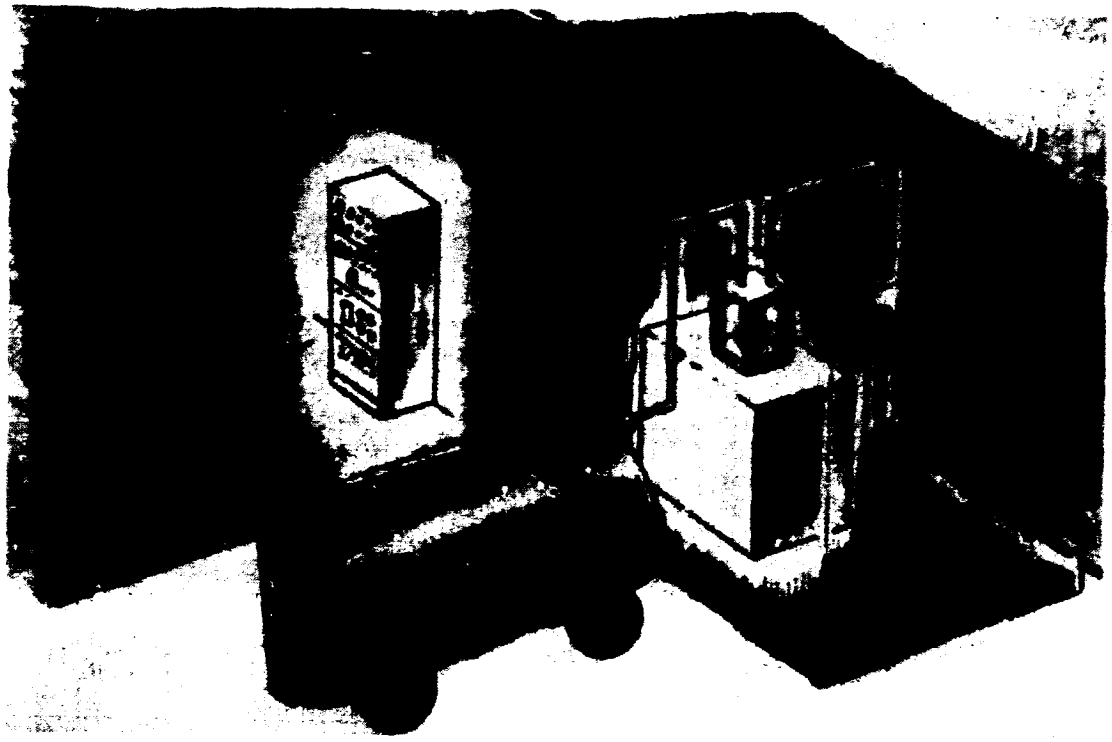

(a)

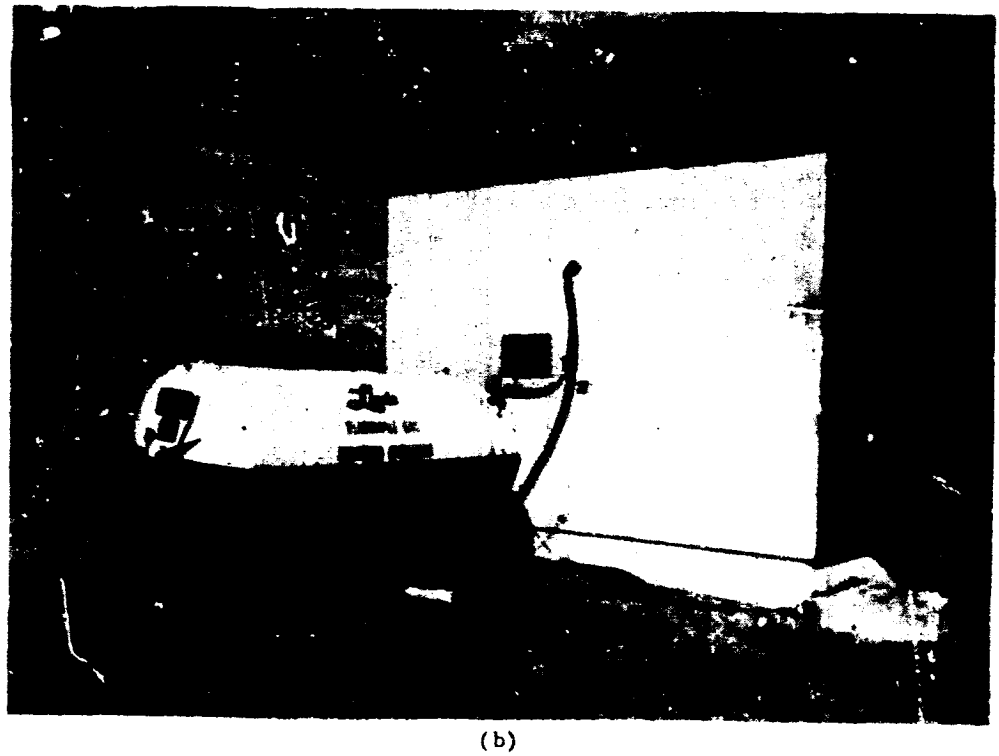

(b)

Fig. 15 Liquid Hydrogen Fatigue-Testing Facility

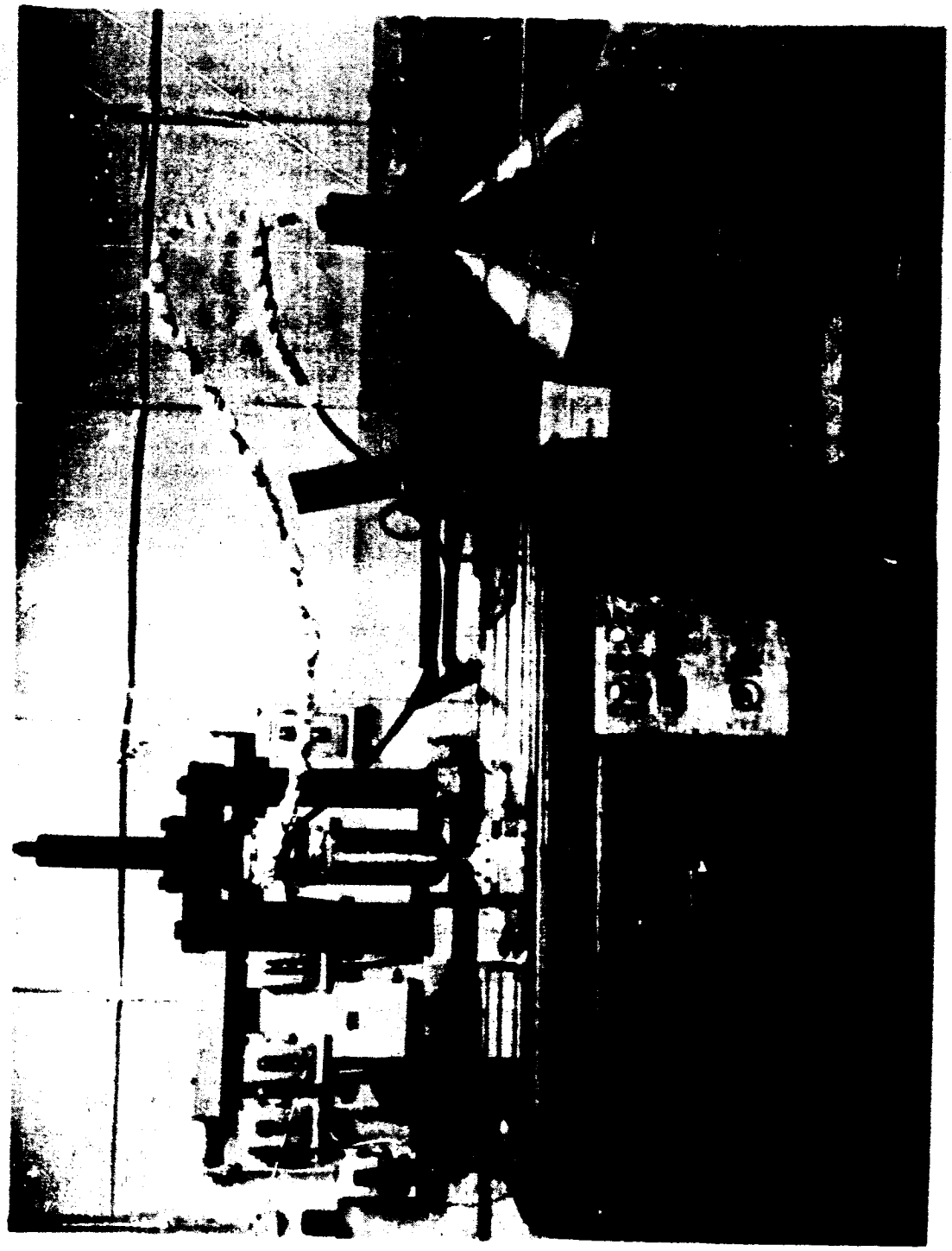

Fig. 26 Liquid Nitrogen Fatigue-Testing Facility

V. TEST PROCEDURE

Specimens were tested at three temperatures: 70, -320, and -423°F. Cryogenic temperatures were achieved by constant-temperature liquid baths: liquid nitrogen for -320°F and liquid hydrogen for -423°F.

A. TENSION

Parent metal aluminum and stainless steel specimens were tested at constant test machine platen speed corresponding to an approximate strain rate of 0.010 in./in./min in the elastic range. After the specimen yielded, platen speed was increased tenfold. Welded specimens were tested to failure at a constant platen speed equivalent to 0.010 in./in./min. Titanium specimens were similarly evaluated except that the test speed was one-half that used for aluminum specimens.

The equipment and techniques used for tensile evaluation are similar to those described in the literature (Ref 1 and 2). Type AB-3 or FA-100-12 resistance strain gages bonded with EPY 400 or Narmco 7343 adhesive were used for strain measurement on tensile specimens. Specimens were single-gaged except for one specimen of each type that was double-gaged for modulus determination. To establish accurate modulus data, the specimen was strained in the elastic range at least three times. The same specimen was used at each of the three temperatures. Strain gages were calibrated using a tapered cantilever beam device to indicate strain sensitivity (or gage factor) at each temperature so that modulus data could be properly converted to correct for temperature effects.

B. FATIGUE

Specimens for fatigue-testing were hand-polished on their edges to remove all evidence of machining marks. All specimens were prepared with the as-received surfaces intact. Afterwards, the specimens were carefully measured and then installed in the cryostat. The cryostat was inserted into the fatigue machine and the entire unit flushed with inert gas for a minimum of 5 minutes before the liquid hydrogen fill process. After testing, the cryostat was thoroughly flushed with warmed nitrogen gas before opening.

Except for the cryogenic aspects, testing was performed in a routine manner. To obtain extra data, some of the discontinued specimens were rerun at high stresses to produce low cycle failures. Results obtained from rerun specimens compared favorably with data obtained from previously untested specimens.

VI. EXPERIMENTAL RESULTS

Tension-testing at all temperatures and liquid hydrogen fatigue testing were performed at the Denver facility. Fatigue-testing at room and at liquid nitrogen temperatures was performed at the Baltimore Division.

A. TENSION TESTS

Tension tests were performed at 70, -320, and -423°F to provide data on:

Ultimate strength;

Yield strength;

Elongation;

Modulus of elasticity;

Notch strength;

Weld strength.

Triplicate tests were performed for each condition. Results of these tests are shown graphically in Fig. 17 thru 27. Detailed test data are given in Appendix B (Tables B-1 thru B-9).

B. FATIGUE TESTS

Fatigue tests were performed to provide S/N curves at 70, -320, and -423°F. A stress ratio (R) of -1 was used for all aluminum and stainless steel specimens. The titanium specimens were not sufficiently flat to permit fully reversed stressing and were tested under tension/tension loading at a stress ratio of 0.01.

Fatigue test results are illustrated in Fig. 28 thru 56. Circles are used to denote data points of specimens tested for the first time. Discontinued specimens are identified by an arrow extending to the right. Reruns of discontinued specimens are shown by square symbols. Detailed tabular presentations of these data are given in Appendix C.

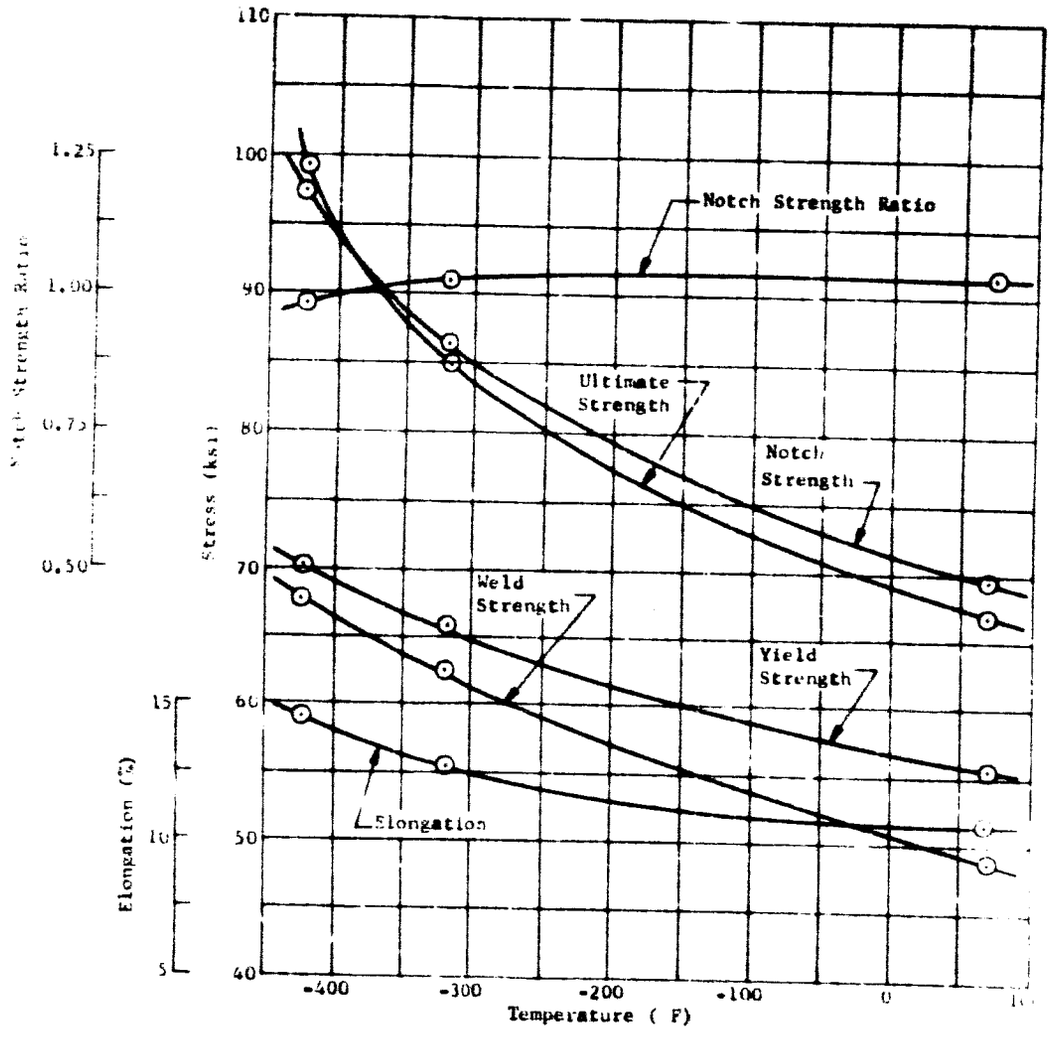

Fig. 18 Tensile Properties of 2219-T87 Aluminum Alloy at Cryogenic Temperature

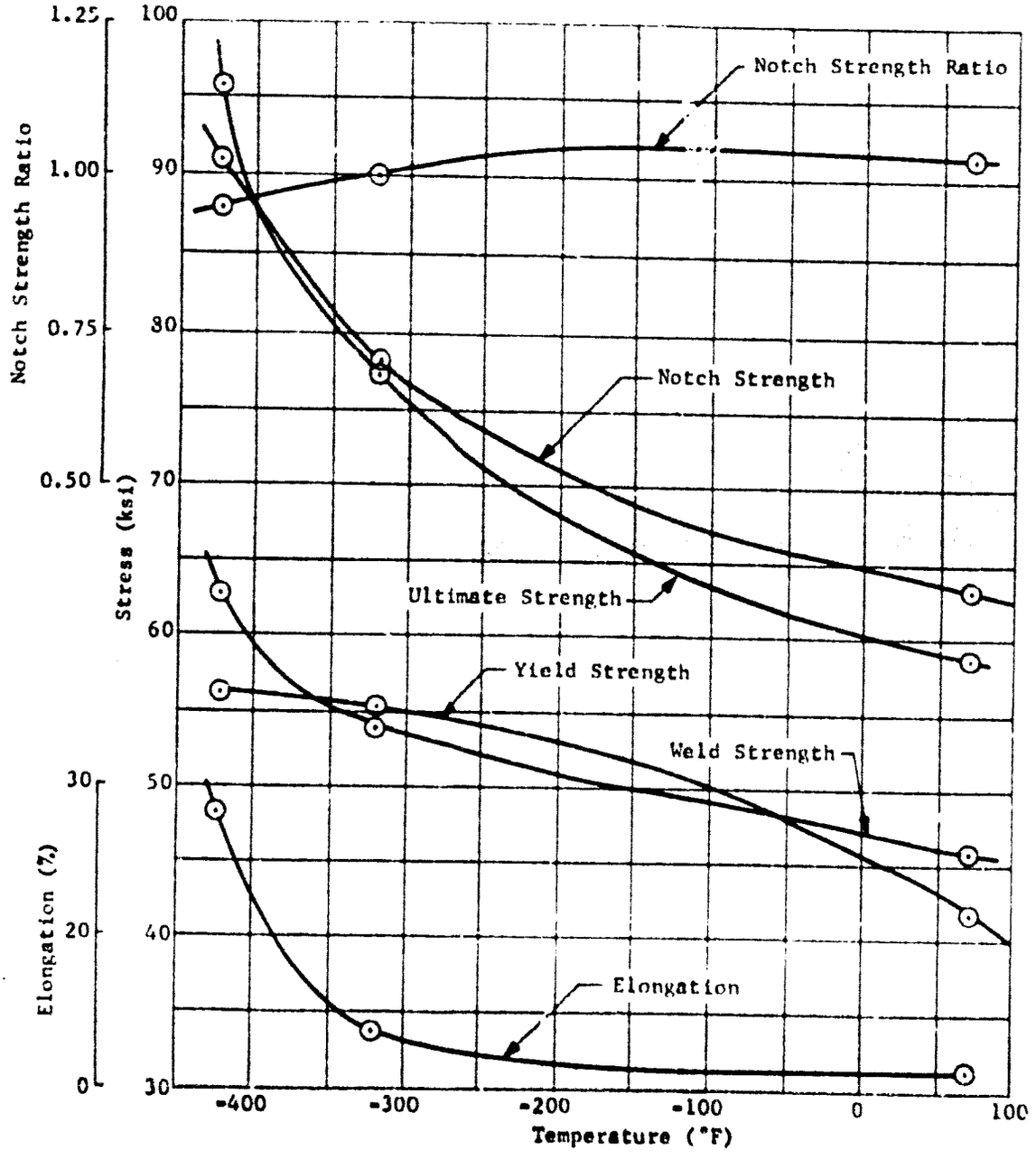

Fig. 19 Tensile Properties of 2219-T62 Aluminum Alloy at Cryogenic Temperatures

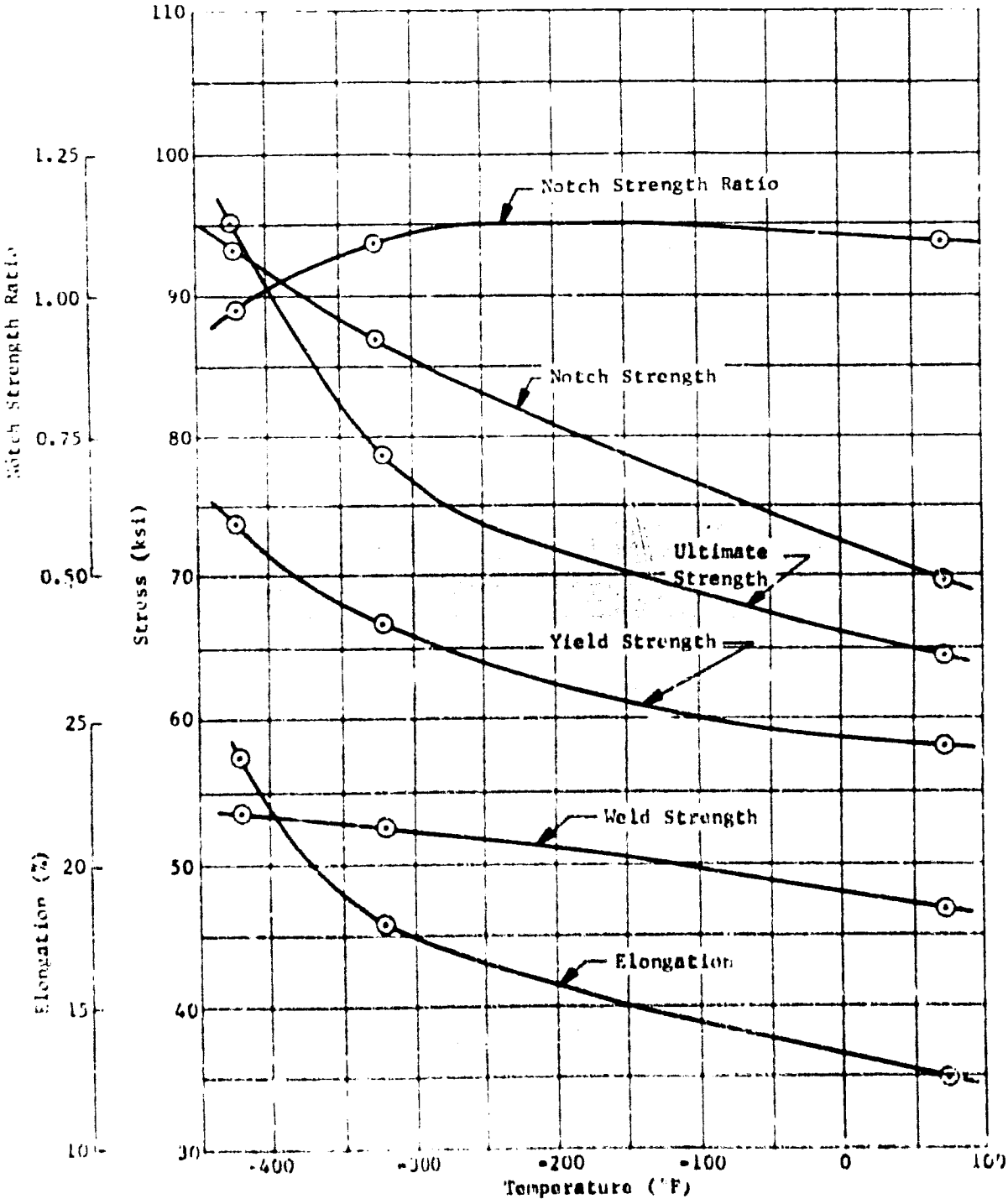

Fig. 20 Tensile Properties of 7039-T6 Aluminum Alloy at Cryogenic Temperatures

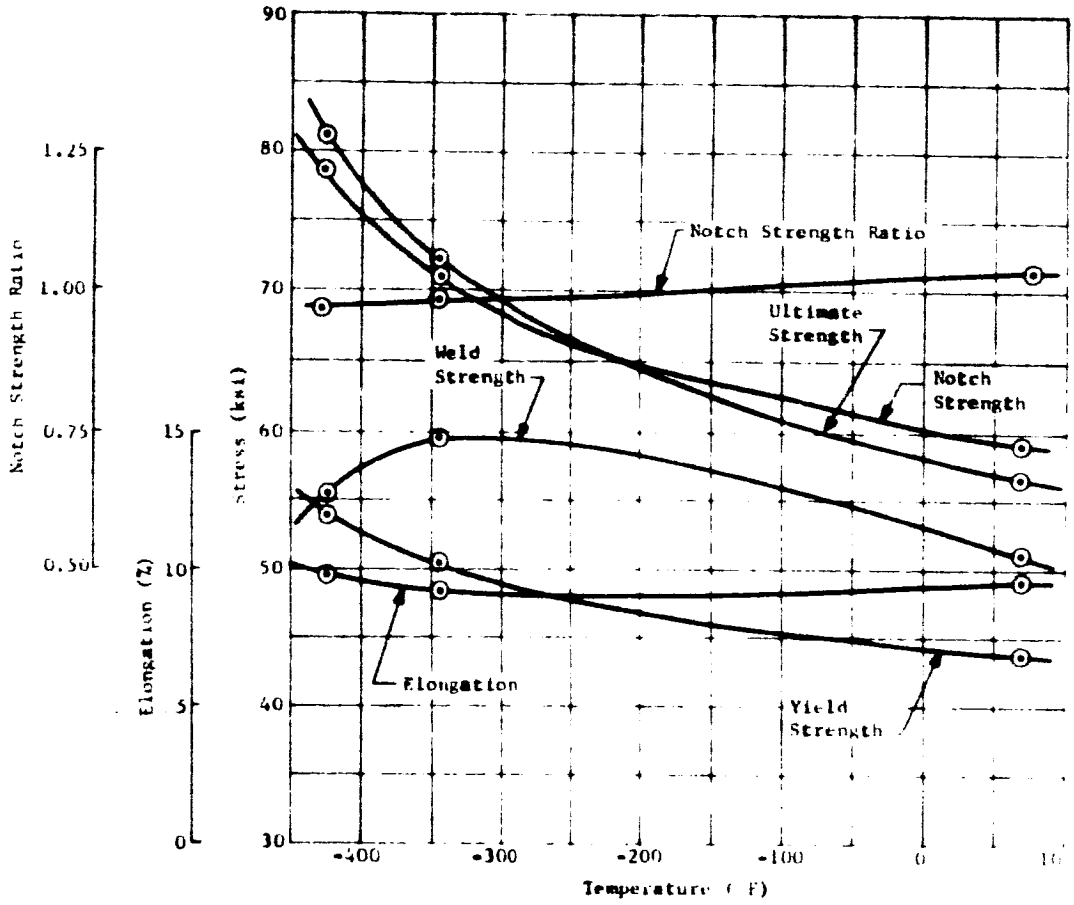

Fig. 21 Tensile Properties of 5456-H343 Aluminum Alloy at Cryogenic Temperatures

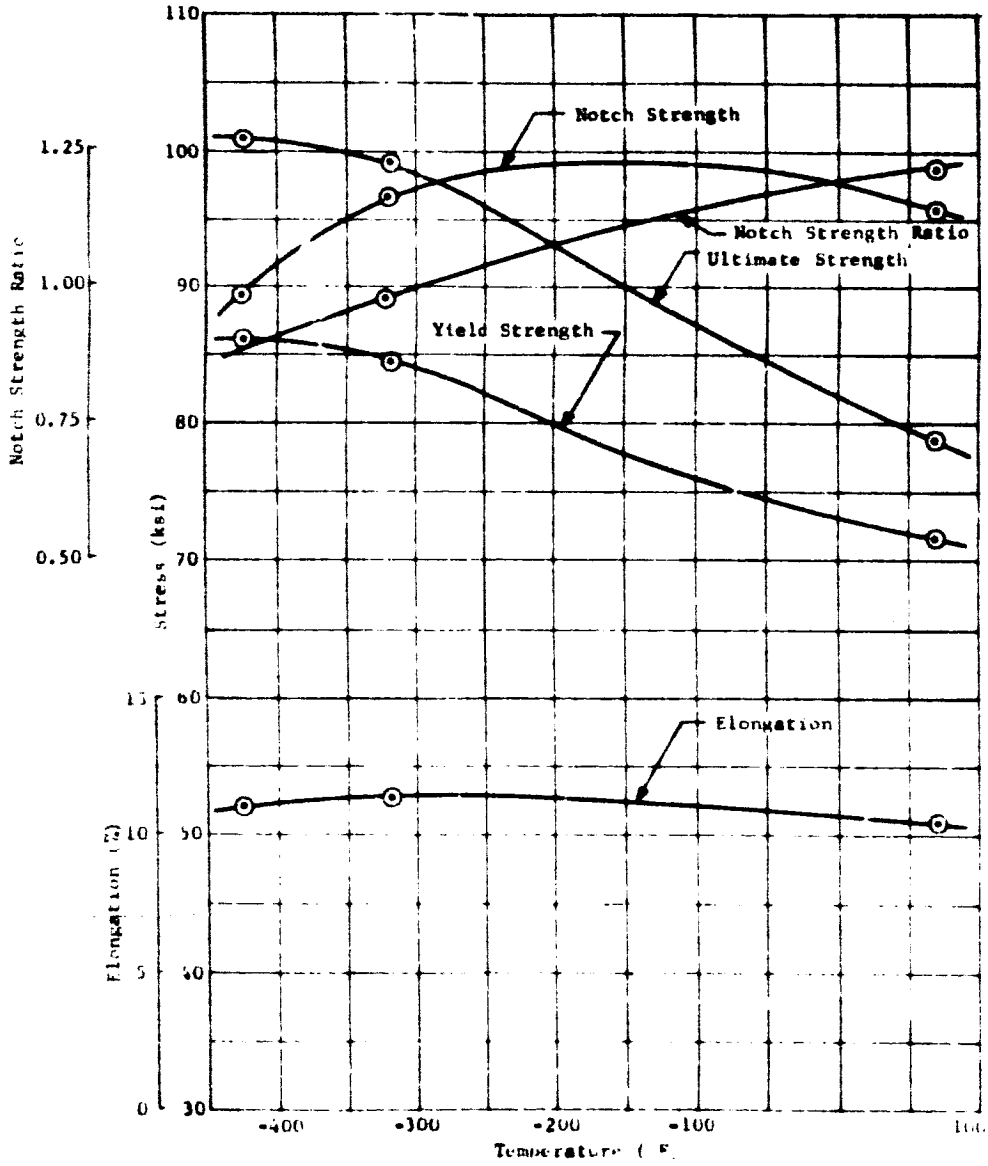

Fig. 22 Tensile Properties of 7075-T6 Aluminum Alloy at Cryogenic Temperatures

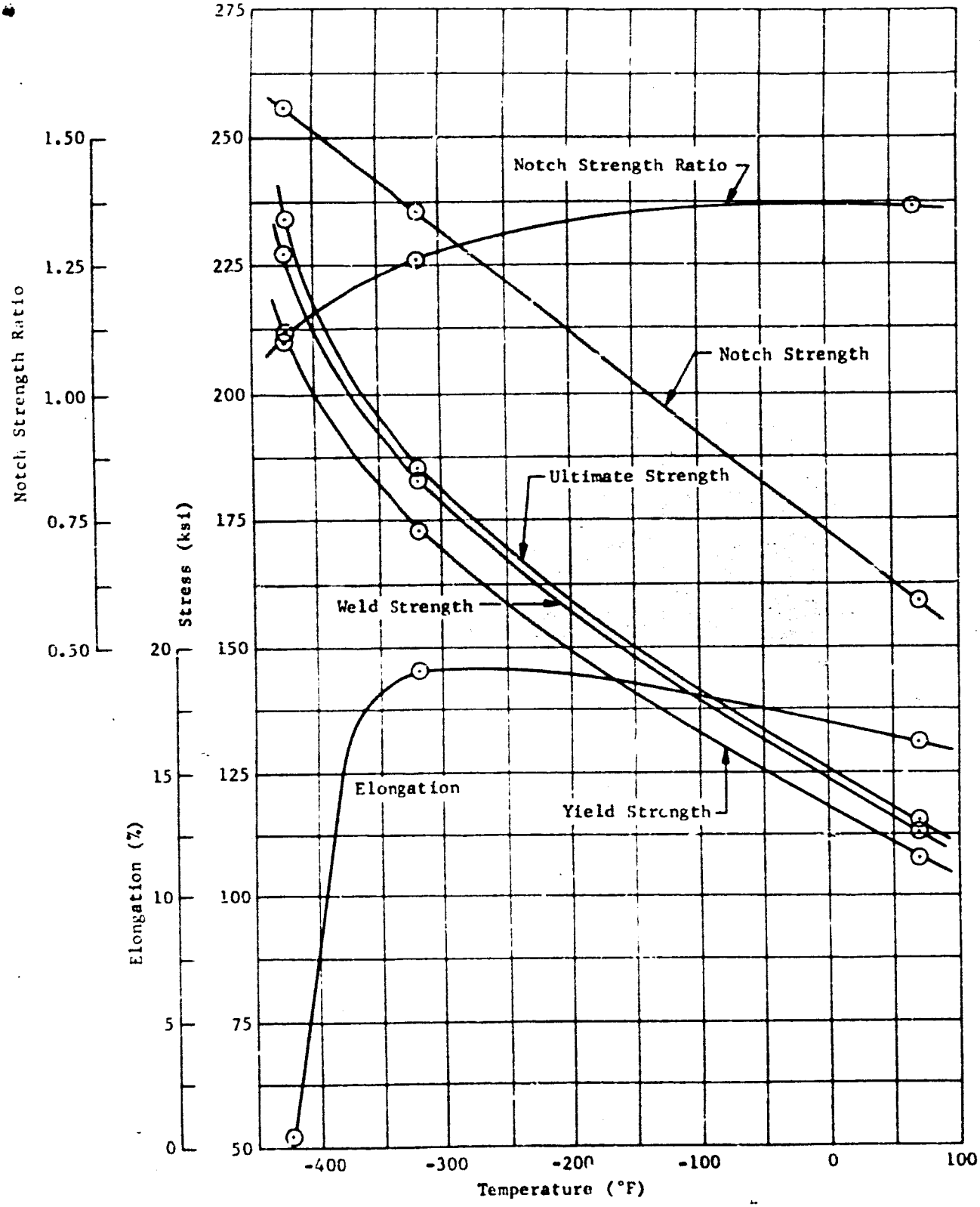

Fig. 24 Tensile Properties of 5Al-2.5Sn Titanium Alloy at Cryogenic Temperatures

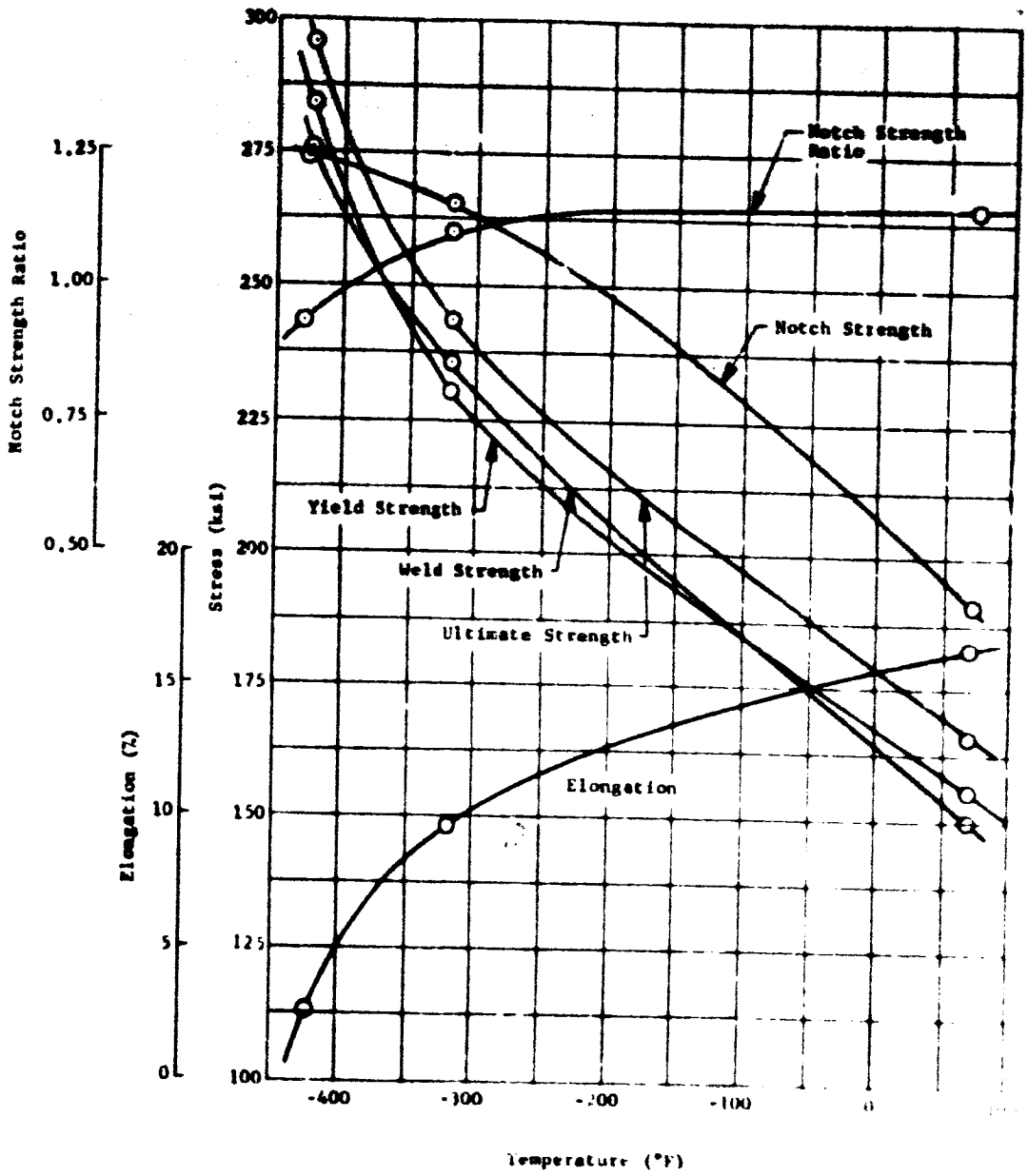

Fig. 25 Tensile Properties of 6Al-4V Titanium Alloy at Cryogenic Temperatures

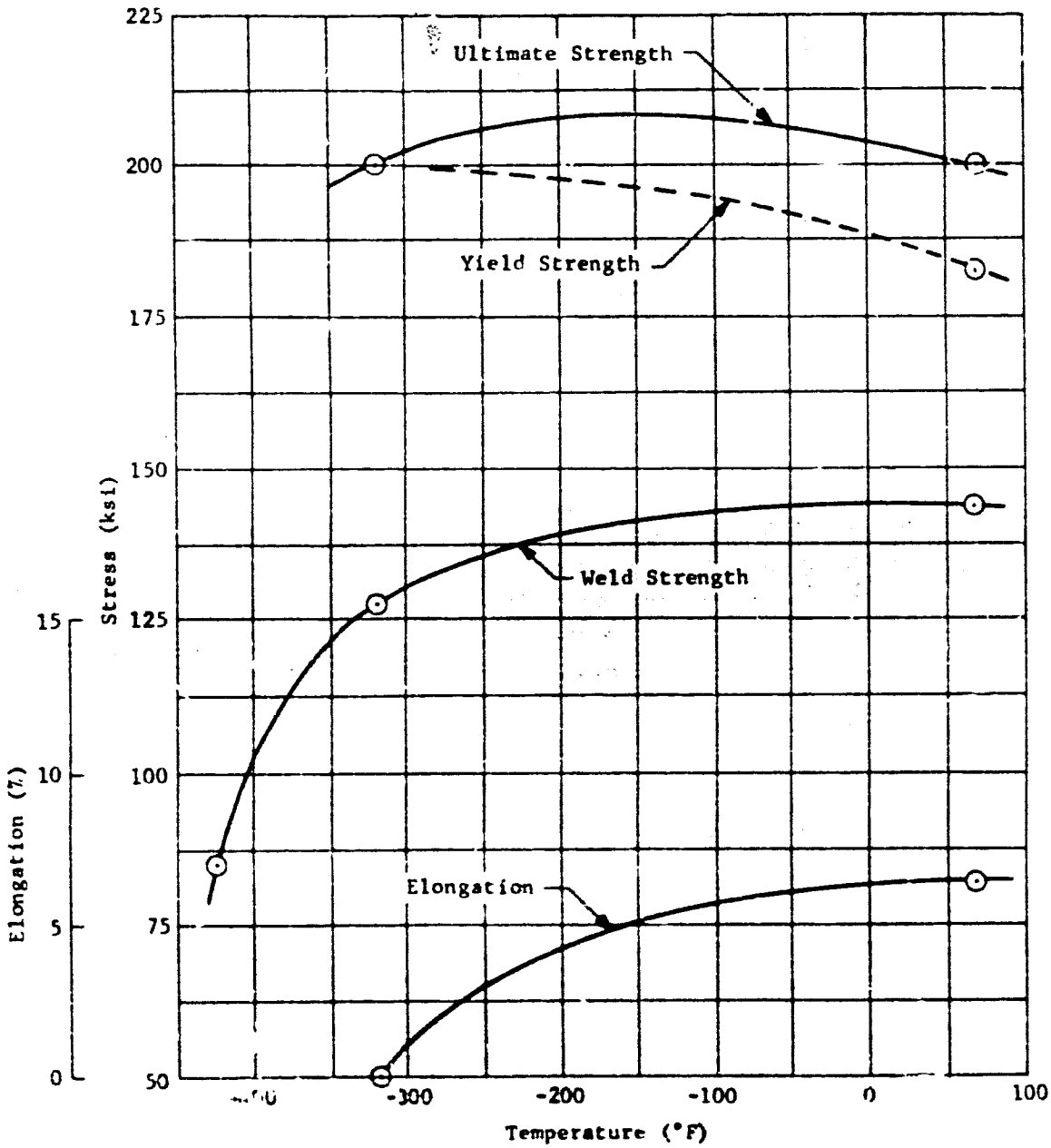

Fig. 26 Tensile Properties of 13V-11Cr-3Al Titanium Alloy at Cryogenic Temperatures

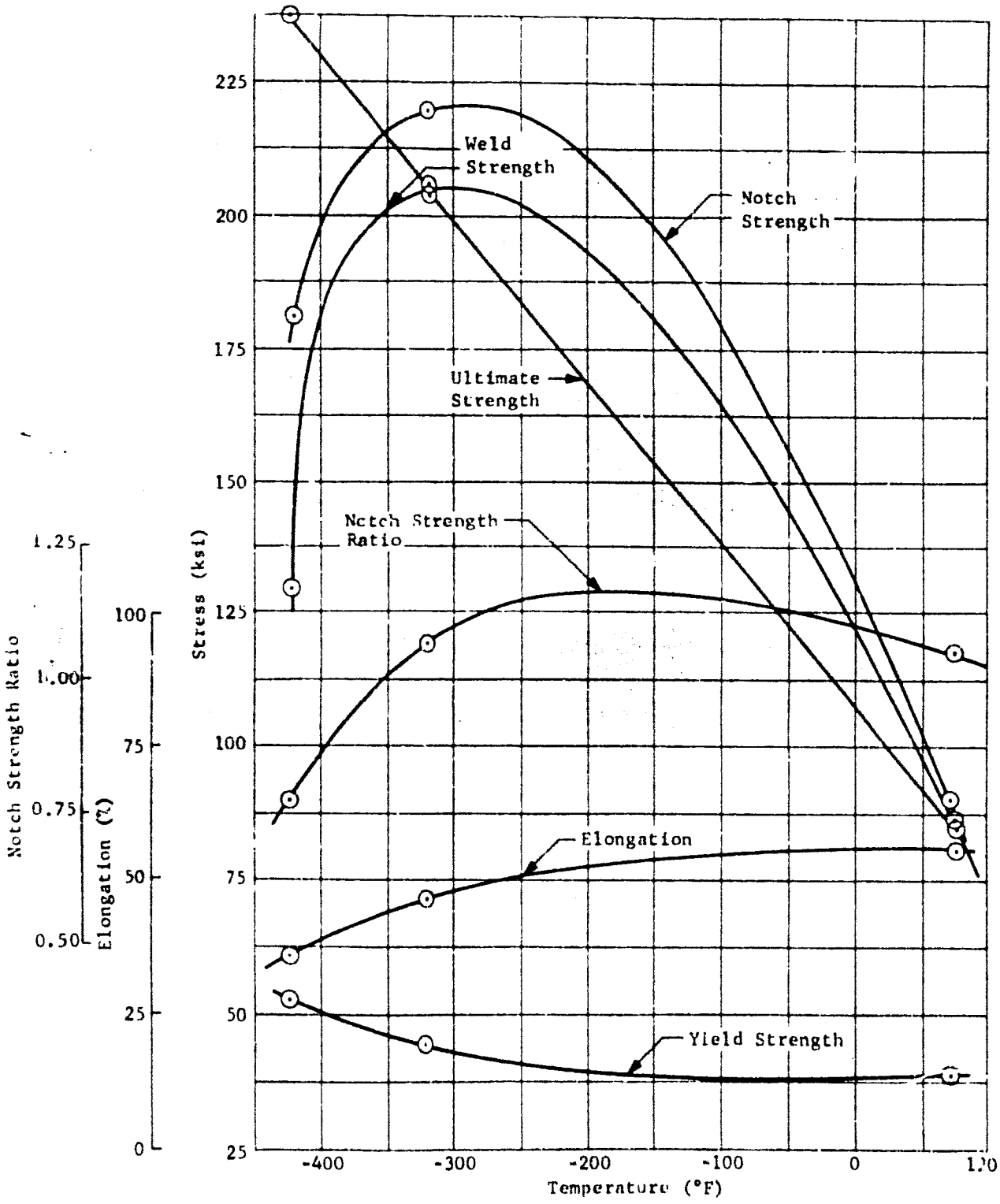

Fig. 27 Tensile Properties of 321 Stainless Steel Alloy at Cryogenic Temperatures

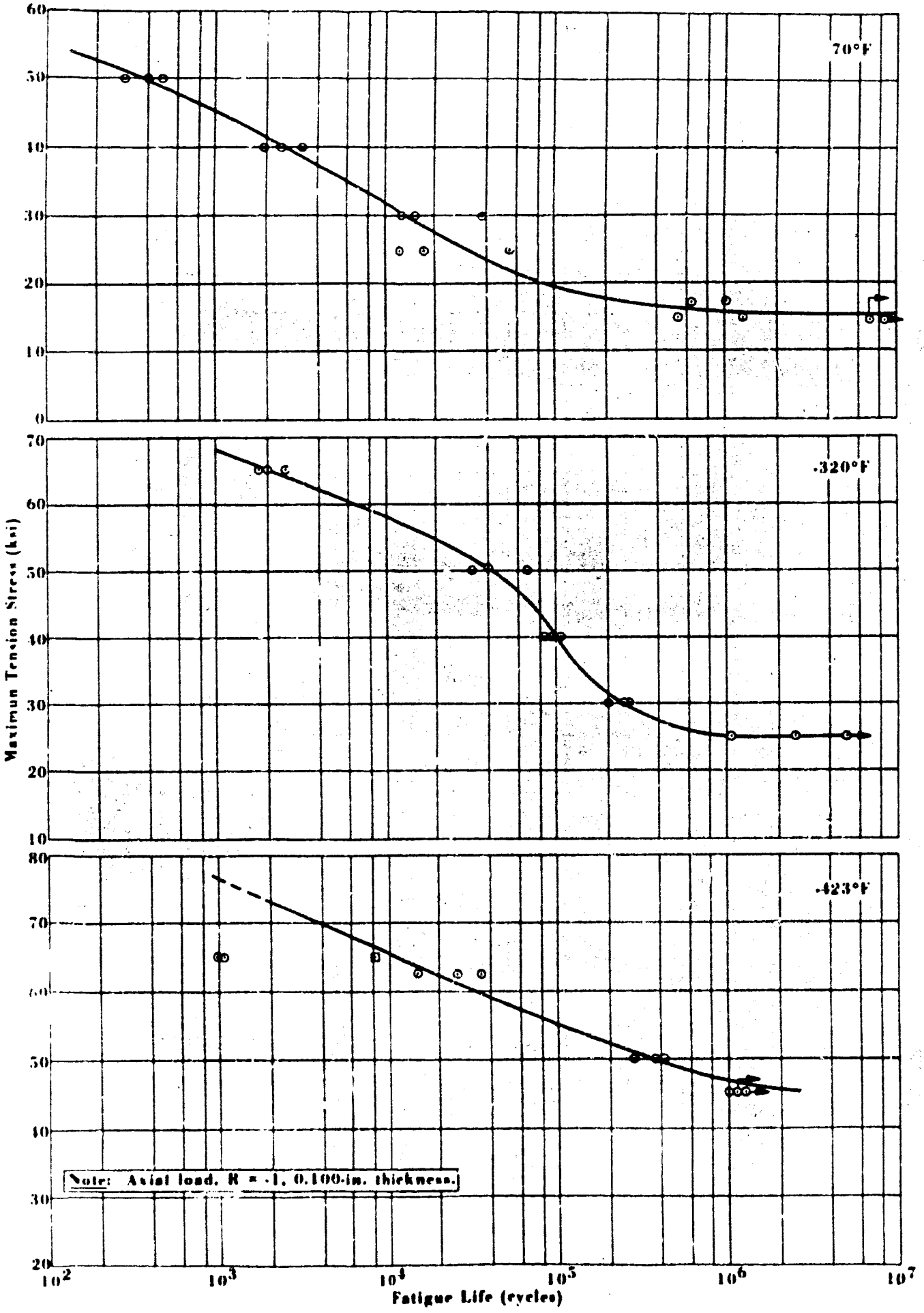

Fig. 28 Fatigue Properties of Unnotched 2014-T6 Aluminum Alloy

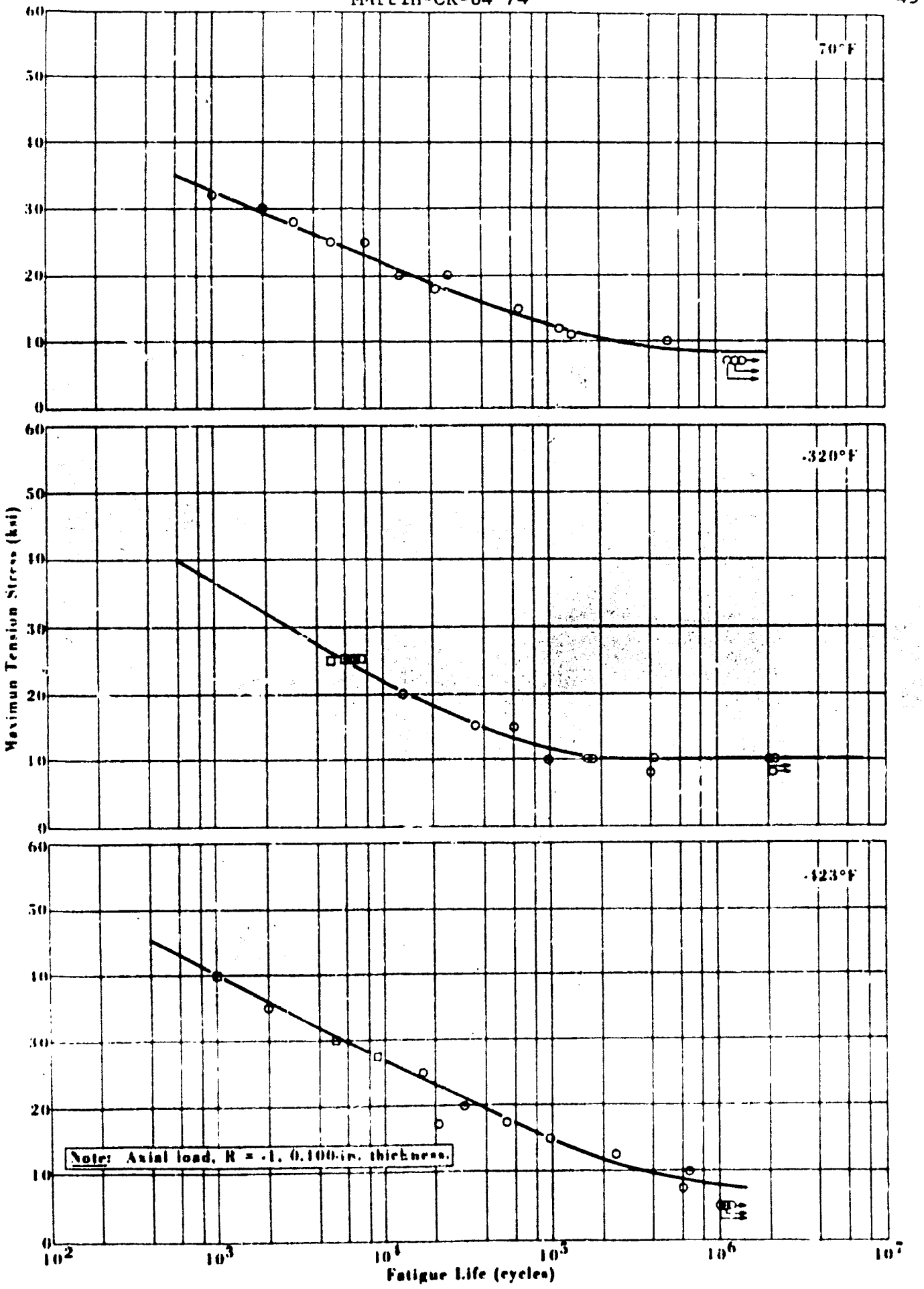

Fig. 29 Fatigue Properties of Notched 2014-T6 Aluminum Alloy

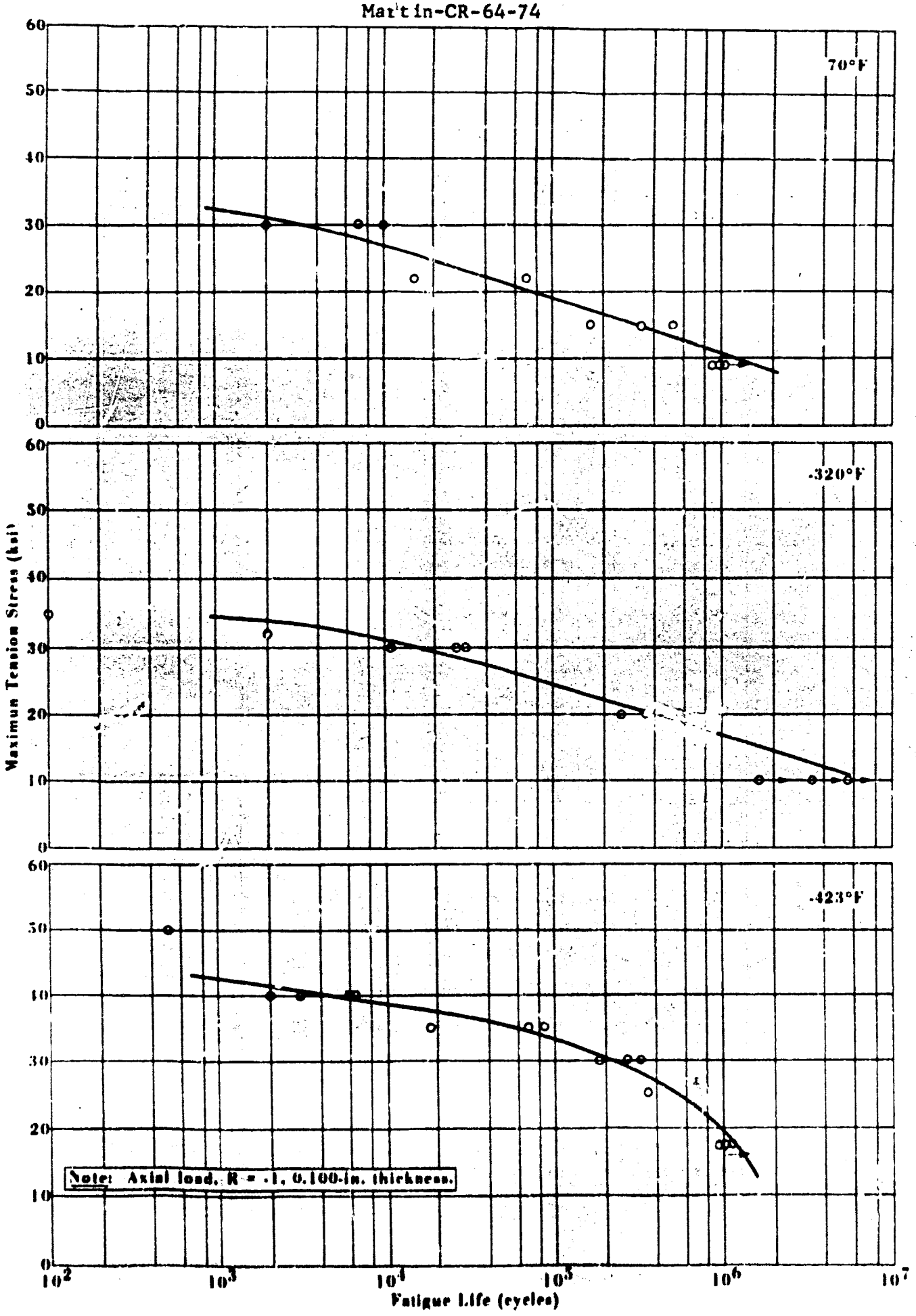

Fig. 30 Fatigue Properties of Welded 2014-T6 Aluminum Alloy

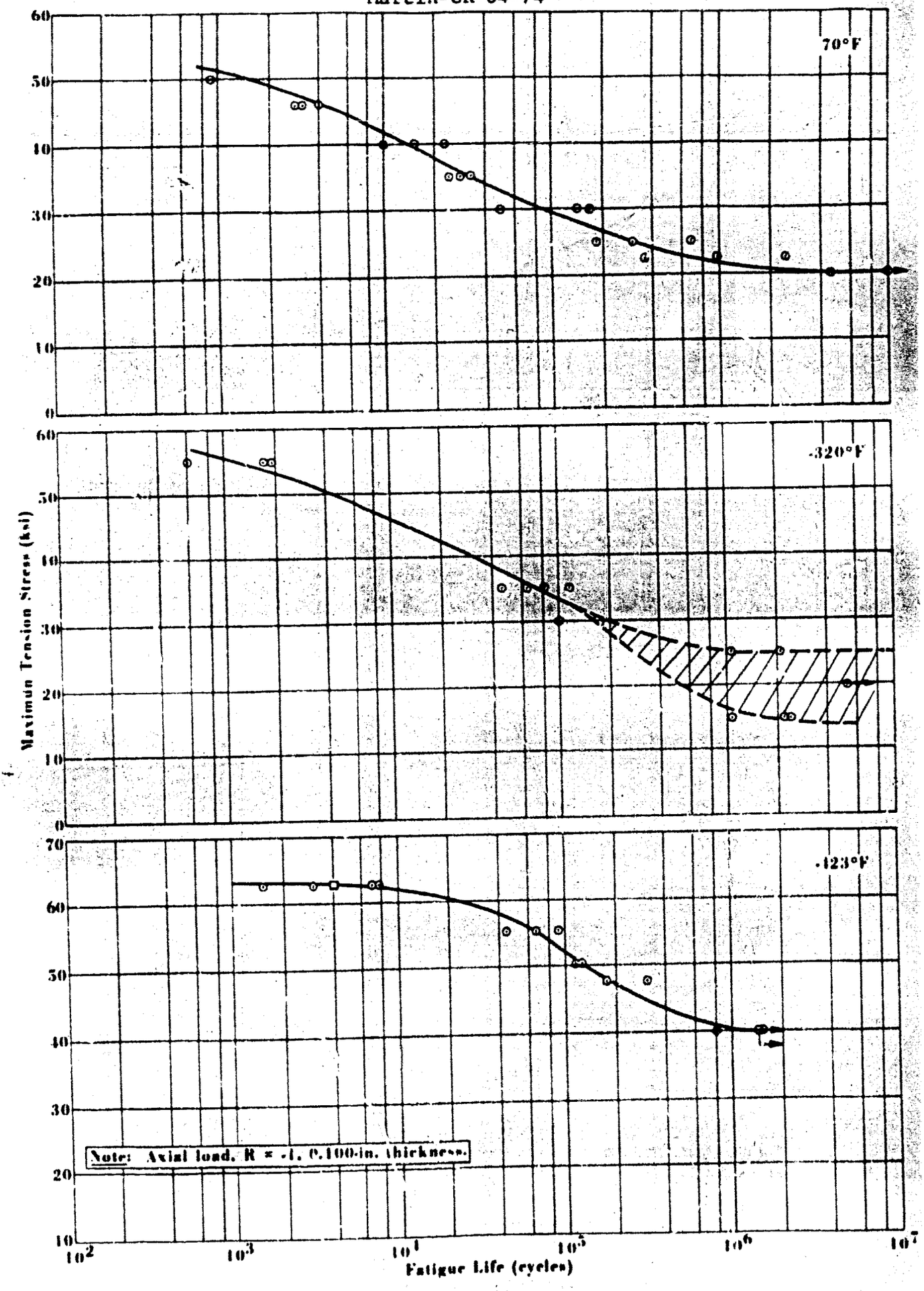

Fig. 31 Fatigue Properties of Unnotched 2219-T87 Aluminum Alloy

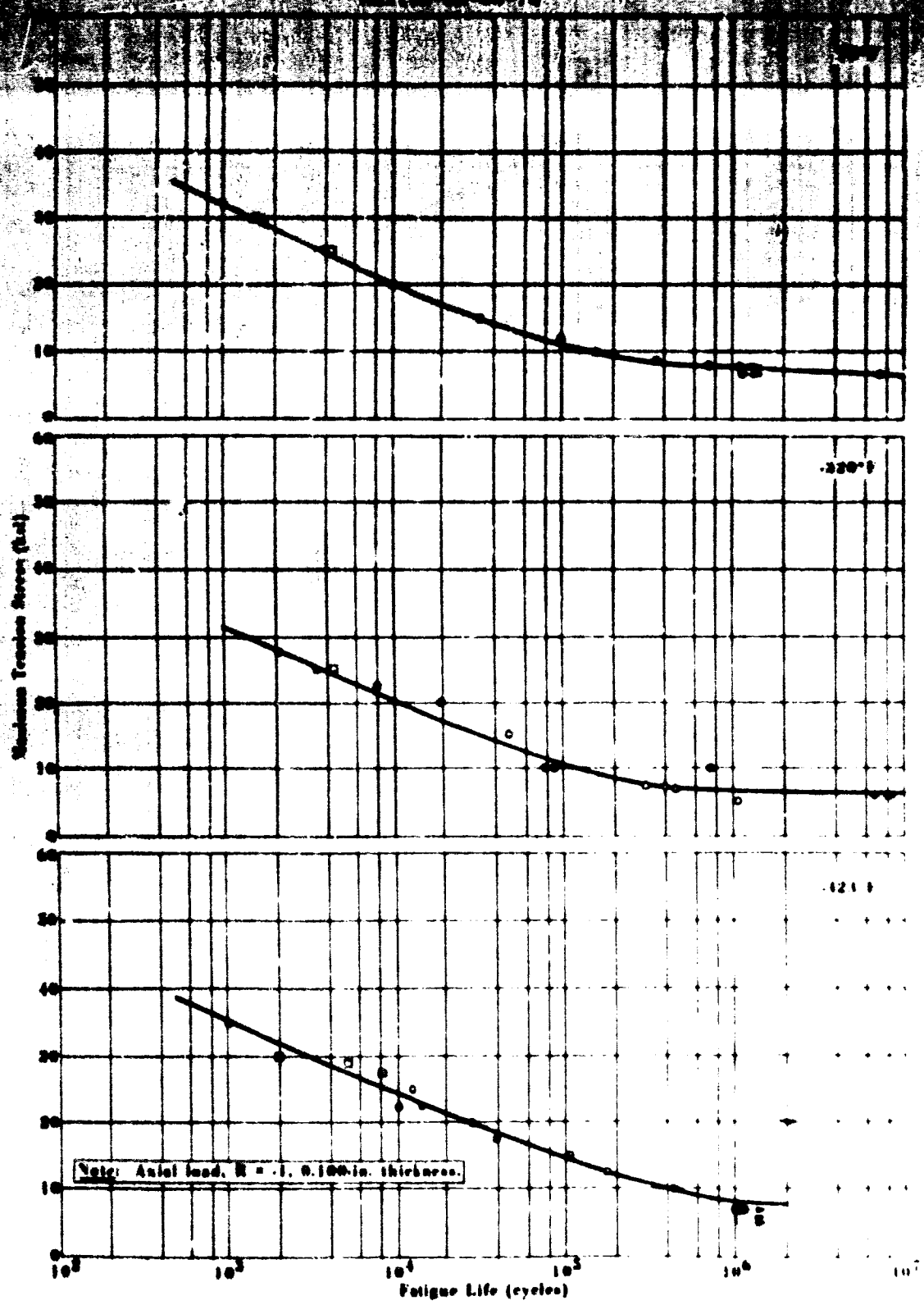

Fig. 32 Fatigue Properties of Notched 2219-T87 Aluminum Alloy

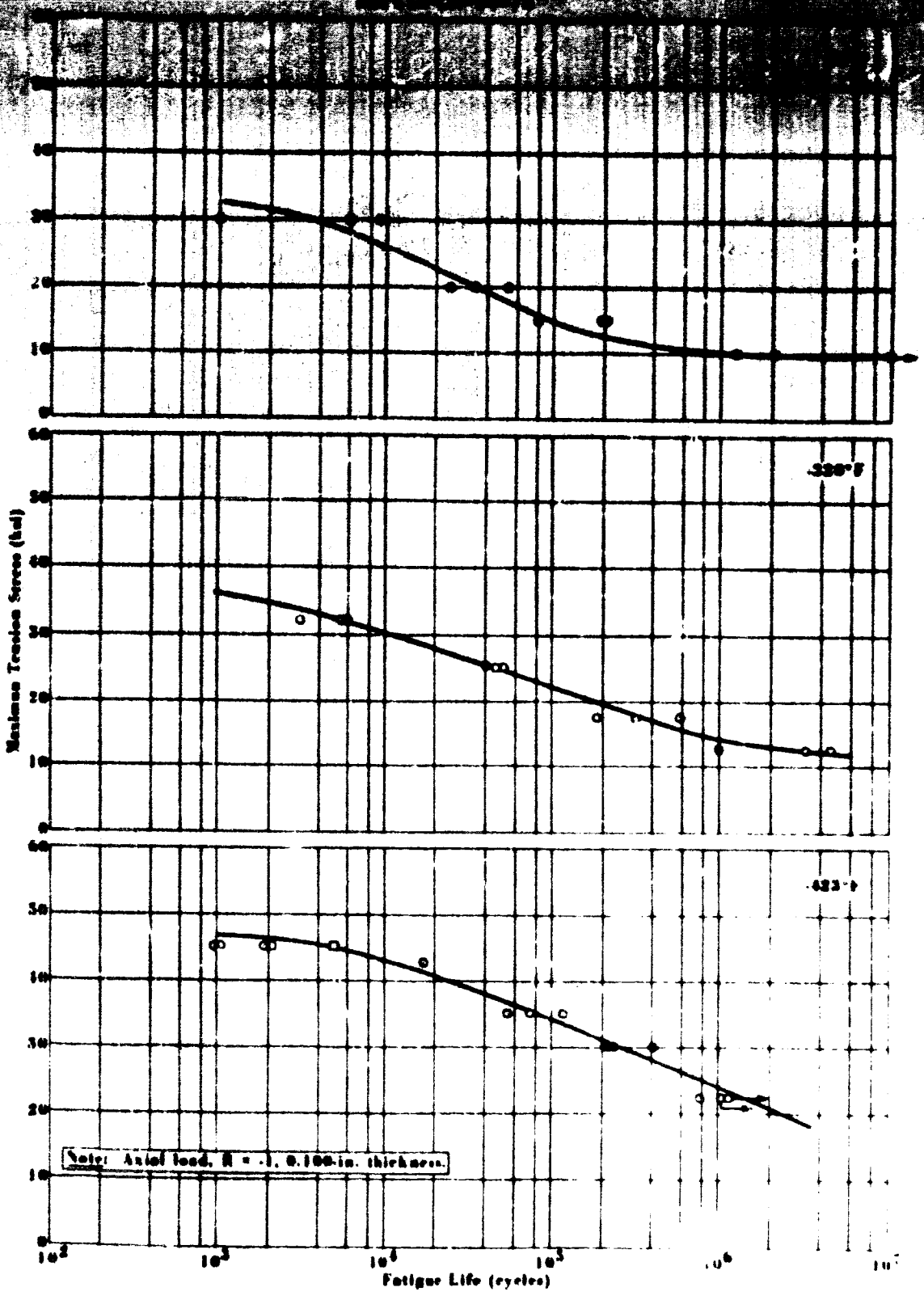

Fig. 33 Fatigue Properties of Welded 2219-T87 Aluminum Alloy

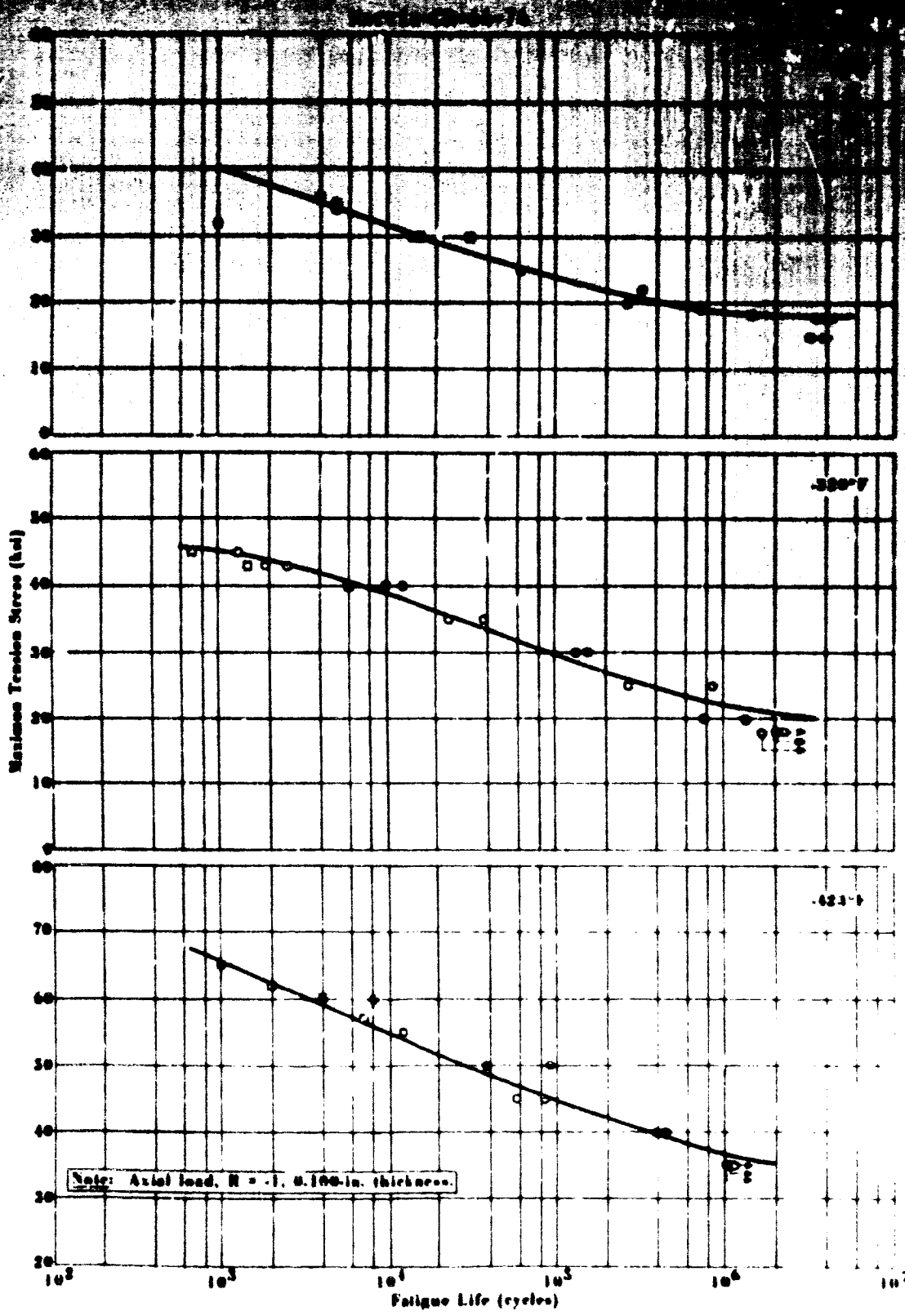

Fig. 34 Fatigue Properties of Unnotched 2219-T62 Aluminum Alloy

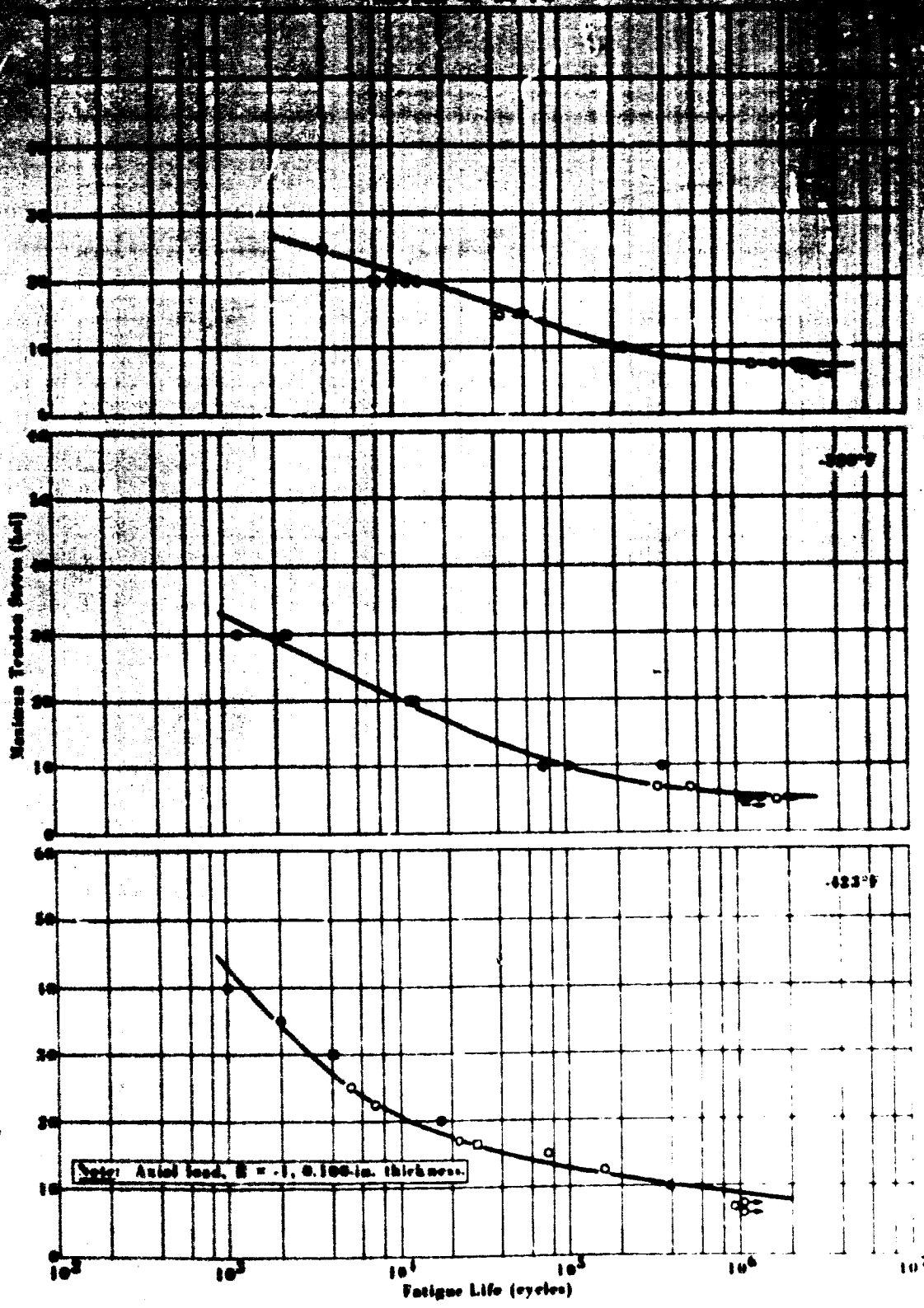

Fig. 35 Fatigue Properties of Notched 2219-T62 Aluminum Alloy

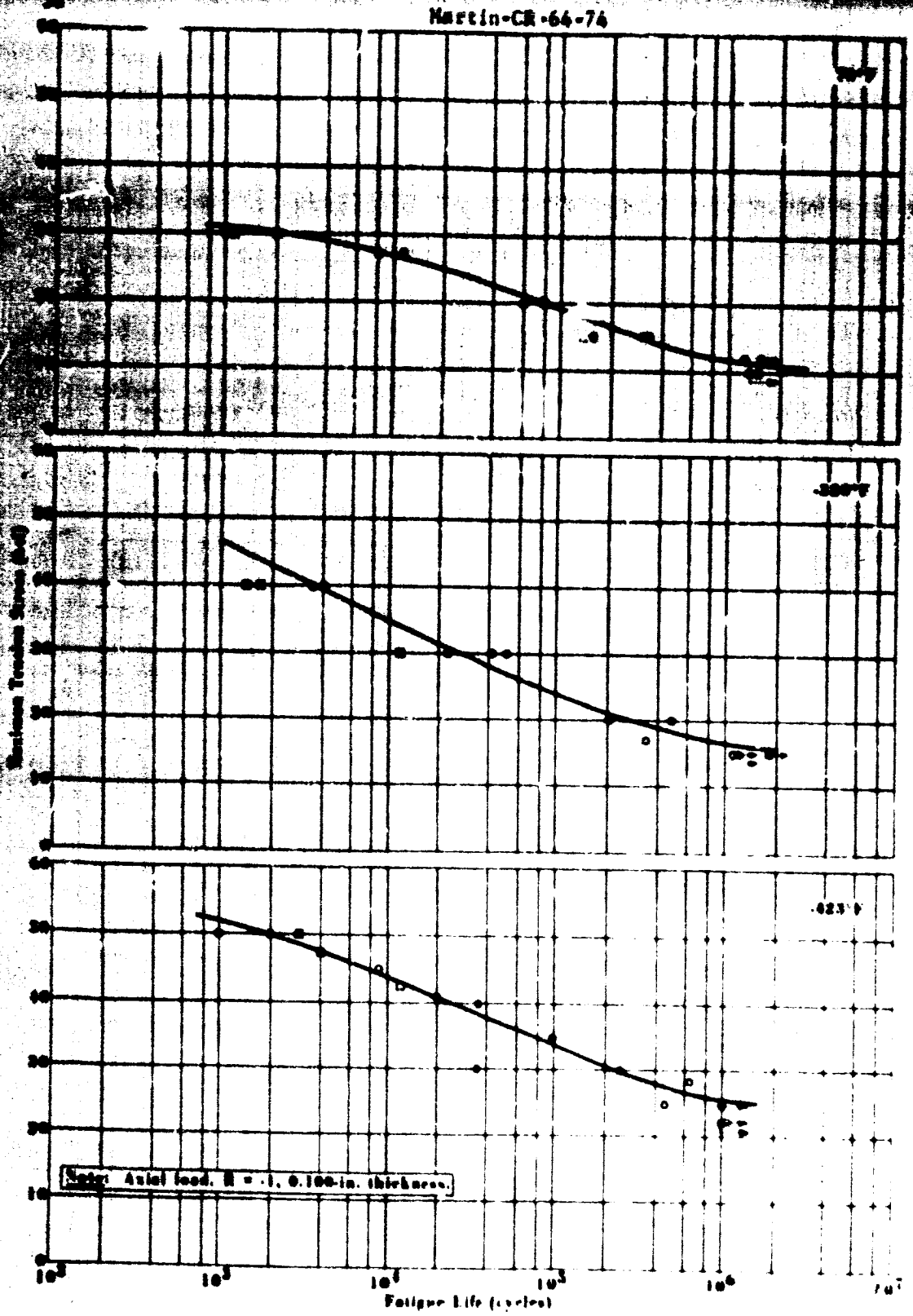

Fig. 36 Fatigue Properties of Welded 2219-T62 Aluminum Alloy

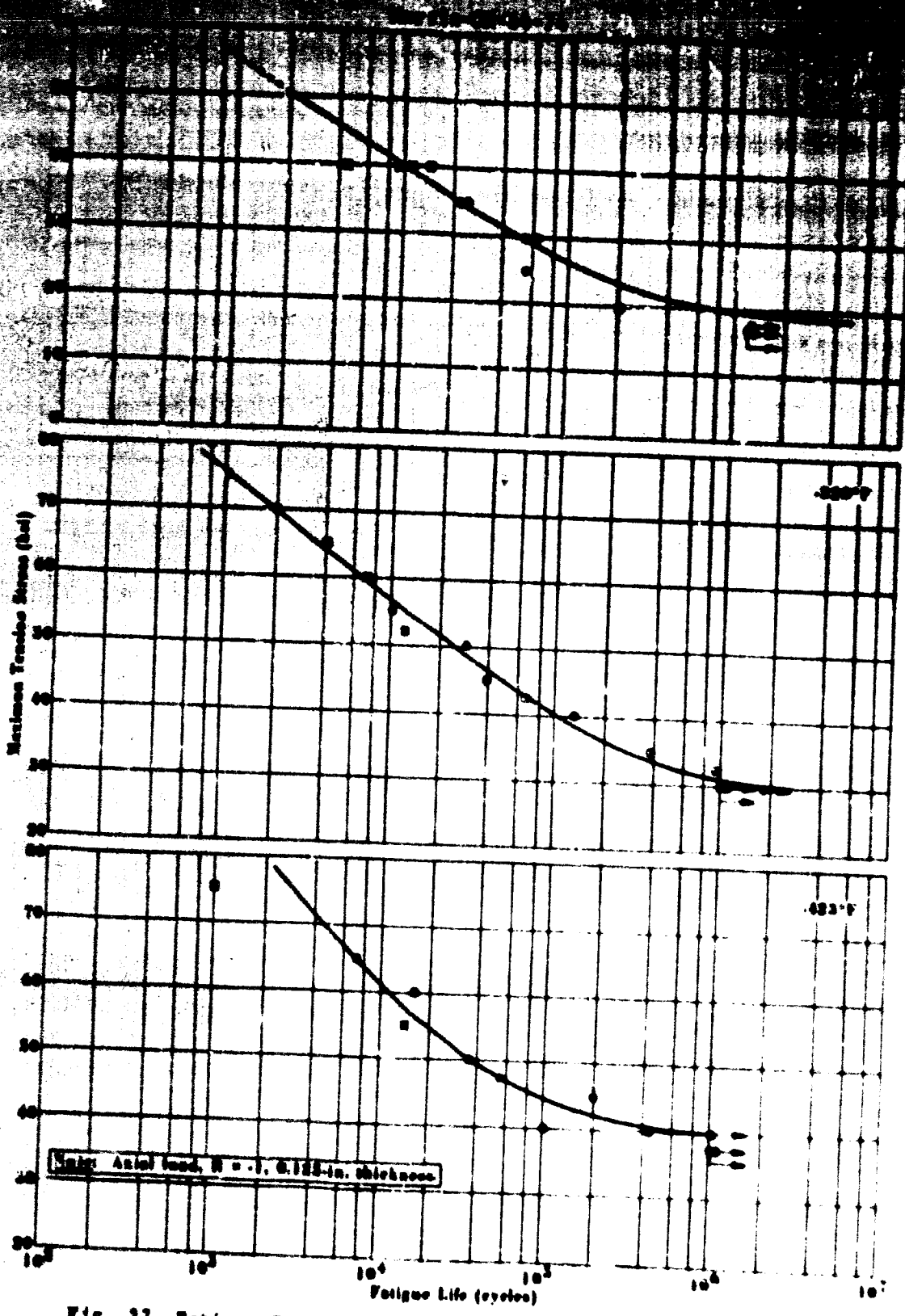

Fig. 37 Fatigue Properties of Unnotched 7039-T6 Aluminum Alloy

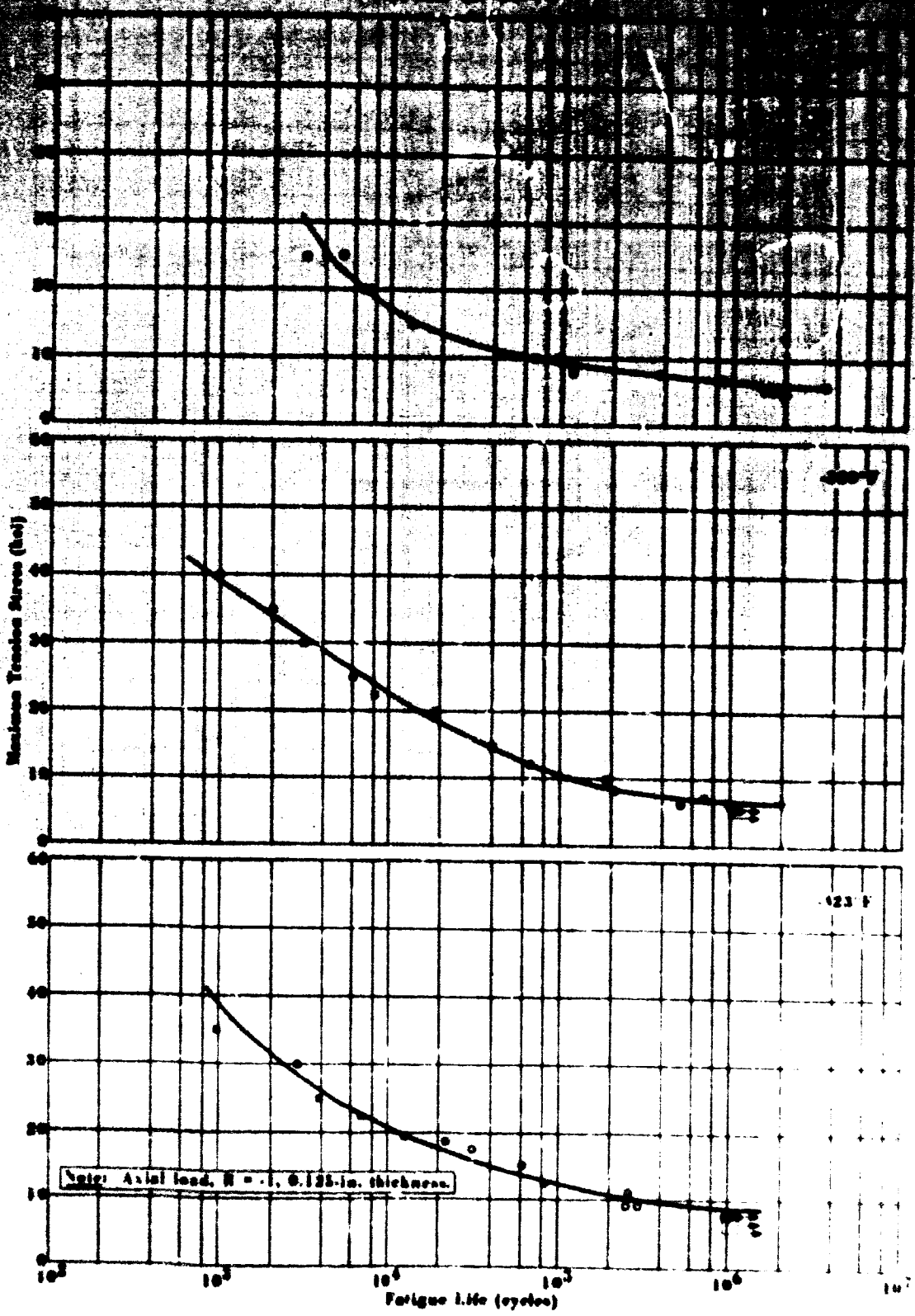

Fig. 38 Fatigue Properties of Notched 7039-T6 Aluminum Alloy

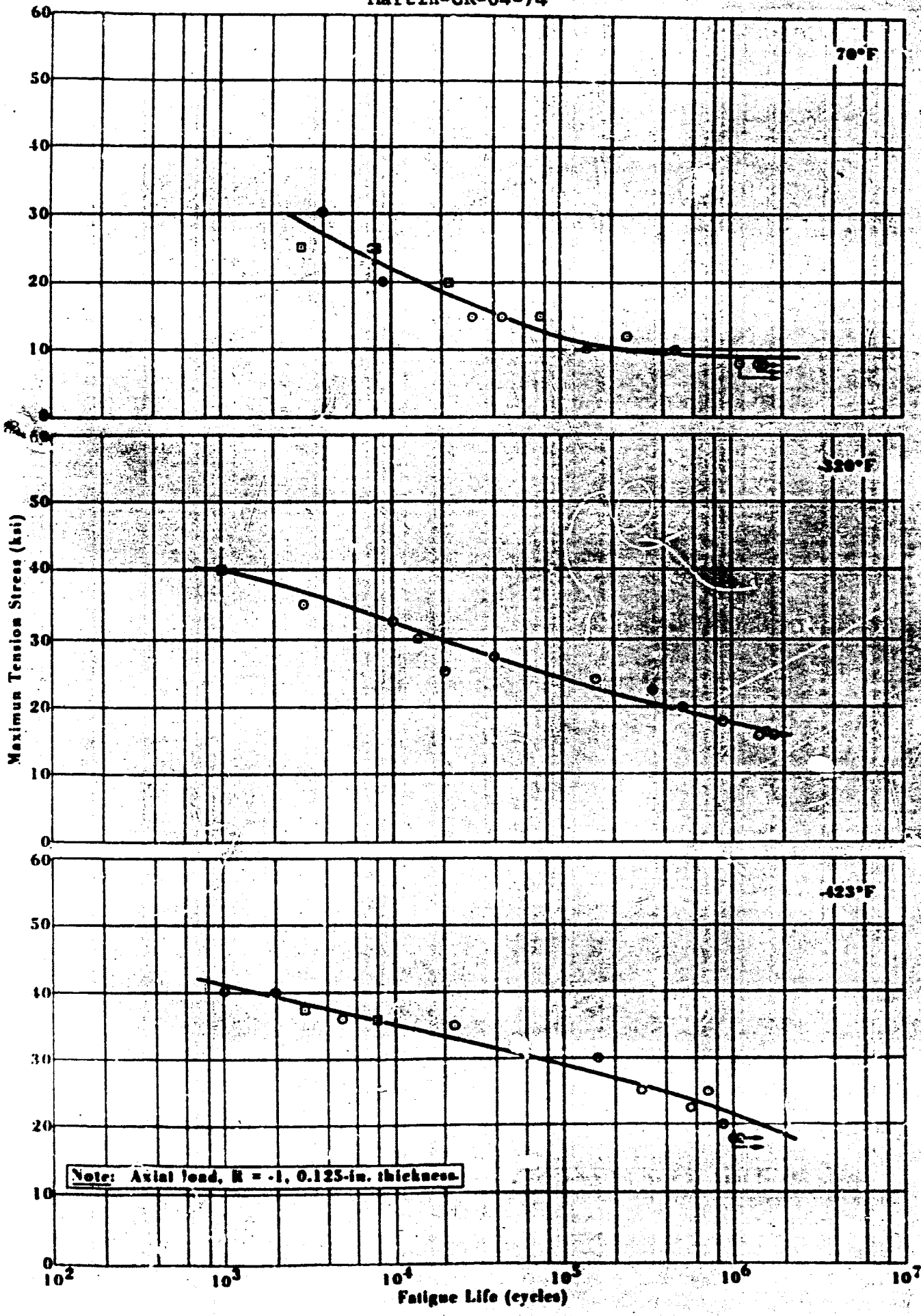

Fig. 39 Fatigue Properties of Welded 7039-T6 Aluminum Alloy

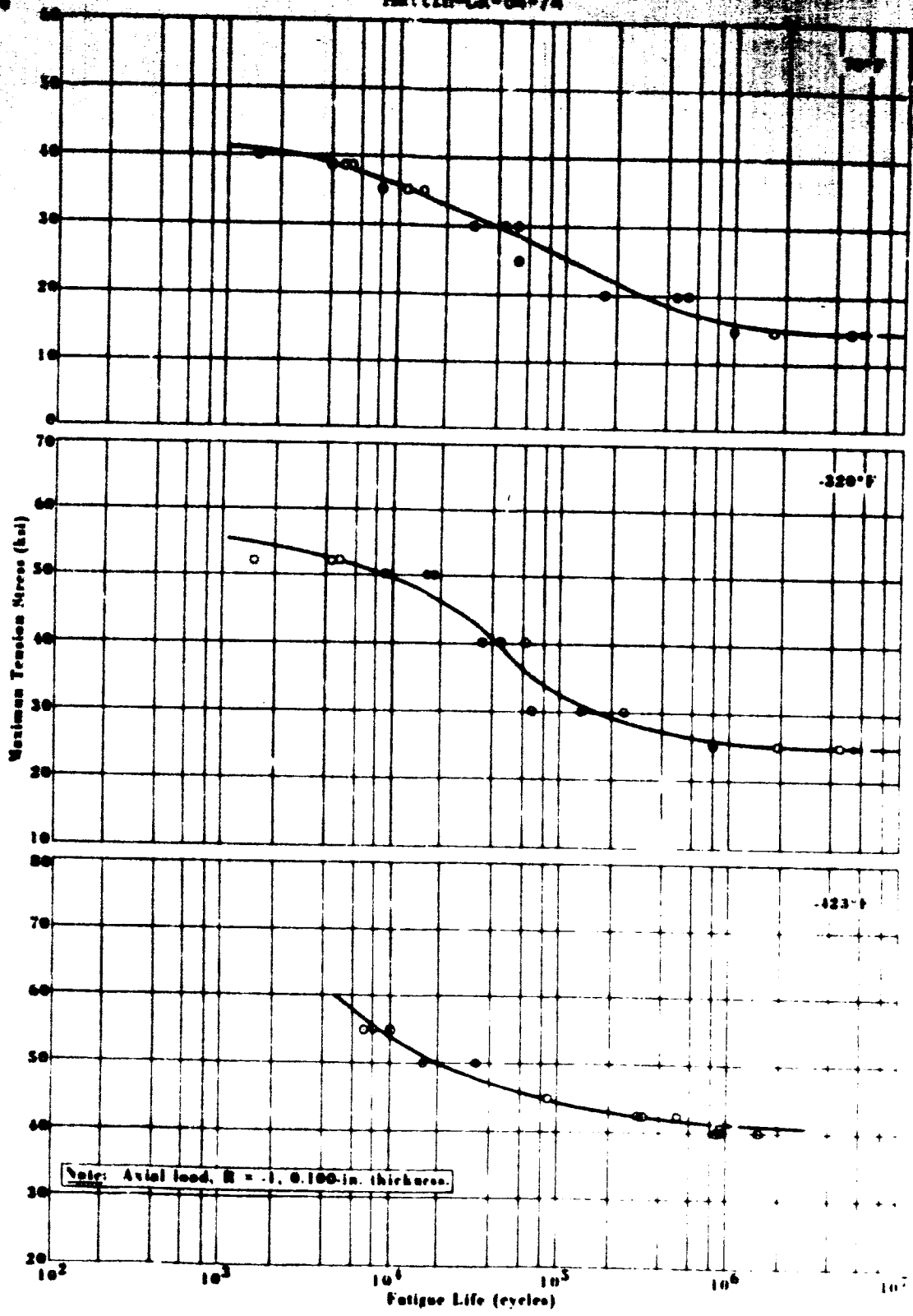

Fig. 40 Fatigue Properties of Unnotched 5456-H343 Aluminum Alloy

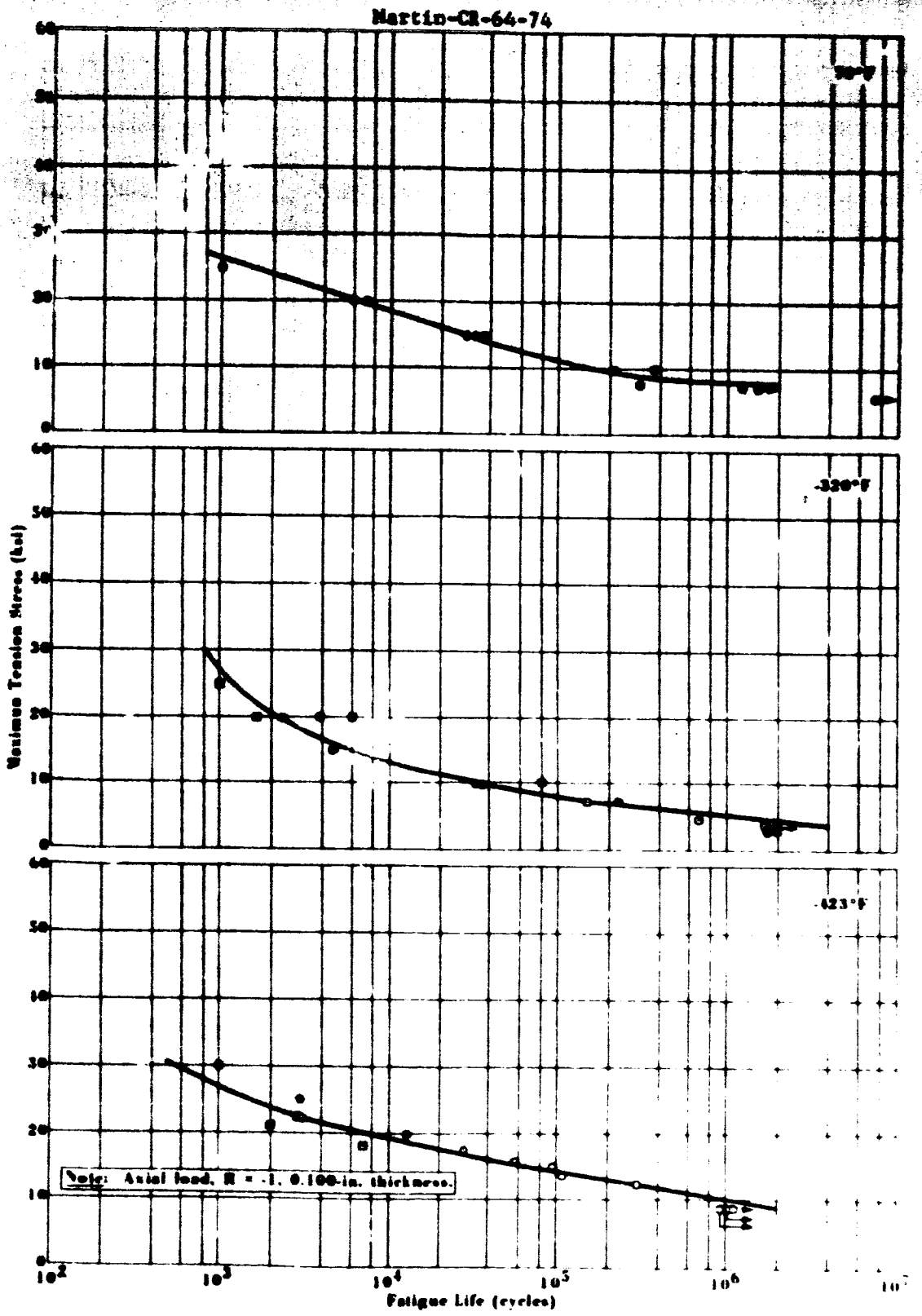

Fig. 41 Fatigue Properties of Notched 5456-H343 Aluminum Alloy

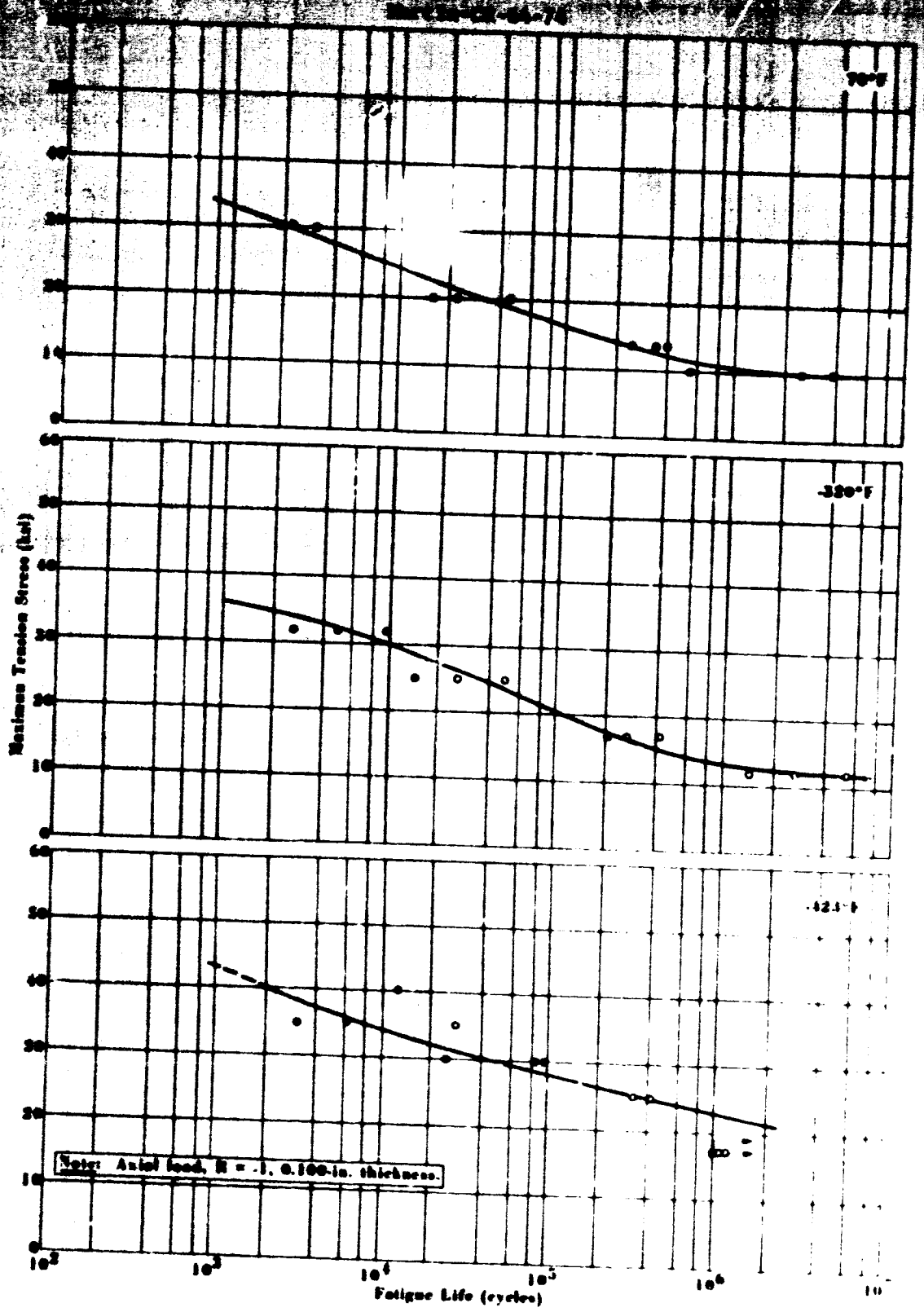

Fig. 42 Fatigue Properties of Welded 5456-H343 Aluminum Alloy

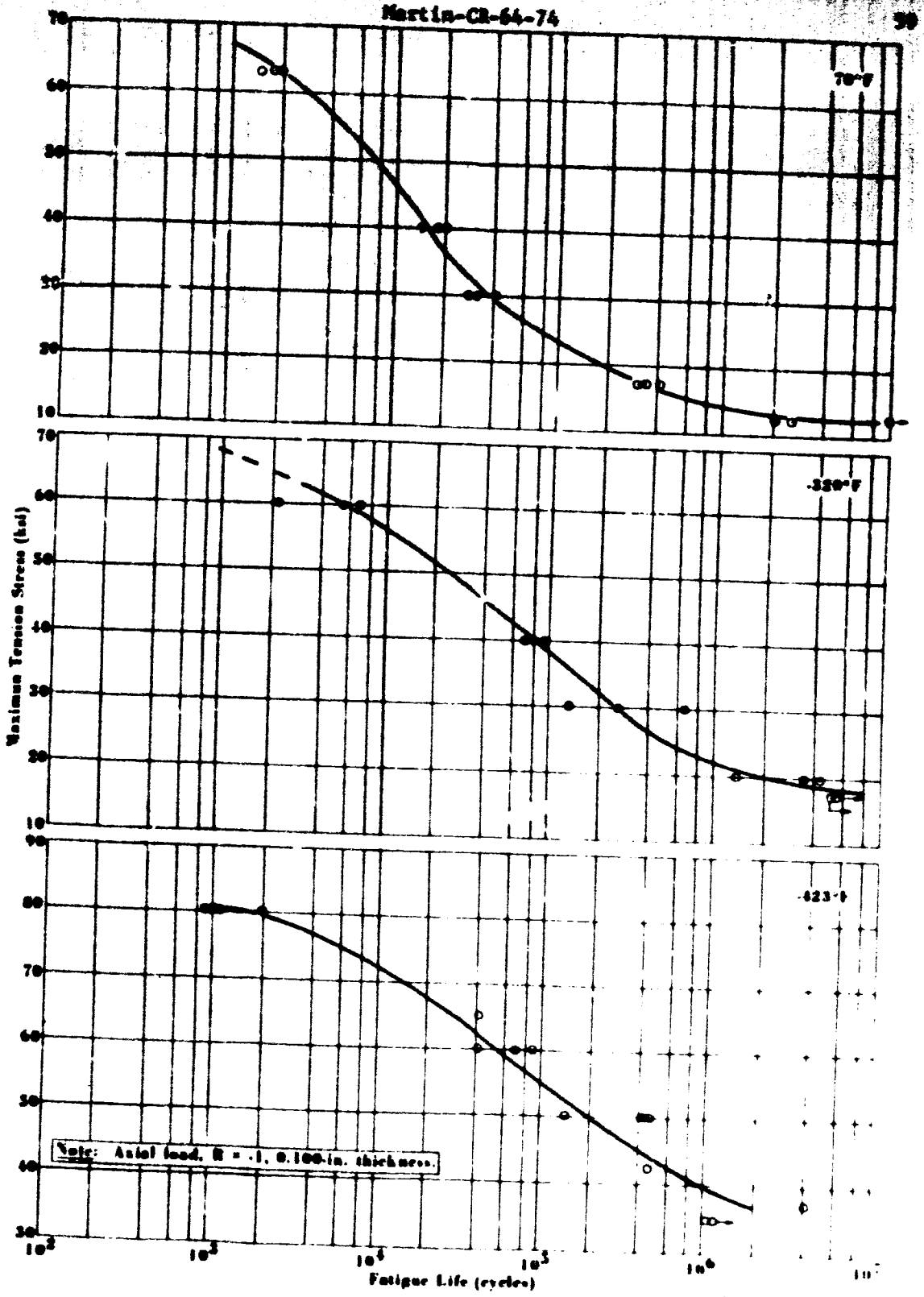

Fig. 43 Fatigue Properties of Unnotched 7075-T6 Aluminum Alloy

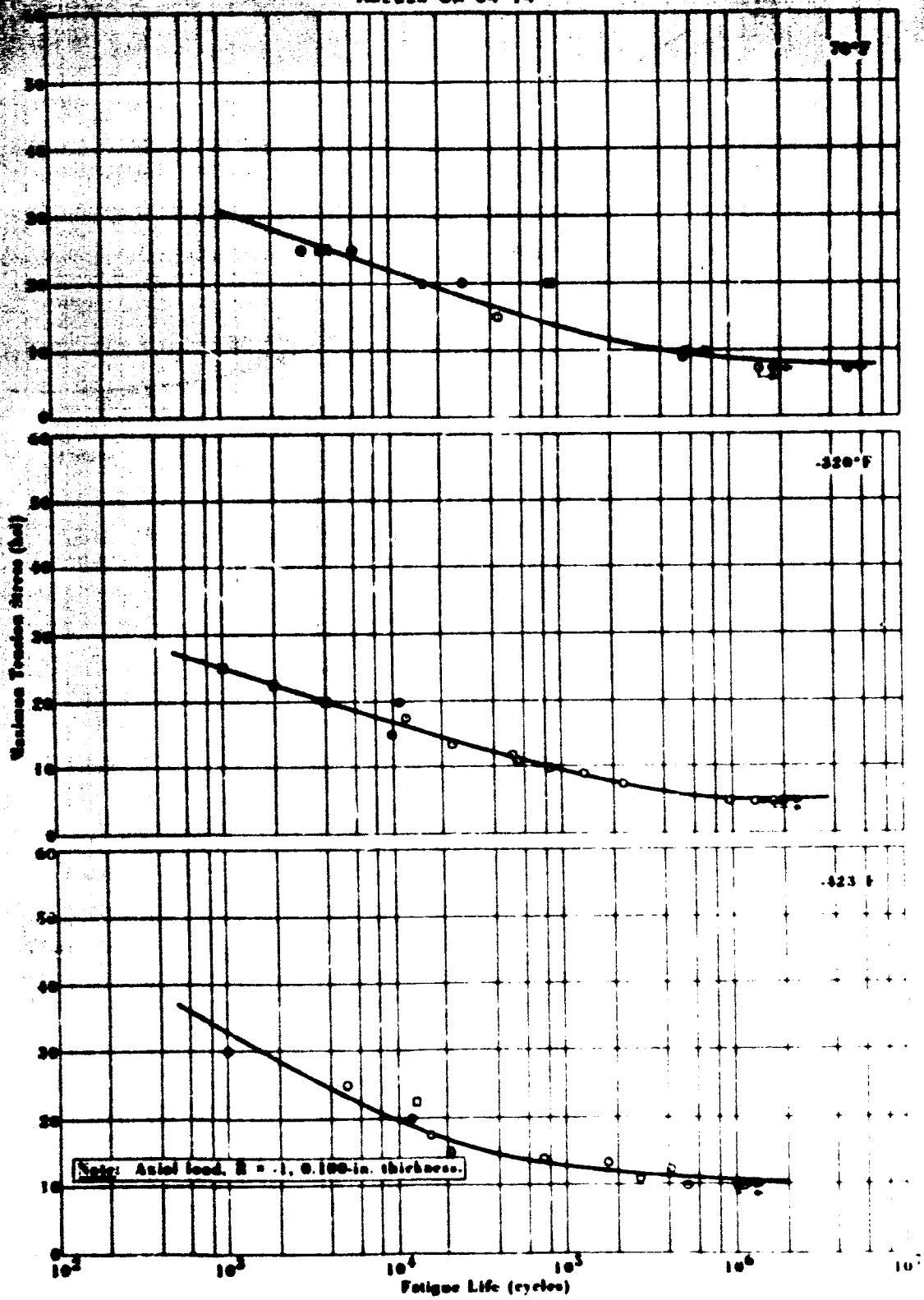

Fig. 44 Fatigue Properties of Notched 7075-T6 Aluminum Alloy

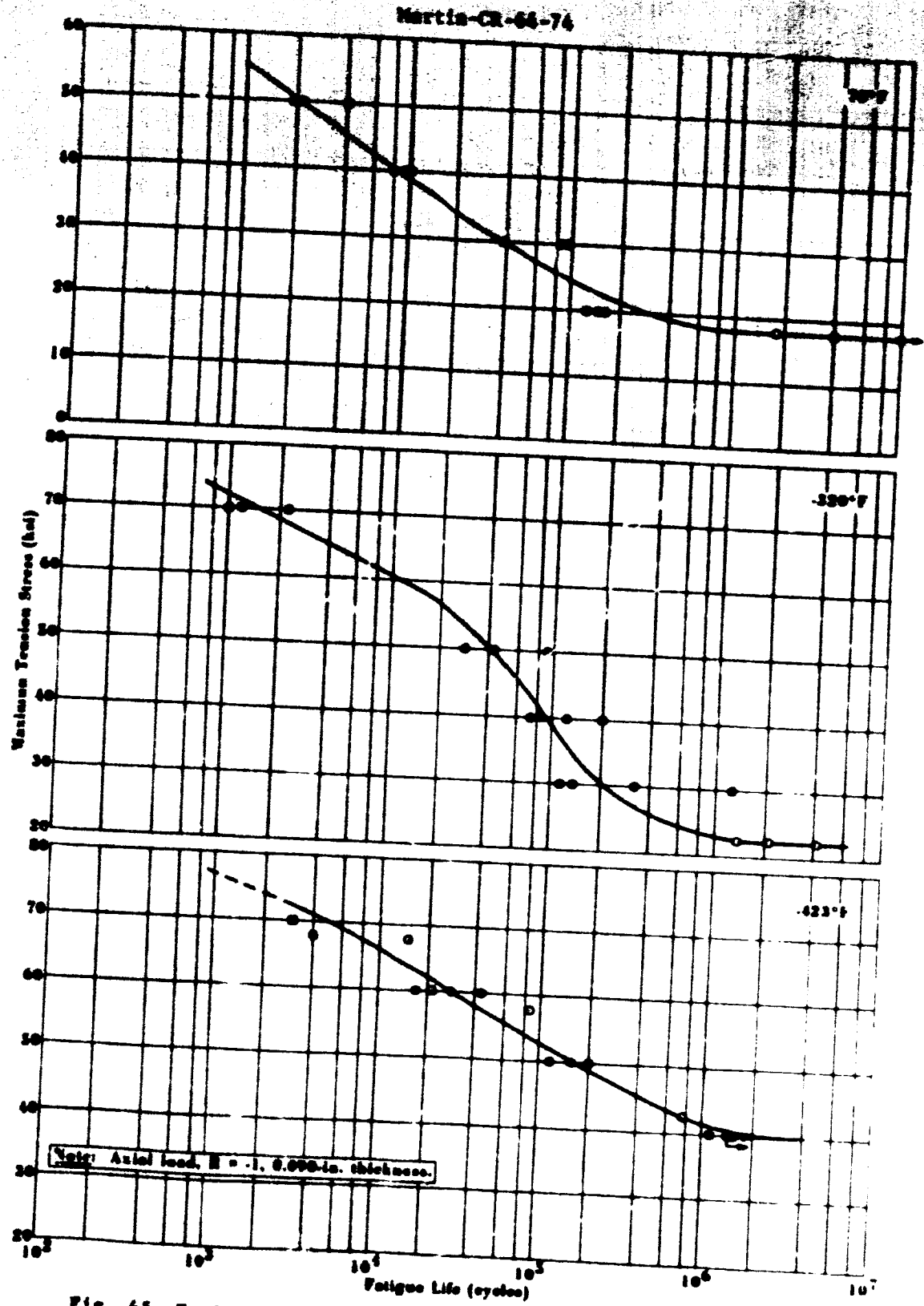

Fig. 45 Fatigue Properties of Unnotched 2020-T6 Aluminum Alloy

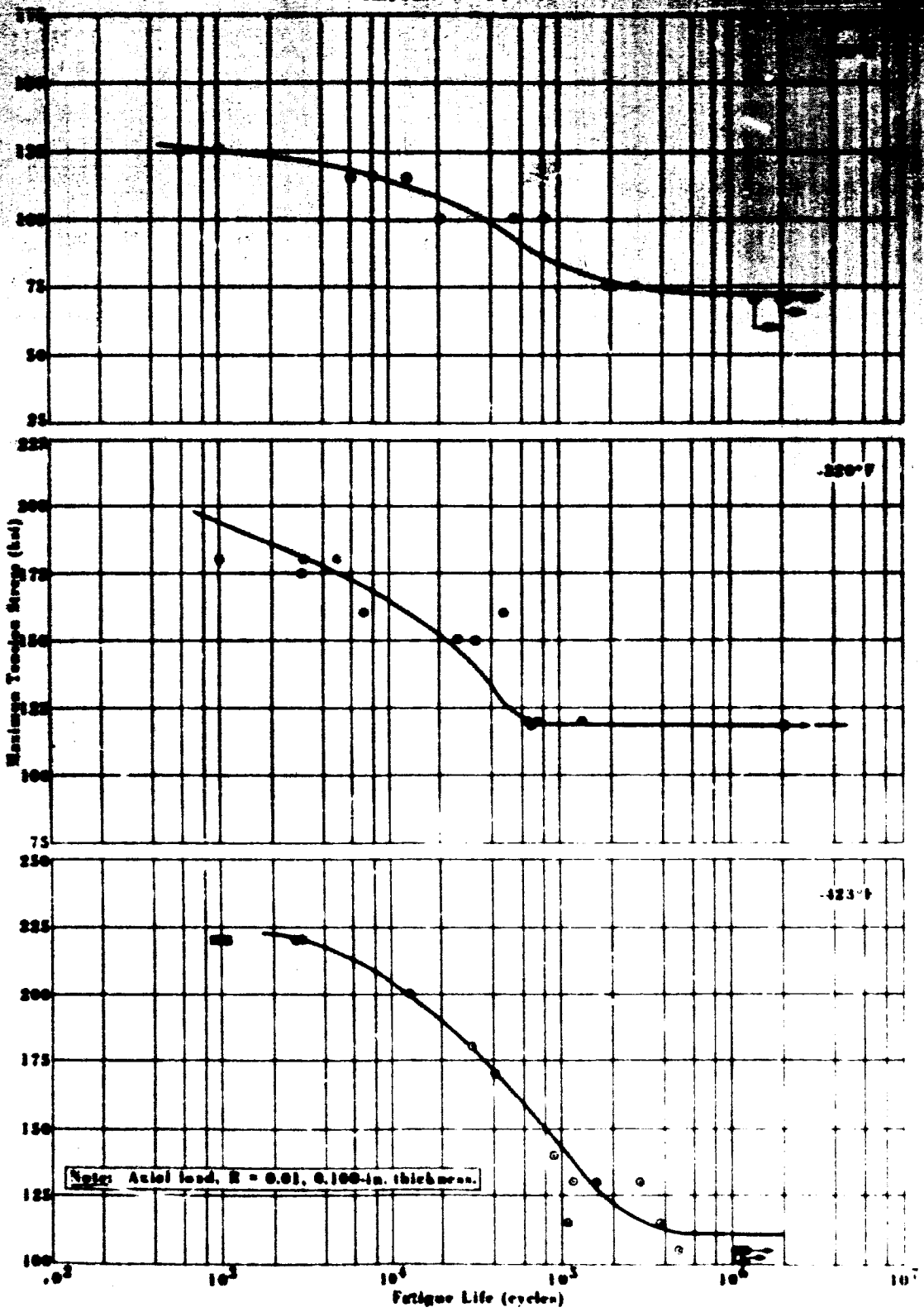

Fig. 46 Fatigue Properties of Unnotched 5Al-2.5Sn (Annealed) Titanium Alloy

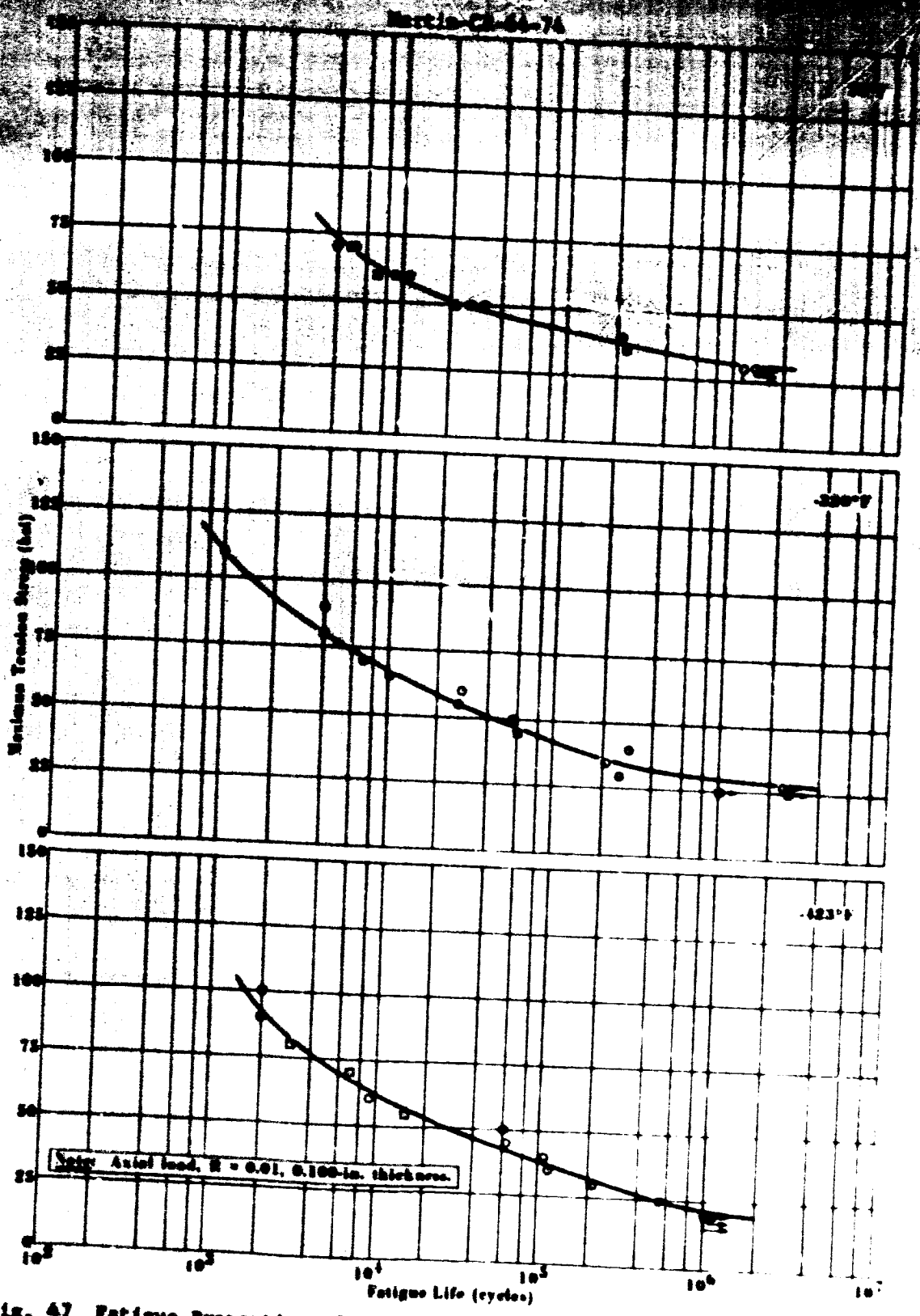

Fig. 47 Fatigue Properties of Notched 5Al-2.5Sn (Annealed) Titanium Alloy

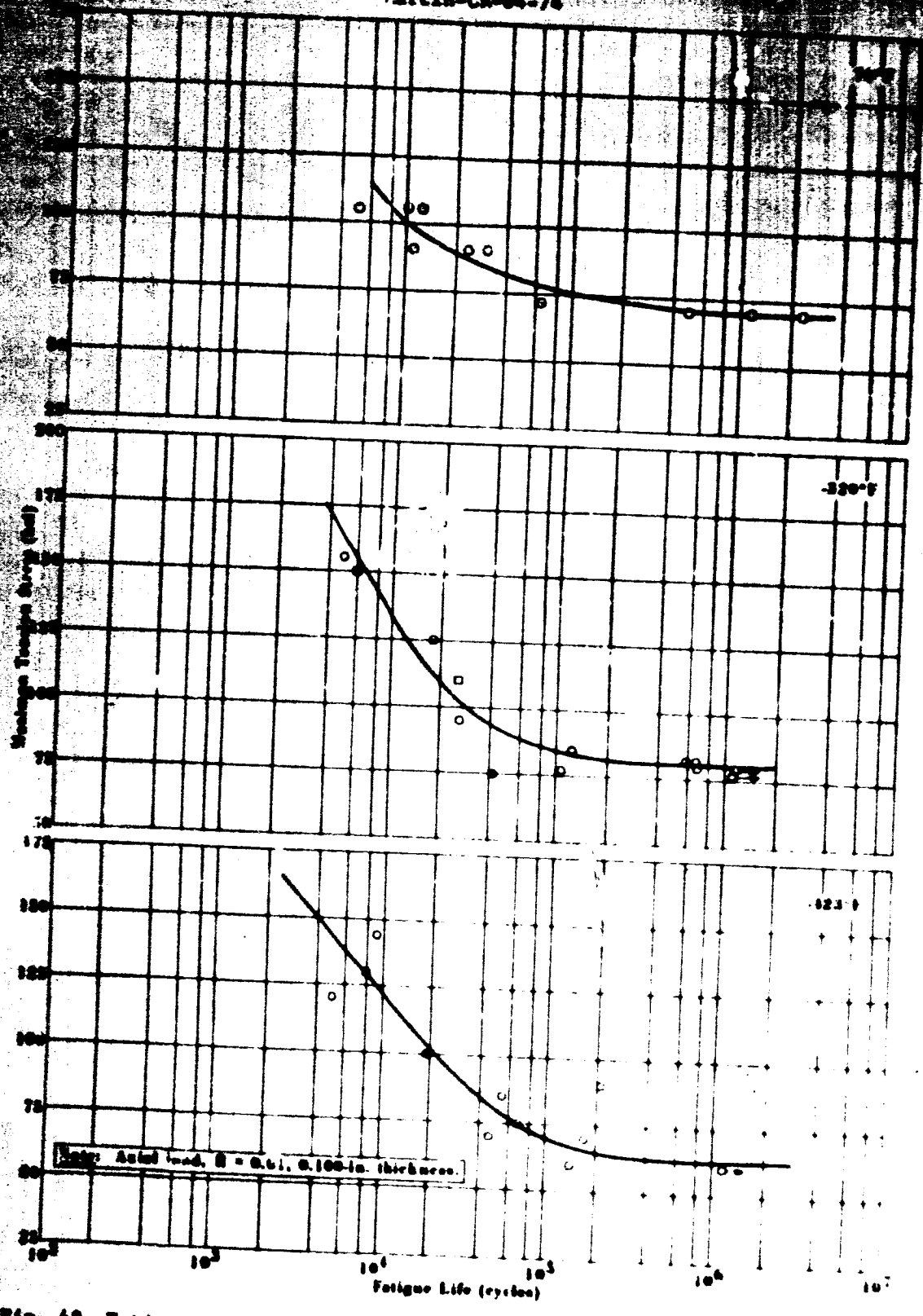

Fig. 48 Fatigue Properties of Welded 5Al-2.5Sn (Annealed) Titanium Alloy

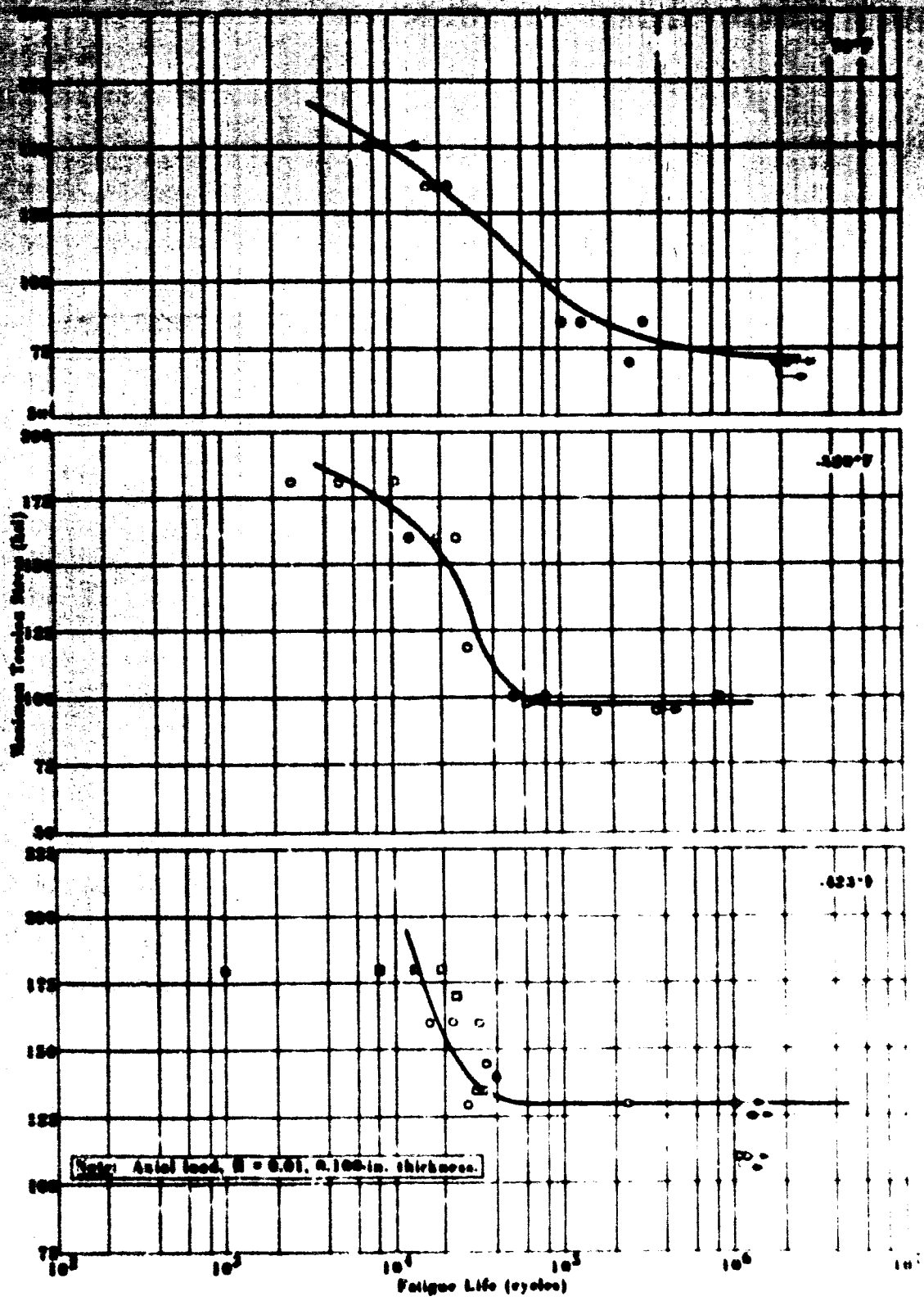

Fig. 49 Fatigue Properties of Unnotched 6Al-4V (Solution Treated and Aged) Titanium Alloy

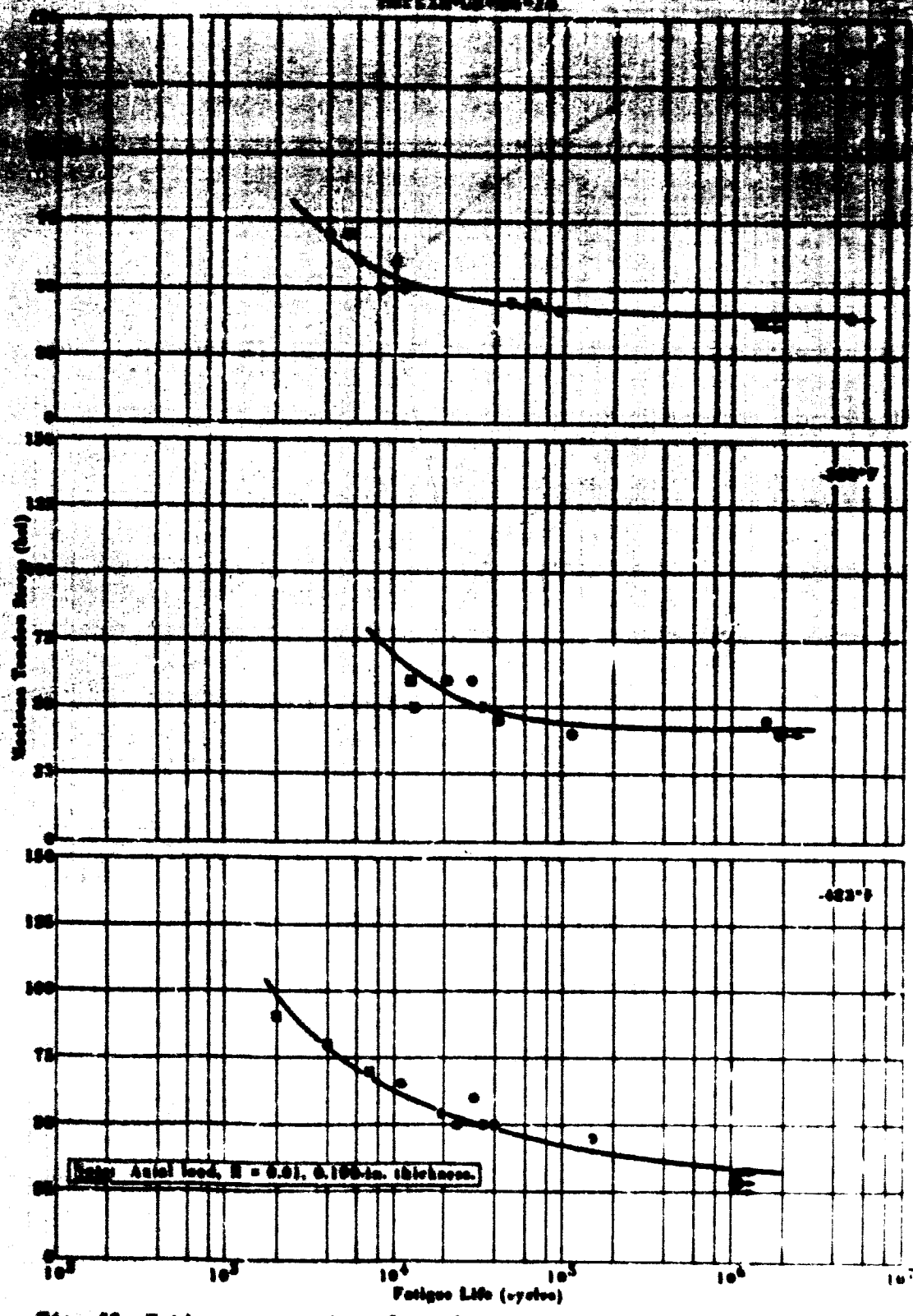

Fig. 30 Fatigue Properties of Notched 6Al-4V (Solution Treated and Aged) Titanium Alloy

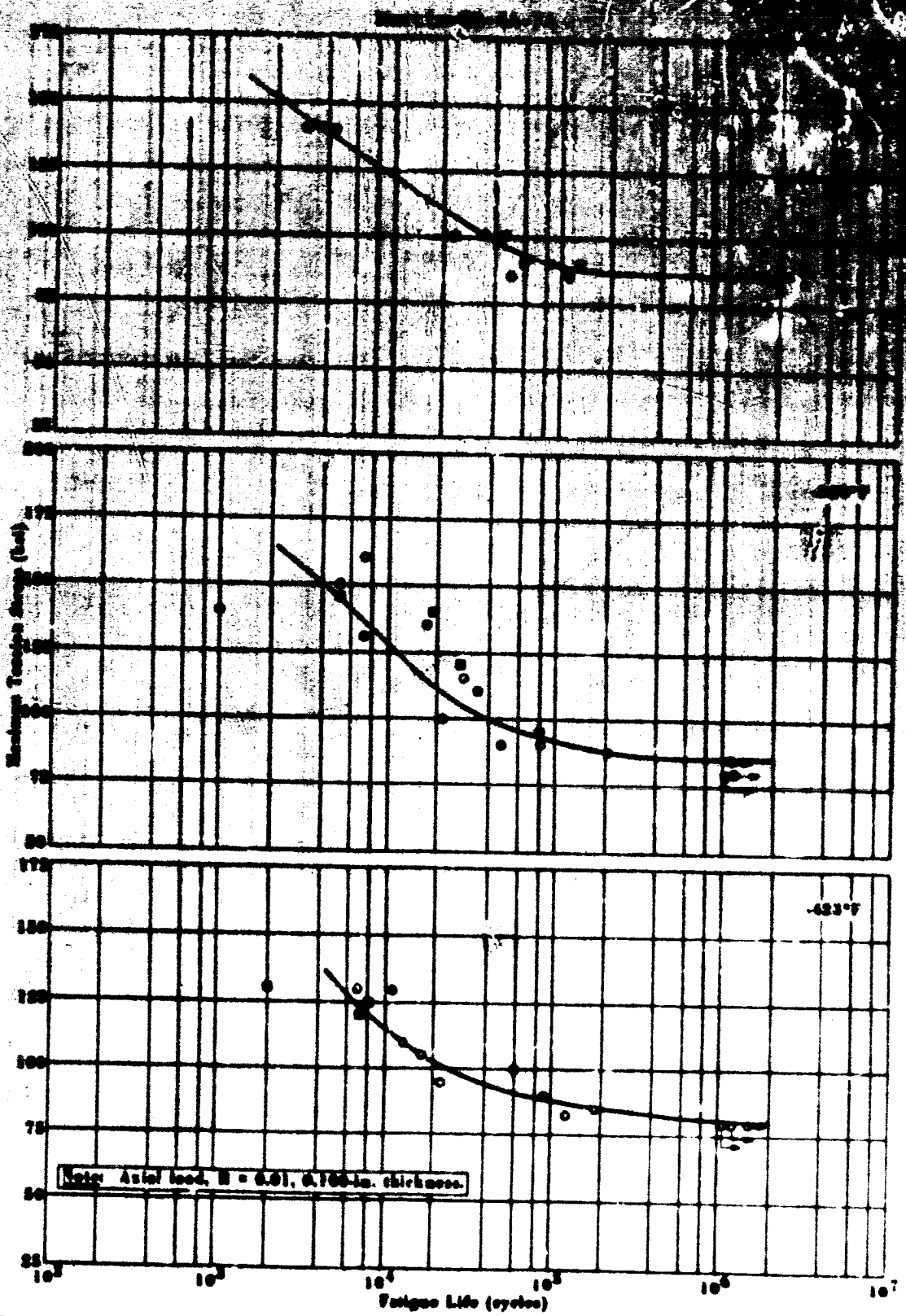

Fig. 51 Fatigue Properties of Welded 6Al-4V (Solution Treated and Aged) Titanium Alloy

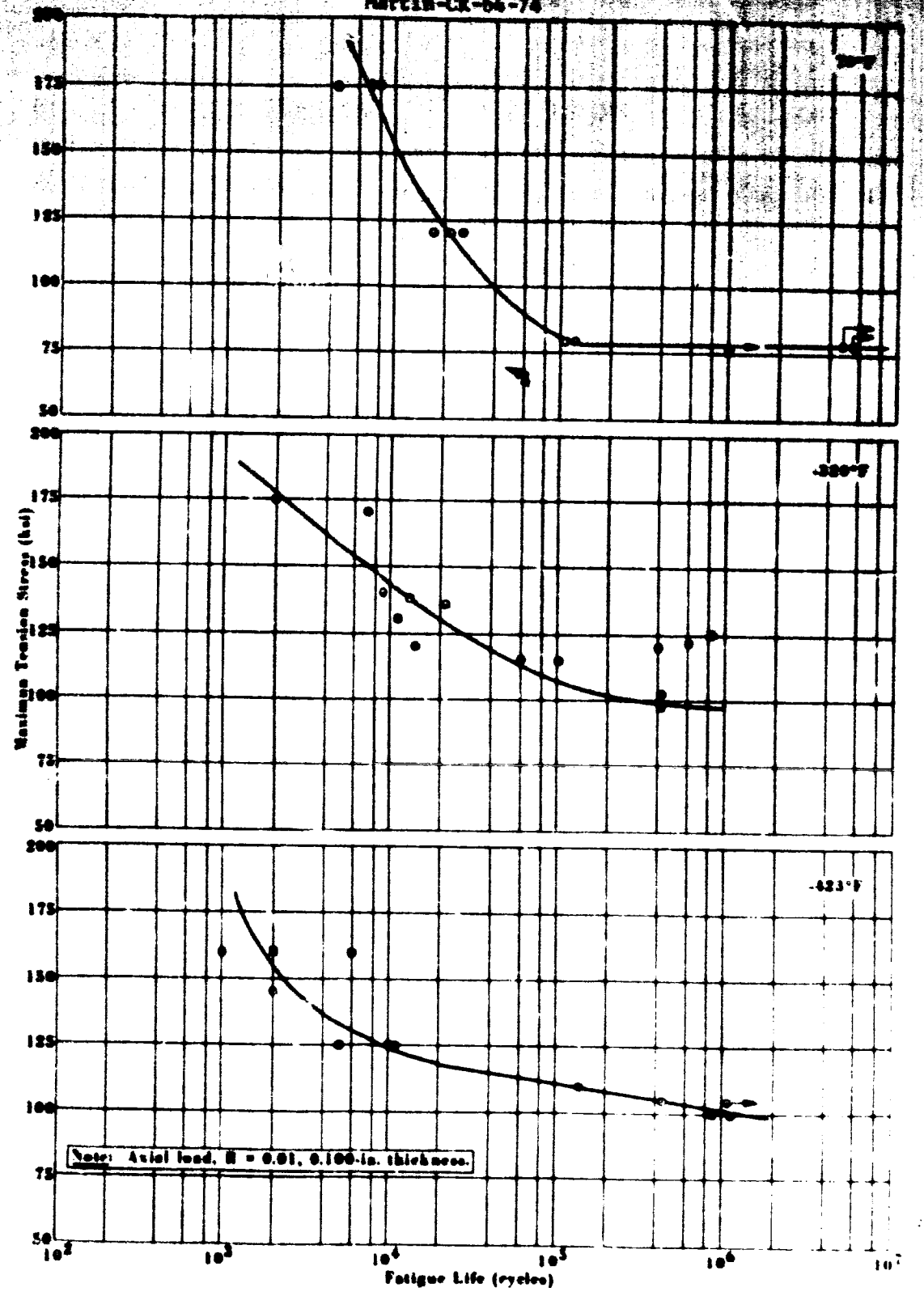

Fig. 52 Fatigue Properties of Unnotched 13V-11Cr-3Al (Solution Treated and Aged) Titanium Alloy

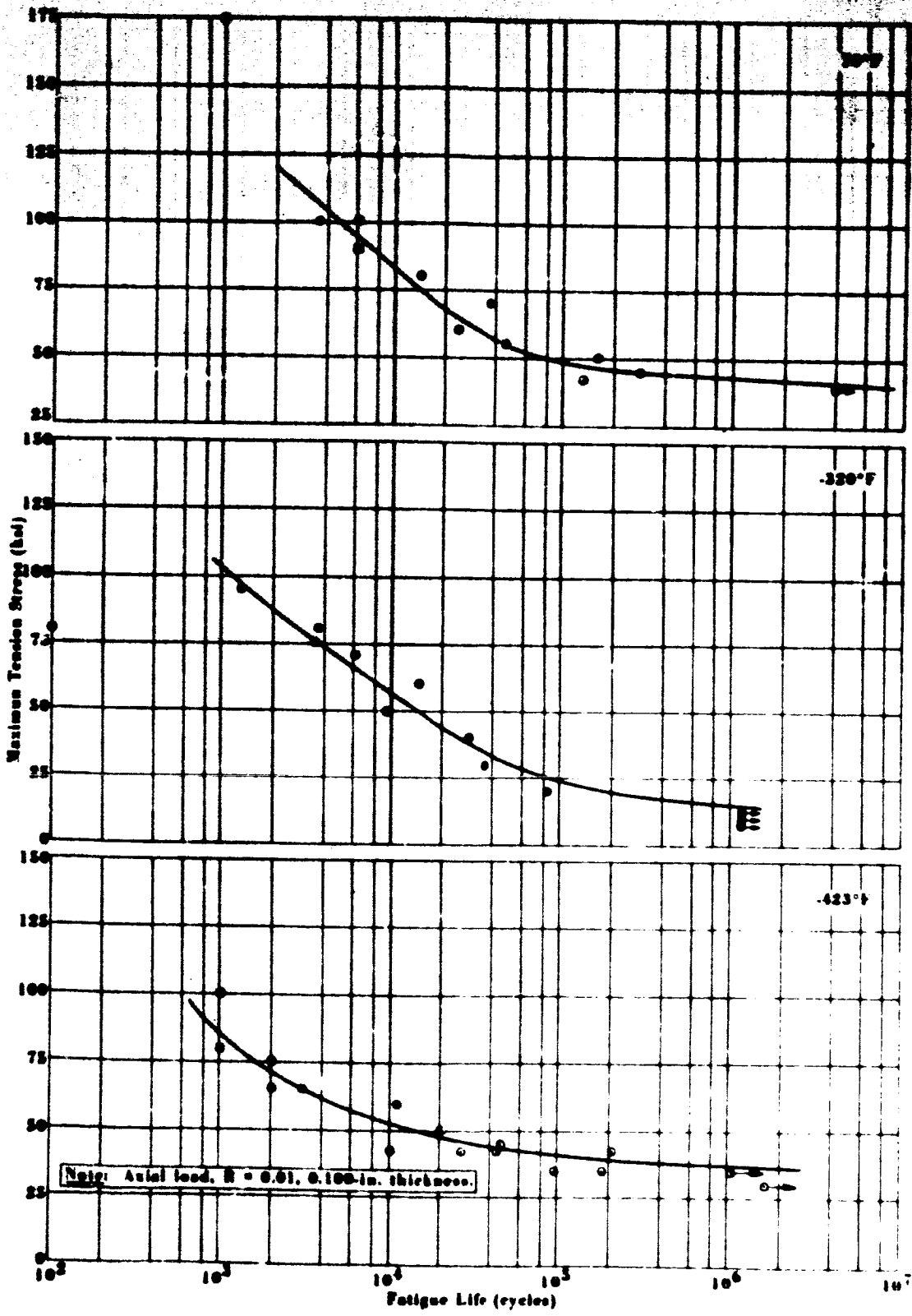

Fig. 53 Fatigue Properties of Welded 13V-11Cr-3Al (Solution Treated and Aged) Titanium Alloy

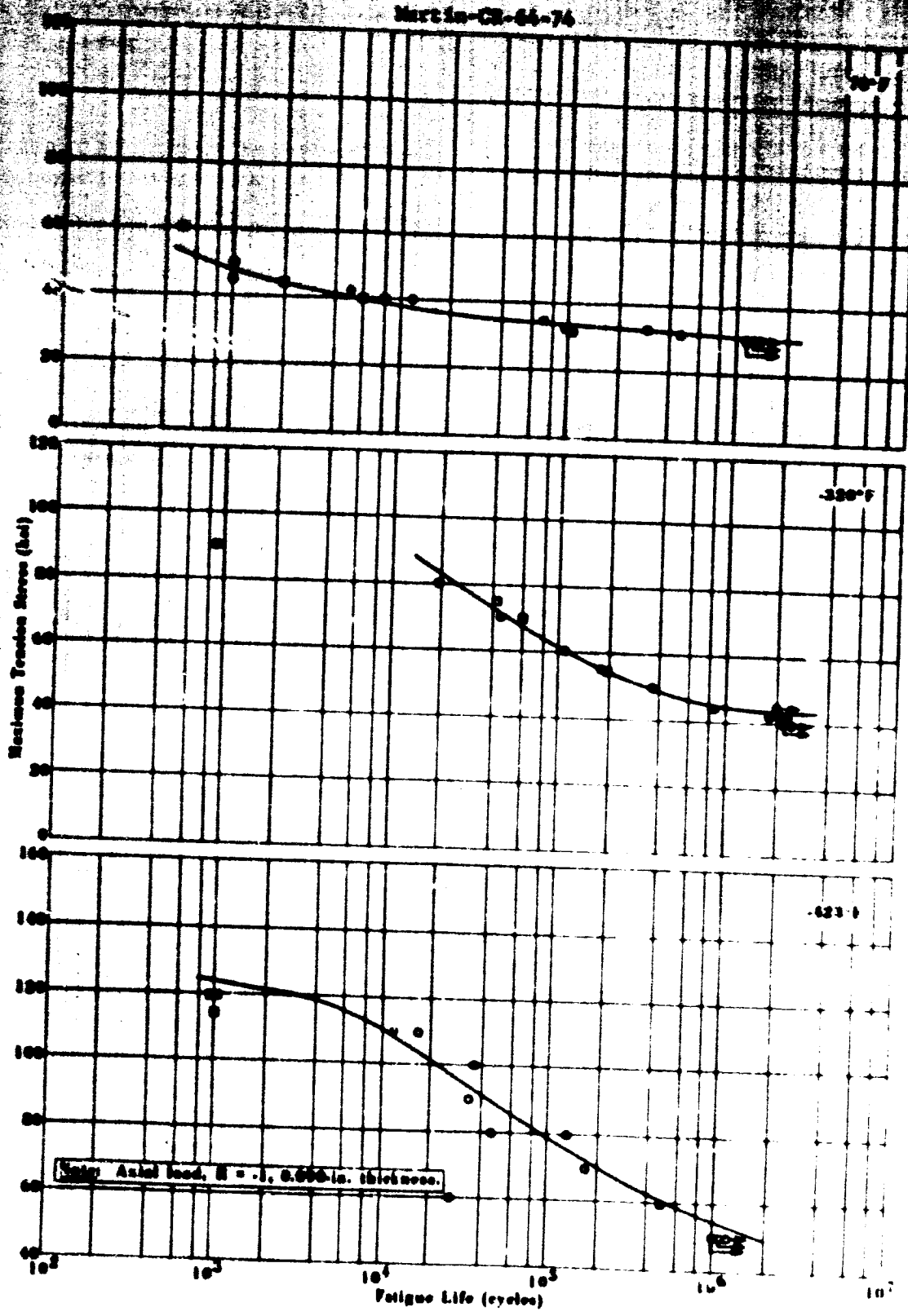

Fig. 54 Fatigue Properties of Unnotched 321 (Annealed) Stainless Steel

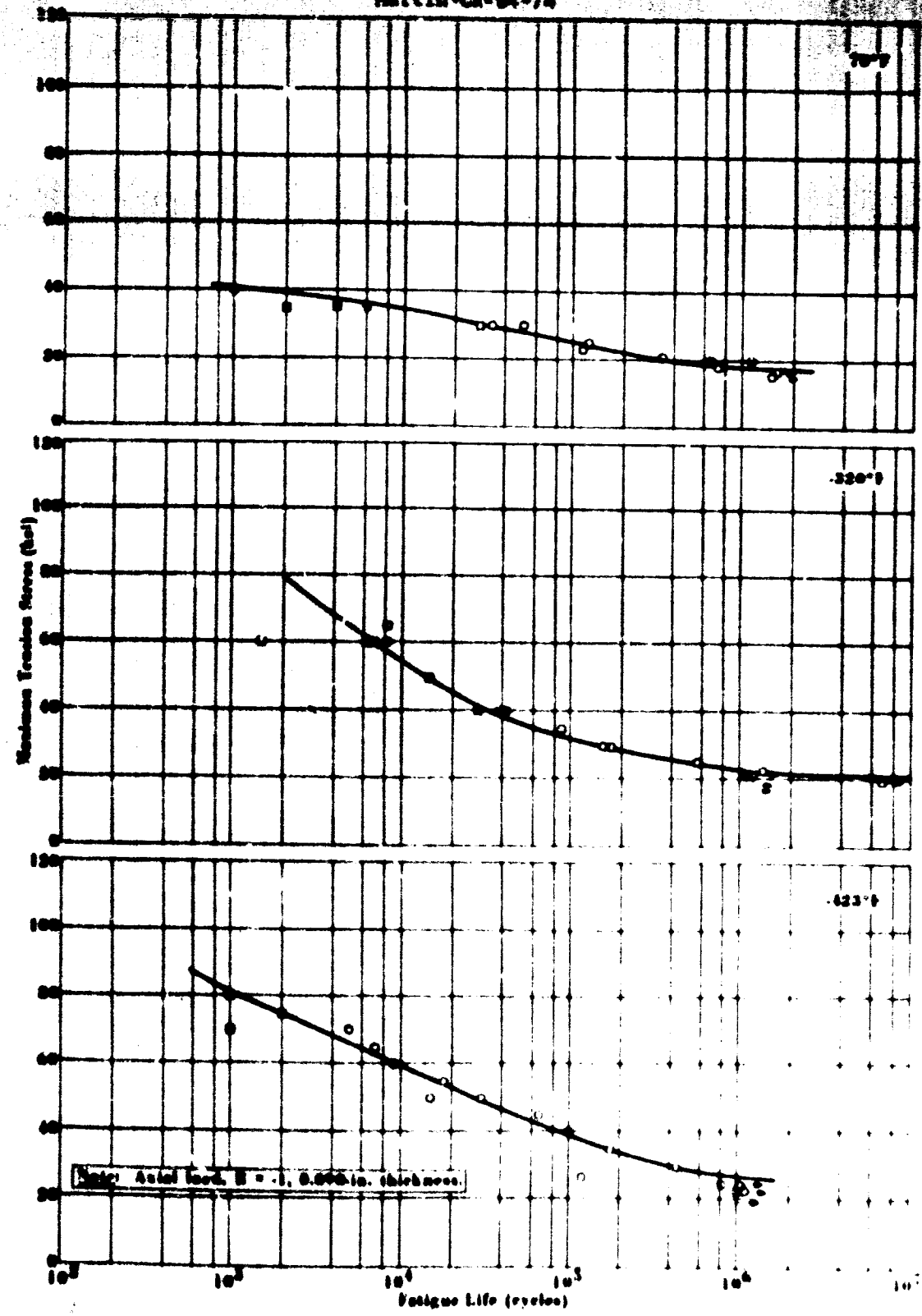

Fig. 55 Fatigue Properties of Notched 321 (Annealed) Stainless Steel

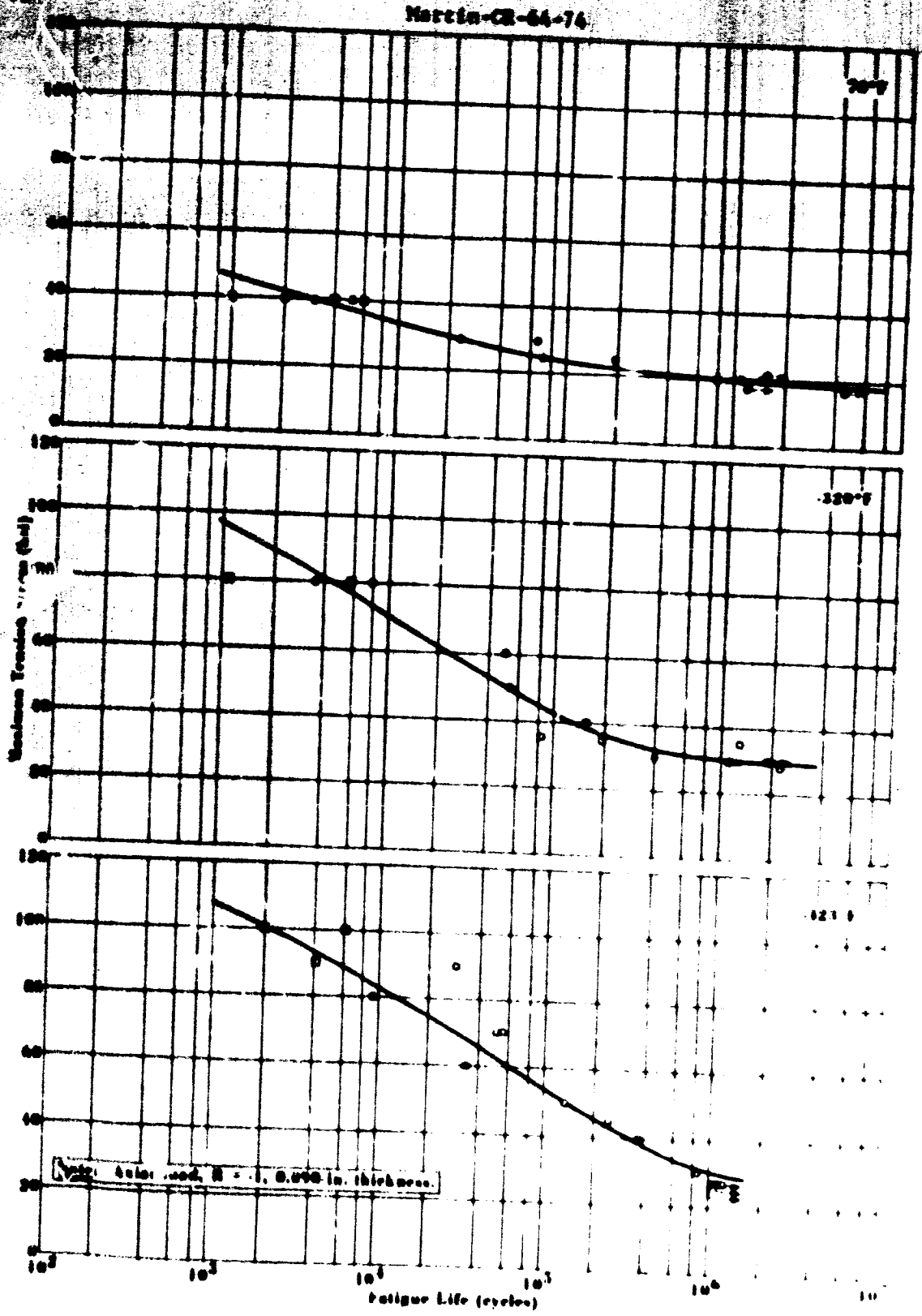

Fig. 56 Fatigue Properties of Welded 321 (Annealed) Stainless Steel

VII. DISCUSSION OF RESULTS

A. ALUMINUM ALLOYS

Of the six aluminum compositions employed in this study, four are being used or have been considered for cryogenic service. These alloys are 2014, 2219, 7039, and 5456. The other two compositions, 2020 and 7075, have not been contenders for cryogenic service primarily because they are nonweldable grades. In addition, the 7075 is known to exhibit poor toughness characteristics at cryogenic temperatures. However, these latter compositions were included in the study for comparative purposes.

1. Tension Properties

The mechanical properties of the 2014-T6 and 2219-T87 alloys (Fig. 17 and 18, respectively) are very similar and in substantial agreement with the data of others (Ref 3 and 4). These alloys are characterized by a greater temperature dependence of strength from -320 to -423°F than from 70 to -320°F. Yield and weld strengths show a relatively constant rate of increase with decreasing temperature. Elongation increases approximately 50% from 70 to -423°F. The principal difference in properties of these alloys is the significantly lower yield strength in the 2219-T87 alloy. The notch strength ratio values are quite high. However, it should be recognized that most aluminum alloys exhibit good notch toughness with the relatively low stress concentration factor ($K_t = 3.5$) used for this work.

The 2219-T62 alloy (Fig. 19) exhibits significantly lower strength, particularly yield strength, than the 2219-T87 composition. This difference results from the absence, in the -T62 temper, of post-solution heat treatment straining used to achieve additional aging response in the -T87 temper. Ductility increases with reduction in temperature, similarly to the 2014-T6 and 2219-T87 alloys. Weld strength is comparable to the 2219-T87. Notch toughness is maintained at high levels down to -423°F.

The 7039-T6 alloy (Fig. 20) exhibits the characteristic increases in unnotched tension properties observed for the 2014 and 2219 alloys. Notch properties are also similar to the former alloys. Unlike the 2014-2219 alloys, weld strength does not increase significantly with decrease in temperature.

The 5456-H343 alloy (Fig. 21) exhibits approximately 20% lower ultimate strength than the 2014-2219 alloys. The ratio of yield/ultimate strength is rather low. Elongation is relatively independent of temperature. At 70 to -320°F, weld strength increases, but then decreases with further temperature reduction. This decrease in weld strength and flat ductility curve is suggestive of loss of toughness at low temperatures. The notch data show good retention of toughness down to -423°F. However, it should be noted that the stress concentration (K_t) is not great. Results of other studies (Ref 3 and 5) using sharper notches (K_t = 6.3-8) have shown lower toughness for this alloy at -423°F than for the 2000 series alloys.

The 7075-T6 material (Fig. 22) shows evidence of the onset of brittle action at -423°F. Ultimate and yield strengths flatten out between -320 and -423°F. Elongation is relatively independent of temperature. Notch tests show a moderate loss of toughness with reduction in temperature. Data obtained by Christian and Watson (Ref 6) using a sharper notch show a significant loss of toughness at low temperatures.

The 2020-T6 alloy (Fig. 23) shows very high strength properties. Room temperature ultimate strength is equal to the strength of 5456-H343 at -423°F. Although this composition is expected to exhibit poor toughness at cryogenic temperatures, the limited evaluation performed is not sufficient to detect such havior. Tensile ductility increases to approximately 10% at -423°F.

Modulus data for the five alloys are given in Fig. 57. Room-temperature results are slightly lower but agree within 4% with data obtained from the Aluminum Association and from producers. Published data are compared with the experimental data listed on the following page.

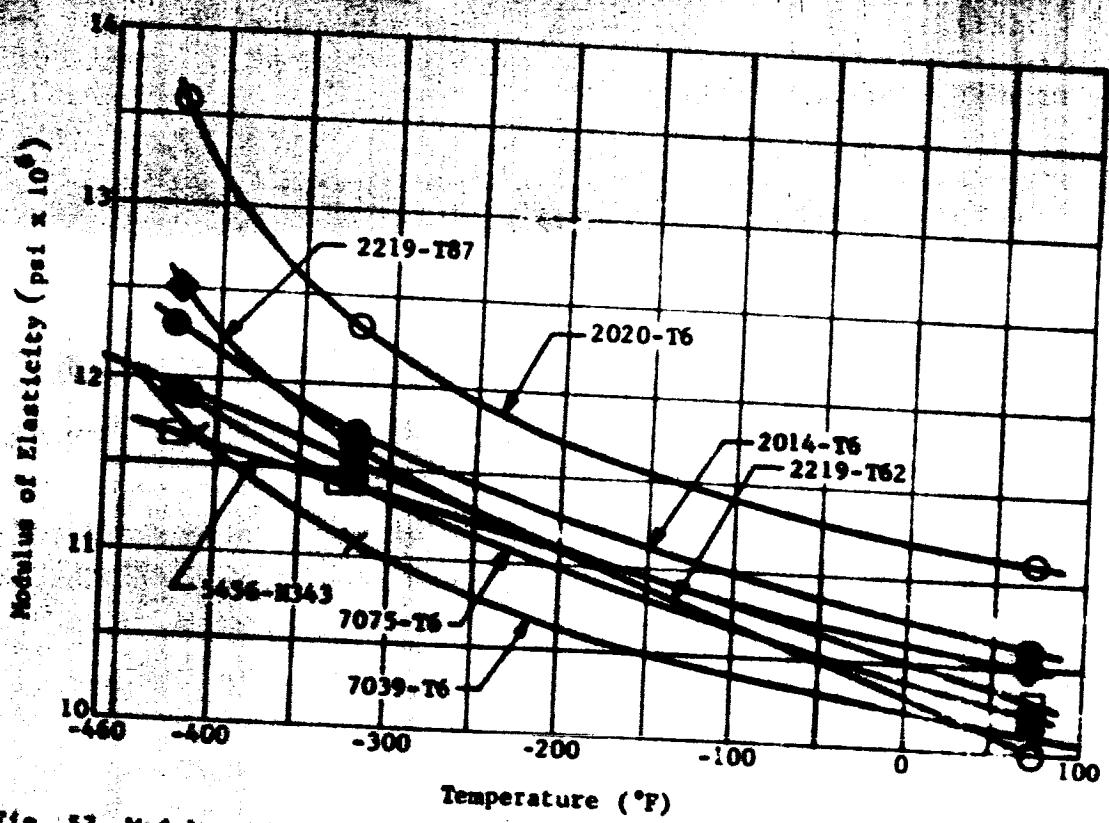

Fig. 57 Modulus of Elasticity of Aluminum Alloys at Cryogenic Temperatures

Alloy	Modulus of Elasticity (psi x 10^6) Experimental	Published
2014-T6	10.6	10.6
2219-T87	10.5	10.6
2219-T62	10.2	10.6
7039-T6	10.0	-
5456-H343	10.2	10.3
7075-T6	10.2	10.4
2020-T6	11.1	11.3

The highest modulus material is the 2020 composition. When introduced, this composition was reported to exhibit a 10% improvement over existing alloys. However, subsequent study showed it to be approximately 5%. Nevertheless, this level is still higher than almost all other aluminum alloys.

There is insufficient reliable data in the literature to confirm the cryogenic modulus data.

2. Fatigue Properties

Fatigue data for the aluminum alloys are presented in the following figures and tables:

Material	Unnotched Figure	Unnotched Table	Notched Figure	Notched Table	Welded Figure	Welded Table
2014-T6	28	B-1	29	B-2	30	B-3
2219-T87	31	B-4	32	B-5	33	B-6
2219-T62	34	B-3	35	B-8	36	B-9
7039-T6	37	B-10	38	B-11	39	B-12
5456-H343	40	B-13	41	B-14	42	B-15
7075-T6	43	B-16	44	B-17		
2020-T6	45	B-18				

e. 2014-T6

The unnotched 2014-T6 alloy exhibits increased strength for 10^6 cycle life of approximately 300% with reduction in temperature from 70 to -423°F. As noted for static behavior, strengthening is greatest between -320 and -423°F. The fatigue ratio* increased from 0.23 to 0.48 with reduction in temperature. The curves obtained at 70 and -423°F were significantly flatter than the -320°F curve which showed a slight knee. Although the reason for this is not completely known, a slight misalignment may be responsible for this condition. Testing performed on similar aluminum alloys at -320°F during the second year's effort did not show this behavior. Alignment accuracy achieved during the latter period is believed to be superior to that attained during the first year.

Notch test results show a significant decrease in fatigue strength compared to the unnotched data. The fatigue strength reduction factor (K_f)†, also known as fatigue notch factor, was rather poor. At 10^6 cycles, the factor increased from 2.0 at 70°F to 6.0 at -423°F. The low cycle (10^3) end of the curve showed a less significant effect with an initial value of 1.4 at 70°F, which increased to almost 2.0 at low temperatures.

Welded joints also show a loss of strength compared to the unnotched material. However, comparing the 70°F static 2014-T6 weld joint efficiency (80%) with the ratio of weld fatigue strength/unwelded fatigue strength (69%), a very good retention of weld strength under dynamic loading is evident. At cryogenic temperatures, a marked decrease in this strength ratio is noted.

$$*\text{Fatigue ratio} = \frac{S_u \text{ (static tensile strength)}}{S_n \text{ (fatigue strength at n cycles)}}$$

†Fatigue strength reduction factor or fatigue notch factor -

$$(K_f) = \frac{\text{Fatigue strength of unnotched specimens at n cycles}}{\text{Fatigue strength of notched specimens at n cycles}}$$

b. 2219-T37

Unnotched specimens of 2219-T87 alloy show behavior similar to the 2014-T6 except that a higher fatigue strength at 70°F (10^6 cycles) is observed. The fatigue ratio is the highest obtained at room temperature for all the aluminum alloys evaluated. The increase in fatigue strength with reduction in temperature is not quite 200%, somewhat lower than the 2014-T6 value. As a result, the fatigue ratio at lower temperatures is not the best of the series. 2014-T6, which has similar static strengthening, exhibits a higher fatigue ratio at -423°F. A decrease in fatigue ratio is indicated at -320°F; however, the magnitude of this decrease is not known because of the uncertain fatigue strength at 10^6 cycles.

The knee at -320°F is apparent, but somewhat flatter than found in the 2014-T6. The portion of the curve for fatigue life exceeding 10^5 cycles is presented as a spread band because of conflicting data points. The lower portion of the band gives a strength level lower than attained at 70°F. The upper stress level, 25,000 psi, is closer to the anticipated strength based on comparison with data for similar compositions.

The results of notch fatigue tests show behavior almost identical with the 2014-T6 alloy. The strengthening with reduction in temperature at the lower cycle portion of the curve is even less noticable than for 2014-T6. The fatigue strength reduction factor (K_f) increased from 2.8 to 5.0 with decreasing temperature at 10^6 cycles. At 10^3 cycles, an insignificant increase from 1.6 to 1.8 is noted.

The weld behavior is characterized by similarly flat curves showing major strengthening between -320 and -423°F. The fatigue strength at 70°F (10^6 cycles) is similar to the value for 2014-T6, but superior at -423°F. The fatigue ratio (10^6 cycles) increases from 0.20 to 0.28 as temperature is lowered.

c. 2219-T62

As anticipated, 2219-T62 exhibits slightly lower unnotched fatigue strength properties than its companion material, 2219-T87. This small diminuation is approximately proportional to the lower static strength of the -T62 material. The knee observed for 2219-T87 and 2014-T6 at -320°F was not apparent in this test series conducted during the second year. Curves at all three temperatures were rather flat, and quite similar in shape. The fatigue ratio was almost identical to the 2219-T87 data. Unlike the data for the previous alloy, where the magnitude of the decrease in fatigue ratio was uncertain, this series shows a decrease of approximately 10% at -320°F.

Notch fatigue tests showed strengthening with reduction in temperature at 10^3 cycles. The curves converged rapidly and showed little temperature dependency of strength from 10^4 through 10^6 cycles. The reduction factor (K_f) at 10^6 cycles increases from 2.4 to 2.6 with decreasing temperature.

The behavior of welded specimens agreed extremely well with that observed for the -T87 specimens. Strengths at 10^6 cycles for each temperature agreed within 2 ksi. The shapes of the corresponding curves were very similar. This behavior is not unexpected, since the static weld behavior of as-welded 2219 is essentially independent of temper. The 10^6 cycle strength values of -T62 and -T87 at -423°F were the highest attained in the aluminum weld studies.

d. 7039-T6

The unnotched 7039-T6 composition shows a significant amount of strengthening between 70 and -320°F in the 10^3 to 10^5 cycle range. The amount of strengthening from -320 to -423°F was minor in the above cycle range. However, at 10^6 cycles, the -423°F curve flattens out and a greater strengthening is noted. The fatigue ratio (10^6 cycles) is excellent over the entire temperature range, increasing from 0.31 at 70°F to 0.43 at -423°F.

Notched fatigue testing revealed very similar behavior at -320 and -423°F, with the curves almost coincidental. The 70°F curve is displaced downward slightly from the two cryogenic curves. However, at 10^6 cycles, the strength levels of all three are quite similar. The reduction factor (K_f) increases from 2.9 at 70°F to 4.4 at both -320 and -423°F. Although the room temperature value is not quite as good as noted for several other candidates, the 423°F value is one of the best determined in this study.

Testing of welded specimens reveals the principal strengthening to occur between 70 and -320°F, similar to the parent metal tests. Only minor strengthening occurs from -320 to -423°F. The fatigue ratio increases from 0.19 to 0.37 with lowering of temperature.

e. 5456-H343

The behavior of unnotched 5456-H343 is characterized by the -320°F knee observed during the first year's testing. The strength values at 10^6 cycles for all temperatures are very similar to those obtained for 2014-T6. The fatigue ratio increases from 0.28 at 70°F to 0.53 at -423°F. The -423°F value is the highest attained in the testing of unnotched aluminum alloys. Although the -423°F fatigue strength is similar to that found for 2014-T6, the static strength is significantly lower; hence, the superior fatigue ratio.

The notch fatigue test results showed a larger spread in 10^6 cycle strength than the previously discussed compositions. However, this spread was not great. The lowest strength was detected at -320°F. At the two extremes, 70 and -423°F, the reduction factor (K_f) values were quite outstanding. Although 5456-H343 shows evidence of a greater loss of toughness in static testing at -423°F with sharp notches than the 2000 series alloys, dynamic testing with a milder notch does not cause a significant loss of strength.

Testing of welded material showed similarly shaped flat curves for all temperatures. Strengthening at 10^6 cycles was greater between -320 and -423°F than from 70 to -320°F.

The fatigue ratio was constant at 0.22 for both 70 and -320°F and then increased to 0.42 at -423°F. The latter value matched the best value obtained at -423°F for all aluminum alloys evaluated.

f. 7075-T6

Unnotched fatigue behavior of this composition was characterized by similar shaped, steep curves. The strengths at 10^6 cycles were among the lowest obtained. The fatigue ratios at 70 and -320°F were the lowest found in this study. At -423°F, the fatigue ratio (0.40) corresponded to the value obtained for the tougher 2000 series alloys. However, a study of the static tensile results shows a flattening out of the tensile strength between -320 and -423°F that is suggestive of the onset of brittle behavior. Therefore, with little static property strengthening, the fatigue ratio can be deceivingly good.

The notch test results showed behavior similar to the 5456-H343, with a minimum in 10^6 cycle strength at -320°F. The fatigue strength reduction factor (K_f) varied from 1.7 at 70, to 4.4 at -320, decreasing to 3.6 at -423°F. The values at 70 and -423°F are the lowest obtained in notch testing and therefore suggest the best notch behavior. However, K_f is based on the unnotched strength values. As noted above the room temperature fatigue ratio is very poor and the -423°F value is misleading. Therefore, it is difficult to accept the K_f data as calculated without interpretation.

g. 2020-T6

The unnotched 2020-T6 alloy showed strength values comparable to the 5456 composition. However, because of the much higher static tensile properties, 2020-T6 exhibits relatively high fatigue ratio values. The knee at -320°F is typical of other aluminum alloys tested during the first year.

h. Comparison of Results

A brief comparison of test results is presented in Table 5. This table presents the fatigue strength at 10^6 cycles for each material, test condition, and temperature. In addition, fatigue ratio data are presented for unnotched and welded tests and fatigue strength reduction factor (K_f) for notched specimens.

Table 5 Comparison of Fatigue Properties* for Aluminum Alloys

Material	Temperature (°F)	Unnotched Stress (ksi)	Unnotched Fatigue Ratio†	Notched Stress (ksi)	Notched K_f‡	Notched K_f^{-1}	Welded Stress (ksi)	Welded Fatigue Ratio†
2014-T6	70	16	0.23	[illegible]	2.0	0.50	11	0.20
	-320	[illegible]	0.29	10	2.5	0.40	17	0.26
	-423	47	0.48	8	5.9	0.17	19	0.27
2219-T87	70	22	0.33	8	2.8	0.36	10	0.20
	-320	17 to 25	0.20 to 0.29	[illegible]	2.4 to 3.6	0.42 to 0.28	14	0.22
	-423	40	0.40	8	5.0	0.20	24	0.28
2219-T62	70	19	0.32	8	2.4	0.42	12	0.26
	-320	22	0.29	6	3.7	0.27	16	0.29
	-423	37	0.38	8	4.6	0.22	20	0.42
7039-T6	70	20	0.31	7	2.9	0.34	9	0.19
	-320	31	0.40	7	4.4	0.23	18	0.34
	-423	40	0.43	9	4.4	0.23	22	0.37
5456-H343	70	16	0.28	8	2.0	0.50	11	0.22
	-320	26	0.36	[illegible]	5.2	0.19	13	0.22
	-423	43	0.53	10	4.3	0.23	23	0.42
7075-T6	70	15	0.19	9	1.7	0.59	--	--
	-320	22	0.22	5	4.4	0.23	--	--
	-423	40	0.40	11	3.6	0.28	--	--
2020-T6	70	18	0.22	--	--	--	--	--
	-320	23	0.24	--	--	--	--	--
	-423	41	0.36	--	--	--	--	--

*n = 10^6 cycles.

†Fatigue ratio = $\frac{\text{Sn (fatigue strength at n cycles)}}{\text{Su (static tensile strength)}}$.

‡Fatigue strength reduction factor (K_f) = $\frac{\text{(fatigue strength of unnotched specimens at n cycles)}}{\text{(fatigue strength of notched specimens at n cycles)}}$.

A bar graph presentation of the data is given in Fig. 58. The notch data are presented in terms of the reciprocal of the fatigue strength reduction factor to make the unnotched and welded data more understandable.

The data show that the two 2219 compositions and 7039-T6 exhibit the highest unnotched fatigue ratio at room temperature. At -423°F, the 2014-T6 and 5456-H343 are superior.

The bar graph for notch properties shows the 7075-T6 to be outstanding at 70°F, followed closely by 2014-T6 and 5456-H343. Significant losses in reduction factor occur on cooling to cryogenic temperatures. At -423°F, the 7075-T6, 5456-H343 and 7039-T6 all exhibit comparable properties.

The welded behavior is characterized by 2219-T62 exhibiting the highest 70°F fatigue ratio. At -423°F, both 2219-T62 and 5456-H343 exhibit the best behavior.

i. Effect of Stress Ratio

The results of two tests performed under tension/tension loading show the effect of stress ratio on fatigue properties. Although insufficient data are presented for a quantitative analysis of the effect, the marked increase in life is apparent. Figure 59 compares 2219-T87 parent metal and 2014-T6 welded properties tested at R = -1 with points obtained for R = 0 at -423°F.

It is proposed to study the effect of stress ratio more thoroughly in future work.

j. Fractured Specimens

Testing under axial loads and fully reversed stressing (R = -1) does not leave much of a surface to study after fracture. The rapid pounding of the matching surfaces after fracture destroys most of the useful information that could be obtained from a surface study. However, some observations have been made.

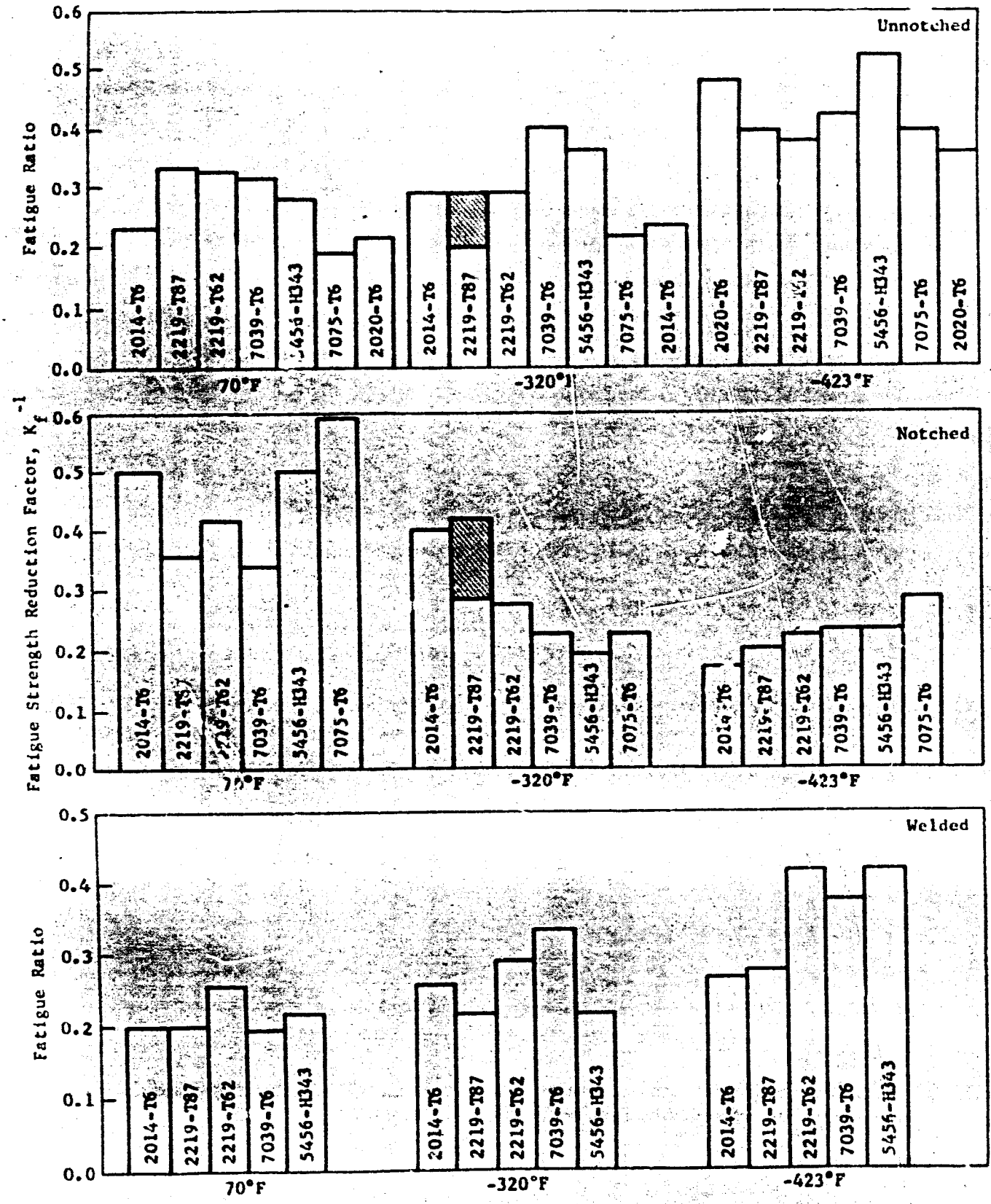

Fig. 58 Comparison of Fatigue Properties for Aluminum Alloys

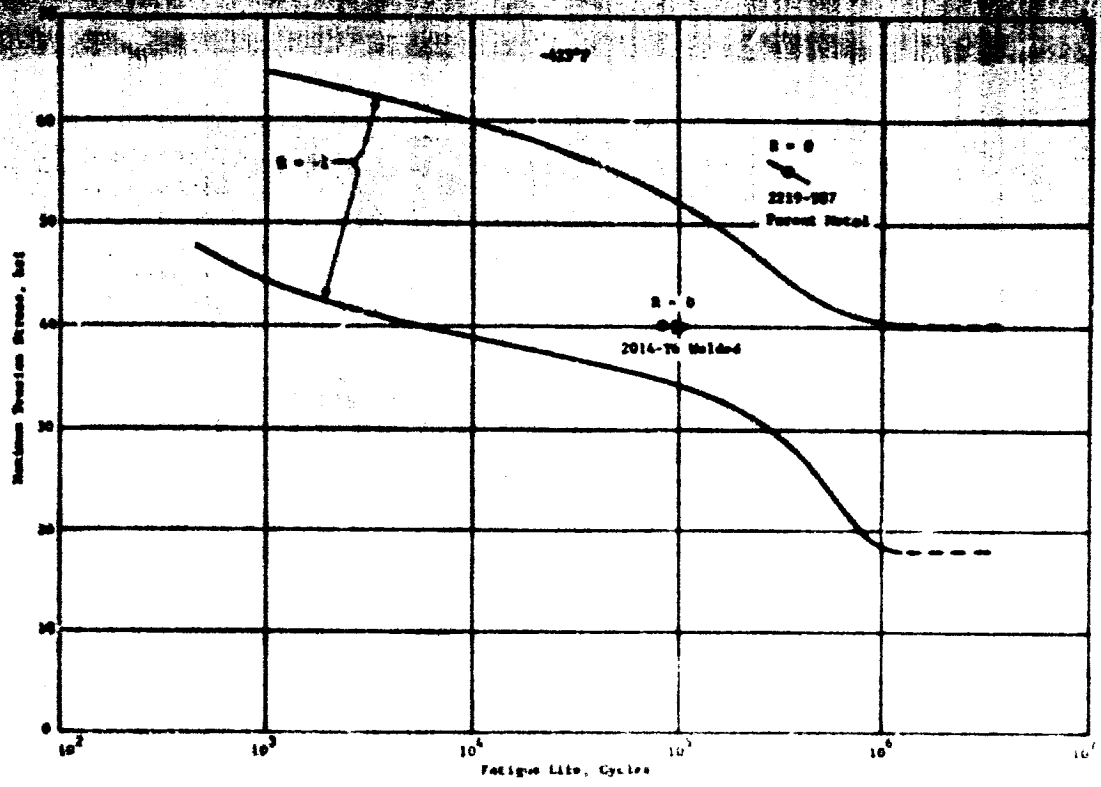

Fig. 59 Effect of Stress Ratio on the Fatigue Properties of Two Aluminum Alloys at -423°F

The 5456-H343, 7075-T6 and 7039-T6 unnotched fatigue specimens showed a laminated appearance. The laminations probably open up after failure as a result of the hammering action. This behavior is typical for the strain hardened 5456 alloy even in static tension failure, but is not observed for the 7075 and 7039 compositions in tension.

Weld fractures occurred at the interface of the fusion zone and heat-affected area.

k. Results of Other Studies

Extensive room temperature tests of two alloys evaluated in this program, 2014-T6 and 7075-T6, have been performed throughout the past years. These results summarized in Ref 7 show a higher stress for failure at 10^7 cycles than reported in this work. The strengths reported for these alloys, 25,000 to 30,000 psi, were primarily obtained using bending techniques. However, some axial data on smooth machined round bars are also included.

Several reasons for the lower strengths obtained in this study must be considered. The endurance limit obtained by bending techniques may be as great as 30% higher than values obtained by axial loading. When round bars are machined, even for axial tests, the surface of the material is removed and defects are removed by polishing. In this study, the surface of the sheet was left in the as-received condition.

The literature is almost void of cryogenic data for comparison purposes. The only data for which a comparison can be made have been generated by Fontana (Ref 8) on 7075-T6 using the flexure technique on polished specimens machined from 0.750-in. diameter bar. These data are compared below:

Temperature (°F)	Stress at 10^6 Cycles (ksi) This Work (Axial Load, R = -1)	Fontana (Flexure, R = -1)
70	15	35
-110	--	38
-320	22	50
-423	41	--

The results of Fontana are significantly higher than obtained in this work.

B. TITANIUM ALLOYS

The titanium alloys evaluated in this program represent each system used commercially: (a) alpha, (b) beta, and (c) alpha-beta. The Ti-5Al-2.5Sn crystallizes in the hexagonal-close-packed structure (alpha) and is characterized by good retention of properties down to very low temperatures. The Ti-13V-11Cr-3Al alloy is a beta-type crystallizing in the body-centered-cubic structure. Body-centered-cubic materials are typified by ductile-brittle transition behavior and, consequently, are not suited for cryogenic service. The Ti-6Al-4V alloy represents the alpha-beta type and combines hexagonal and body-centered-cubic phases. Due to the relatively low percentage of beta phase in this particular

composition, toughness and ductility can be retained to moderately low temperatures. However, below -320°F, there is a marked decrease in mechanical properties. Hence, alpha alloys, such as Ti-5Al-2.5Sn, are clearly the best titanium selection for most applications down to -423°F.

1. Tension Properties

The mechanical properties of the Ti-5Al-2.5Sn alloy are shown in Fig. 24. Strength properties increase almost 100% from 70 to -423°F. Elongation increases slightly from room temperature to -320°F, but decreases sharply to 1.8% at -423°F. This behavior would be expected for normal interstitial Ti-5Al-2.5Sn, but not for low-interstitial grade. A study of the chemical analysis shows both iron and interstitial elements to be quite low. No explanation for this unusual behavior can be found. Plotting the interstitial content of this material with the data previously reported by Schwartzberg and Keys (Ref 9) on interstitial effects in Ti-5Al-2.5Sn shows that the ultimate strength falls slightly above the curve (Fig. 60). Data of Espey, et al. (Ref 10) and Christian (Ref 11) at higher oxygen equivalent contents showed satisfactory ductility.

Weld joint efficiency is very close to 100%. Notch tests show a notch strength ratio exceeding 1.1 at -423°F.

The behavior of the solution-treated and aged Ti-6Al-4V alloy is shown in Fig. 25. Strength increased from 165,000 psi at 70°F to almost 300,000 psi at -423°F. As expected for this composition in the fully heat-treated condition, ductility decreased continuously below room temperature. Weld joint efficiency was very good. Notch properties decreased with reduction in temperature to a strength ratio slightly less than unity at -423°F.

Figure 26 presents tensile data for the Ti-13V-11Cr-3Al alloy. As expected, brittle behavior was observed below room temperature. At room temperature, a strength level of 200,000 psi was achieved while maintaining 6.5% elongation. At -320°F, brittle failures occurred through the pinholes or specimen fillet. No attempt was made to test specimens at -423°F. Weld strength decreased from 144,000 psi at 70°F to 85,000 psi at -423°F.

Modulus data obtained at 70, -110, and -320°F are presented in Fig. 61. Data obtained at -423°F were not satisfactory and are not presented.

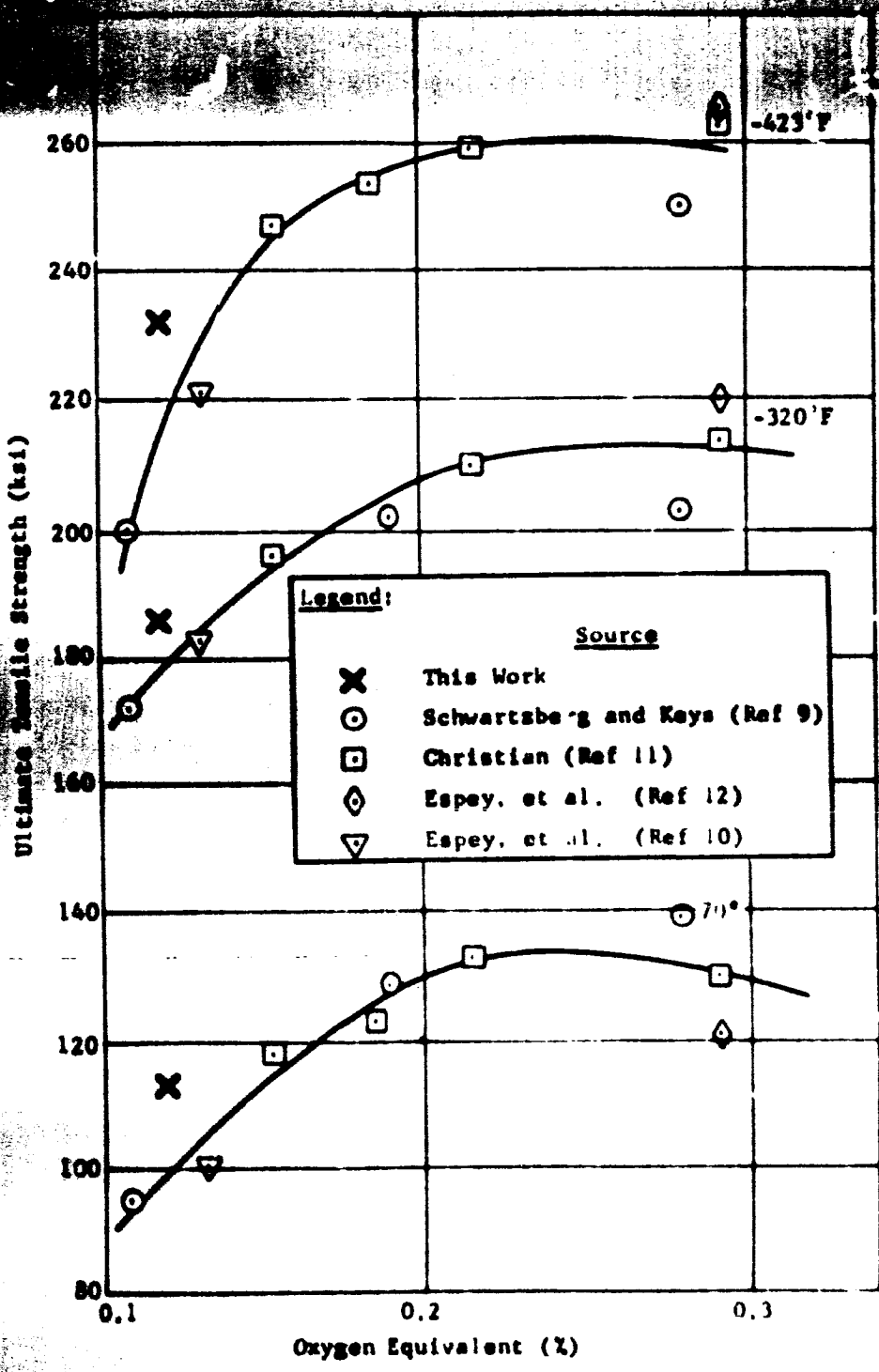

Fig. 60 Effect of Interstitial Content on the Unnotched Tensile Strength of 5Al-2.5Sn Titanium Alloy

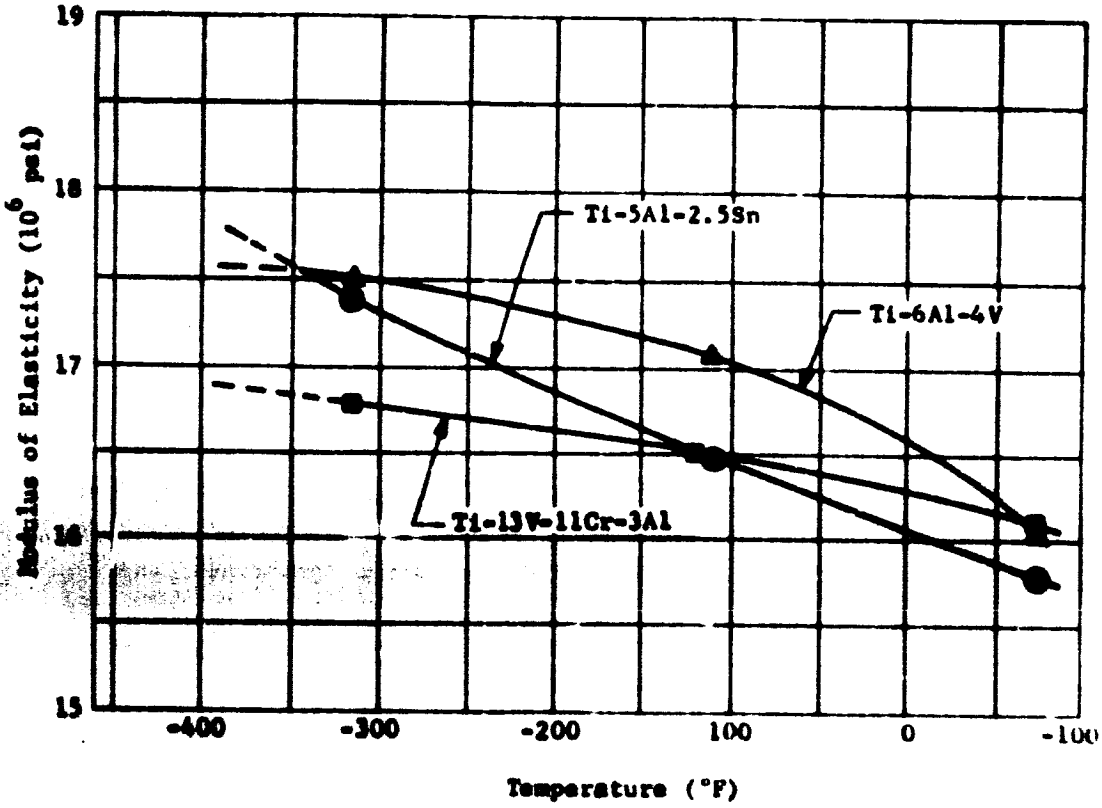

Fig. 61 Modulus of Elasticity of Three Titanium Alloys at Cryogenic Temperatures

2. Fatigue Properties

Fatigue data for titanium alloys are presented in the figures and tables listed below:

Material	Unnotched Figure	Unnotched Table	Notched Figure	Notched Table	Welded Figure	Welded Table
[illegible]	[illegible]	[illegible]	[illegible]	[illegible]	[illegible]	B-21
[illegible]	49	B-22	50	B-23	51	B-24
Ti-13V-11Cr-3Al	52	B-25	--	--	53	B-26

The unnotched curves for the titanium alloys are characterized by a general sharp transition from high strength to the level of the endurance limit and rather flat behavior above 10^5 cycles. The aluminum alloy curves generally are much flatter and exhibit a continuing decrease in strength.

a. Ti-5Al-2.5Sn

The unnotched fatigue data for Ti-5Al-2.5Sn are characterized by a wide variation in low cycle fatigue strength as a function of temperature.

However, at the high cycle end of the test range, the cryogenic properties do not differ widely. The room temperature stress at 10^6 cycles is almost 40,000 psi lower than the cryogenic properties. The fatigue ratio decreases from 0.62 at 70 and -320°F to 0.48 at -423°F. Note that the fatigue ratio values for titanium should not be compared with those obtained for aluminum and stainless steel because of the difference in stress ratio (R). The stress ratio (R = 0.01) used for titanium testing would give better fatigue ratio data than obtainable under fully reversed stressing.

Notched fatigue results showed similar behavior at all three test temperatures. These curves did not show the sharp transition noted for unnotched material. Stress decreased continuously with increasing life throughout the test range. The stresses for 10^6 cycle life at 70 and -320°F were very similar; a small decrease in fatigue strength occurred on cooling to -423°F. The fatigue strength factor (K_f) at 10^6 cycles increased progressively from 2.2 to 4.8 with decreasing temperature.

[illegible] slope [illegible] rather flat [illegible] cycles increased somewhat from [illegible] to -320°F and then decreased to less than the room temperature strength at -423°F. The fatigue ratio (10^6 cycles) decreased continuously from 0.62 to 0.27 with reduction in temperature.

b. Ti-6Al-4V

The unnotched specimens of Ti-6Al-4V exhibit a smaller difference in strength properties at the low cycle end of the curve than for the Ti-5Al-2.5Sn. However, a significant spread between the 10^6 cycle stresses for the three test temperatures is noted. The fatigue ratio (10^6 cycles) is essentially independent of temperature at a value of 0.40 to 0.43. This range is somewhat poorer than observed for the Ti-5Al-2.5Sn.

The notch behavior of this alloy is almost independent of temperature. Curves for the three test temperatures are similarly steep in the 10^3 to 10^4 cycle range and then quite flat to 10^6 to 10^7 cycles. Strength values fall between 40,000 and 43,000 psi at 10^6 cycles.

The fatigue strength reduction factor (K_f) is somewhat better than observed for Ti-5Al-2.5Sn. The values increase from 1.8 to 3.2 for 10^6 cycles strength with reduction in temperature.

Fatigue curves for welded joints show a steep decrease in strength from 10^3 to 10^5 cycles and then flatten out between 10^5 and 10^7 cycles. The three curves are nearly coincidental. The fatigue strength at 10^6 cycles decreases only slightly from 87,000 to 81,000 psi with reduction in temperature. The attendant increase in static strength results in a net decrease in fatigue ratio from 0.53 to 0.27 with reduction in temperature. These values are slightly lower than obtained for Ti-5Al-2.5Sn alloy.

c. Ti-13V-11Cr-3Al

The unnotched test results for Ti-13V-11Cr-3Al show a rather steep 70°F curve from 10^3 to 10^5 cycles. The curve flattens out rapidly and remains flat to 10^7 cycles. The cryogenic curves show a somewhat more gradual decrease in strength to 10^6 cycles. The fatigue ratio at 70°F (10^6 cycles) is slightly lower than obtained for Ti-6Al-4V. The high value obtained at -320°F is somewhat fictitious because the static tensile tests resulted in premature failure.

Welded tests produced curves less steep than noted for the parent metal. The fatigue strength at 10^6 cycles decreased from 70 to -320°F and then increased between -320 and -423°F. The fatigue ratio at 70°F (0.30) was significantly lower than determined for the other two titanium alloys. The fatigue ratio decreased to 0.12 at -320°F and then increased to 0.24 at -423°F. Brittle fracture at both cryogenic temperatures tend to discount the validity of these values.

d. Fractured Specimens

Fracture surfaces were generally too smeared for study. Welded specimen fractures appeared to initiate in the heat affected zone, but progressed through the cast structure.

e. Comparison of Results

A comparison of results is provided in Table 6. The data show the Ti-5Al-2.5Sn composition to exhibit superior unnotched properties, based on fatigue ratio, than the other two materials. Welded Ti-5Al-2.5Sn and Ti-6Al-4V showed fairly similar behavior. The unnotched behavior of Ti-6Al-4V was superior to the Ti-5Al-2.5Sn. Ti-13V-11Cr-3Al showed generally poor properties below room temperature. A bar graph presentation of the data is given in Fig. 62.

Table 6 Comparison of Fatigue Properties* for Titanium Alloys

Material	Temperature (°F)	Unnotched		Notched			Welded	
		Stress (ksi)	Fatigue Ratio†	Stress (ksi)	K_f‡	K_f^{-1}	Stress (ksi)	Fatigue Ratio†
Ti-5Al-2.5Sn	70	72	0.62	32	2.2	0.45	70	0.62
	-320	118	0.62	30	3.9	0.26	82	0.45
	-423	110	0.48	23	4.8	0.21	62	0.27
Ti-6Al-4V	70	73	0.43	41	1.8	0.56	87	0.53
	-320	98	0.40	43	2.3	0.43	86	0.36
	-423	130	0.43	40	3.2	0.31	81	0.27
Ti-13V-11Cr-3Al	70	79	0.40	--	--	--	44	0.30
	-320	97	0.48	--	--	--	15	0.12
	-423	102	--	--	--	--	37	0.24

*$n = 10^6$ cycles.

†Fatigue ratio = $\frac{\text{Sn (fatigue strength at n cycles)}}{\text{Su (static tensile strength)}}$.

‡Fatigue strength reduction factor (K_f) = $\frac{\text{(fatigue strength of unnotched specimens at n cycles)}}{\text{(fatigue strength of notched specimens at n cycles)}}$.

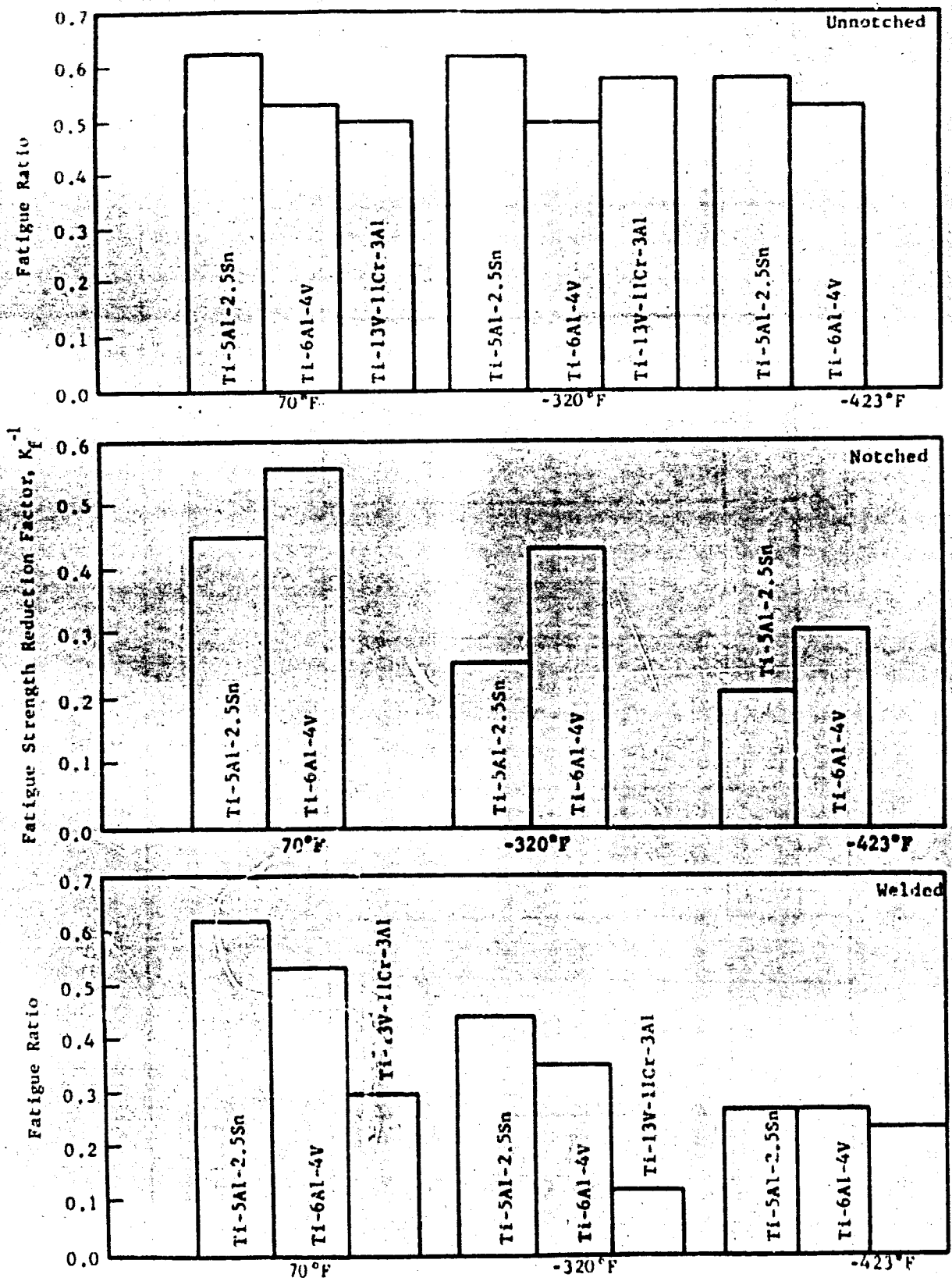

Fig. 62 Comparison of Fatigue Properties for Titanium Alloys

C. STAINLESS STEEL

The 321 grade of stainless steel is typical of the series of austenitic chromium-nickel steels so widely used for cryogenic service because of their excellent low-temperature toughness.

1. Tension Properties

The mechanical properties of 321 stainless steel are given in Fig. 27. The unnotched behavior shows the characteristic rapid linear increase in ultimate strength with very little increase in yield strength, as temperature is decreased. Elongation shows a small decrease with reduction in temperature, but is still quite high (36%) at -423°F.

Notch and weld strengths increase from 70 to -320°F, but decrease somewhat from -320 to -423°F.

2. Fatigue Properties

The unnotched fatigue data (Fig. 54) for 321 stainless steel show a very flat curve at 70 F. Curves obtained at both -320 and -423°F are moderately steep. The fatigue ratio (10^6 cycles) at 70°F is 0.37. This value decreases to 0.21 and 0.23 at -320 and -423°F, respectively. Unlike the aluminum alloys, which show an improvement in fatigue performance at low temperatures as evidenced by an increase in the fatigue ratio, the 321 shows a substantial decrease. However, the absolute strength values of the stainless steel increase with reduction in temperature and exceed the properties obtained in the aluminum alloy study.

Notched test results (Fig. 55) show a flat curve at 70°F and steeper curves at -320 and -423°F. The 10^6 cycle stress level increases from 18 ksi at 70 to 24 and 27 ksi at -320 and -423°F, respectively. The fatigue strength reduction factor (K_f) is exceptionally good. The value for all temperatures varied from 1.8 to 2.0.

The behavior of welded joints (Fig. 56) was very similar to that observed for the unnotched parent metal. Although weld joint efficiency is very high in 321 stainless steel, the welded fatigue specimens attain only approximately two-thirds of the unwelded fatigue strength. The fatigue ratio values are 0.23, 0.15, and 0.24 at 70, -320, and -423°F, respectively.

Data for the three test conditions are summarized in the tabulation below:

	Unnotched		Notched			Welded	
Temperature (°F)	Stress (ksi)	Fatigue Ratio	Stress (ksi)	K_f	K_f^{-1}	Stress (ksi)	Fatigue Ratio
70	32	0.37	3	1.8	0.56	20	0.23
-320	44	0.21	24	1.8	0.56	30	0.15
-423	55	0.23	27	2.0	0.50	31	0.24

VIII. CONCLUSIONS

This program has demonstrated that tension/compression fatigue properties can be obtained under axial loading for flat sheet materials at temperatures down to -423°F. Furthermore, it has been demonstrated that tests at liquid hydrogen temperature can be performed for long periods with automatic fill control.

Data generated for the aluminum alloys show the following:

1) Unnotched 2219 and 7039-T6 exhibit good properties at 70°F;

2) Unnotched 2014-T6 and 5456-H343 were superior at -423°F;

3) Fatigue ratio increases with decrease in temperature for unnotched and welded specimens;

4) Introduction of a mild notch reduces fatigue strength significantly;

5) Notched 5456-H343 and 7075-T6 exhibit superior behavior at 70°F;

6) At -423°F, 5456-H343 and 7039-T6 exhibit the highest notch fatigue properties;

7) Welded joints decrease fatigue properties. This increase is greater than the decrease of strength in static weld behavior compared to parent metal, but not as great as introducing a machined notch;

8) The 2219-T62 alloy showed the highest welded fatigue ratio at 70 and -423°F. The 5456-H343 was comparable to the 2219-T62 at -423°F.

The titanium fatigue test results show the following:

1) Ti-5Al-2.5Sn showed the best unnotched fatigue ratio properties;

2) Welded Ti-5Al-2.5Sn and Ti-6Al-4V showed [illegible] behavior;

3) Notched behavior of Ti-6Al-4V was superior to Ti-5Al-2.5Sn;

4) Ti-13V-11Cr-3Al showed generally poor properties below room temperature.

Test results for 321 stainless steel show:

1) Unnotched fatigue ratio decreases with reduction in temperature;

2) Notched behavior was relatively good and was independent of temperature;

3) Fatigue ratios for welded joints decreased initially with reduction in temperature and then increased.

The following materials appear to be satisfactory for cyclic service at cryogenic temperatures:

Aluminum	Titanium	Stainless Steel
2014-T6	5Al-2.5Sn	321
2219-T87	6Al-4V	
2219-T62		
7039-T6		
5456-H343		

Aluminum alloys 2020-T6 and 7075-T6 appear to be somewhat questionable for service at -423°F. Ti-13V-11Cr-3Al is not recommended for cryogenic service.

REFERENCES

1. R. D. Keys: "A Multiple Tensile Specimen Test Device for Use in Liquid Hydrogen." Advances in Cryogenic Engineering, Vol 7, Plenum Press, New York, 1962.

2. R. Markovich and F. R. Schwartzberg: Testing Techniques and Evaluation of Materials for Use at Liquid Hydrogen Temperature. A-61-4. Martin Company, Denver, Colorado, February 1961. Also, ASTM STP 302, ASTM, Philadelphia, Pennsylvania, 1961.

3. J. L. Christian: Mechanical Properties of Aluminum Alloys at Cryogenic Temperatures. MRG-190. Convair-Astronautics, 2 December 1960.

4. F. R. Schwartzberg and R. D. Keys: Mechanical Properties of 2000 Series Aluminum Alloys at Cryogenic Temperatures. R-61-32. Martin Company, Denver, Colorado, October 1961.

5. Martin Company unpublished data.

6. J. L. Christian and J. F. Watson: "Properties of 7000 Series Aluminum Alloys at Cryogenic Temperatures." Advances in Cryogenic Engineering, Vol 6, Plenum Press, New York, 1961.

7. Strength of Metal Aircraft Elements, MIL-HDBK-5. March 1959.

8. M. G. Fontana: Investigation of Mechanical Properties and Physical Metallurgy of Aircraft Alloys at Very Low Temperatures. WADC TR 5662, Part II. Ohio State University Research Foundation, October 1948.

9. F. R. Schwartzberg and R. D. Keys: Mechanical Properties of an Alpha Titanium Alloy at Cryogenic Temperatures. Paper presented at Annual ASTM Meeting, 23-29 June 1962.

10. G. B Espey, M. H. Jones, and W. F. Brown, Jr: Some Factors Influencing the Fracture Toughness of Sheet Alloys for Use in Lightweight Cryogenic Tankage. ASTM STP 302. ASTM, Philadelphia, Pennsylvania, 1961.

11. J. L. Christian: Mechanical Properties of Titanium and Titanium Alloys at Cryogenic Temperatures. MRG-189. Convair-Astronautics, 14 October 1960.

12. G. B. Espey, M. H. Jones, and W. F. Brown, Jr: Sharp-Edge-Notch Tensile Characteristics of Several High-Strength Titanium Sheet Alloys at Room and Cryogenic Temperatures. ASTM STP 287. ASTM, Philadelphia, Pennsylvania, 1960.

APPENDIX A

CRYOSTAT DRAWINGS

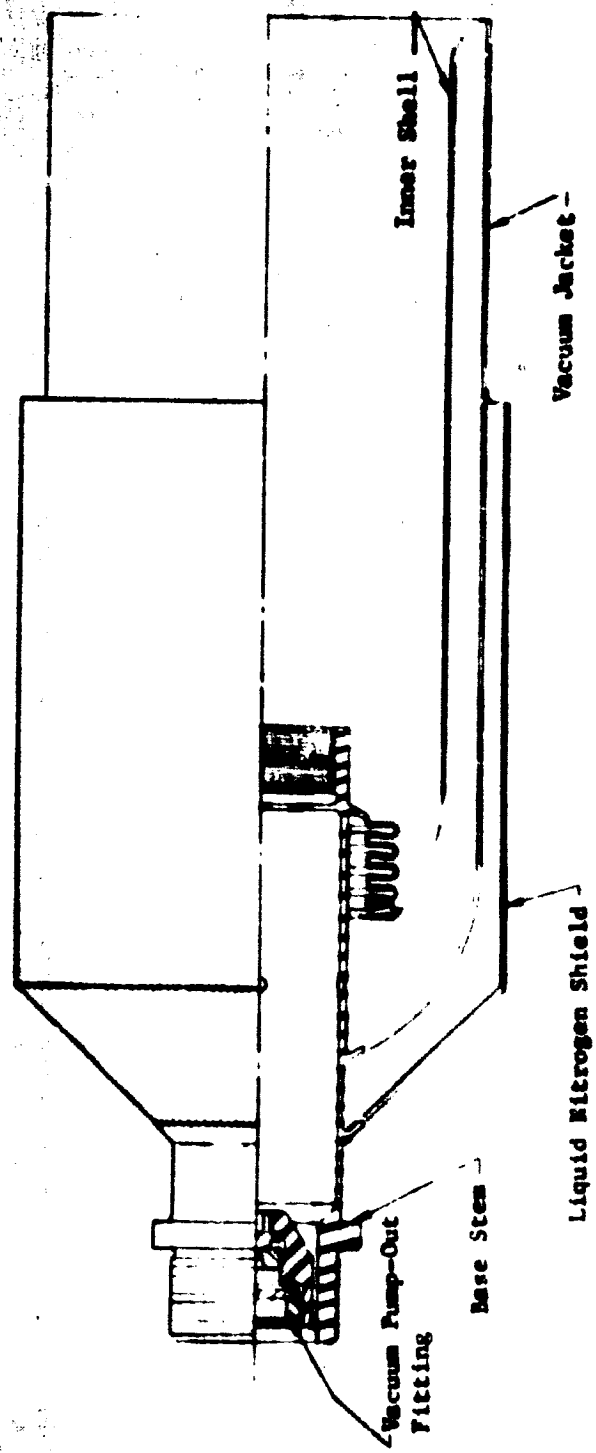

Fig. A-1 Fatigue Cryostat Assembly

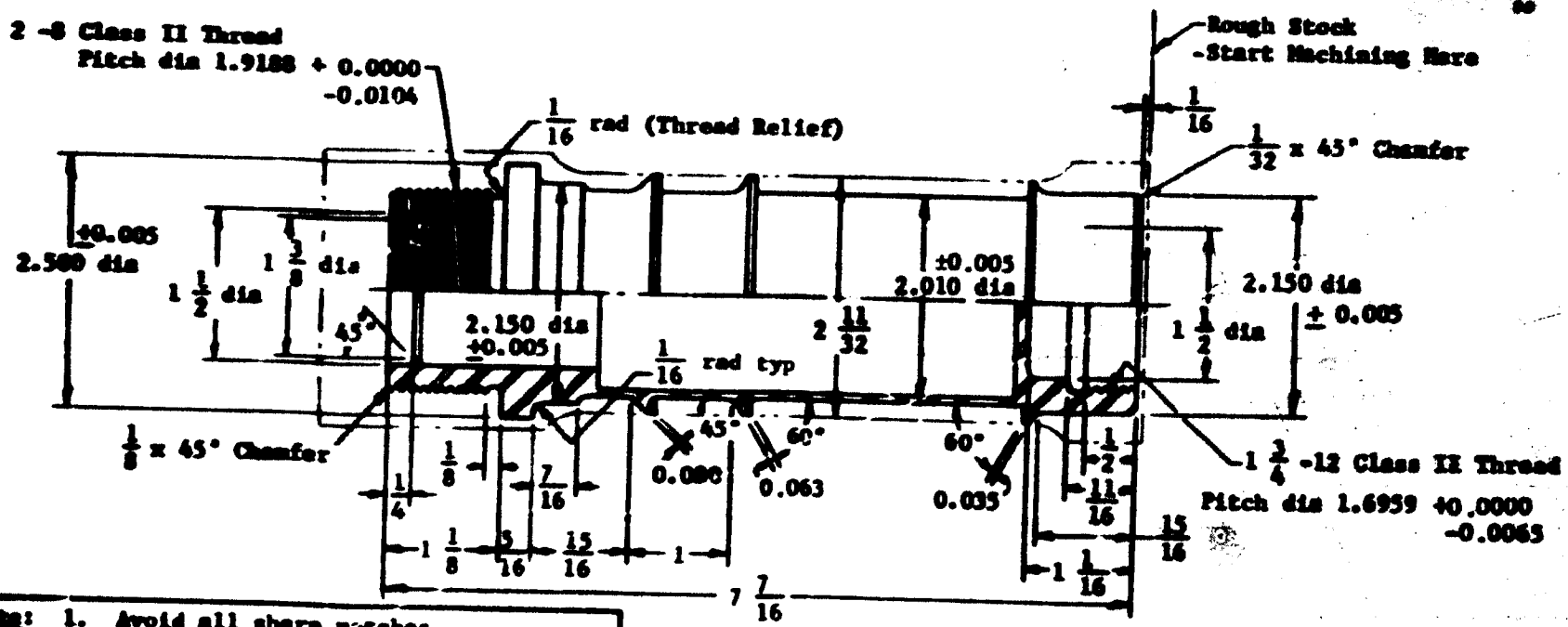

Notes:

1. Avoid all sharp notches.
2. All internal radii = $\frac{1}{16}$.
3. Use smooth radius thread tool.
4. Roll shank to work harden surface (protect threads and end face).
5. Phantom outline indicates stock to be removed.
6. Thread diameters to be concentric with ℄ within 0.002 TIR.
7. All measurements in inches except as noted.

Fig. A-2 Cryostat Base Stem

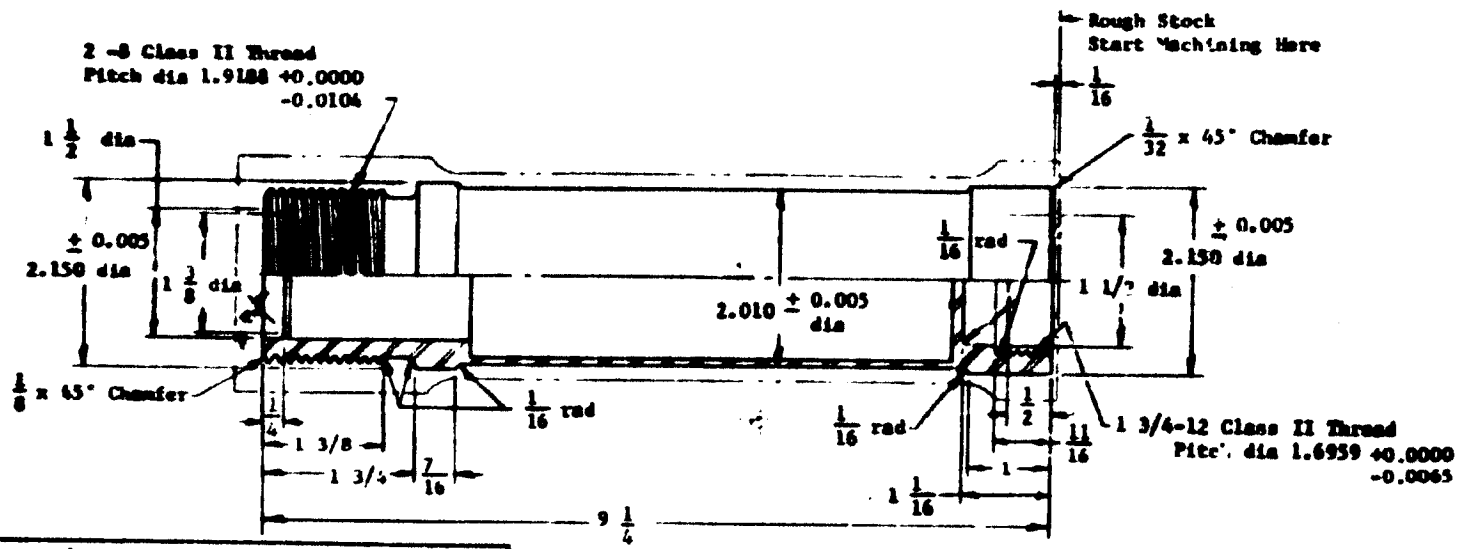

Note:
1. Avoid all sharp notches.
2. Use smooth radius thread tool.
3. Roll shank to work harden surface (protect threads and end faces).
4. Phantom outline indicates stock to be removed.
5. Thread diameters to be concentric with ℄ within 0.002 TIR.
6. All measurements in inches except as noted.

Fig. A-3 Cryostat Top Stem

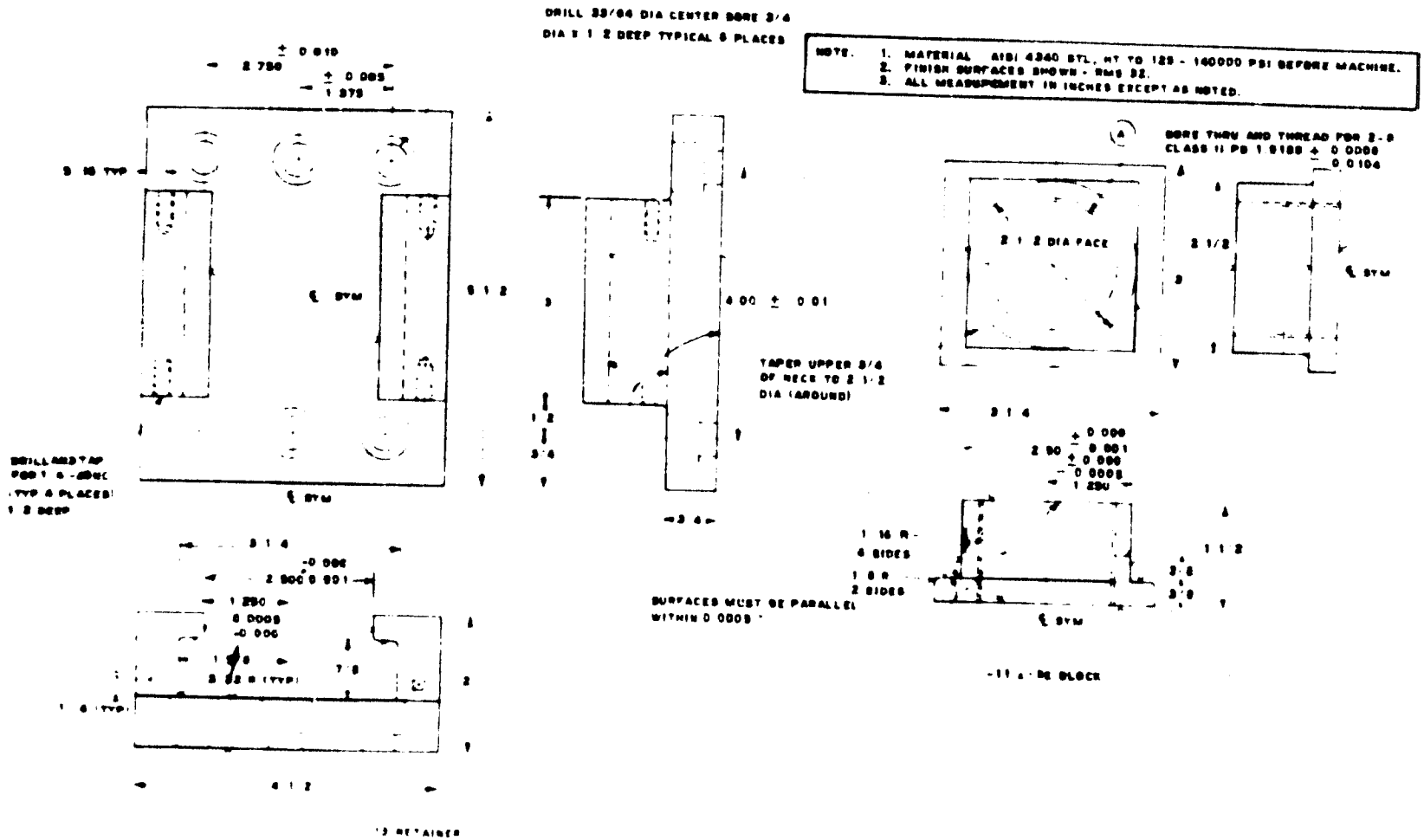

Fig. A-4 Lower Retainer Plate and Base Block

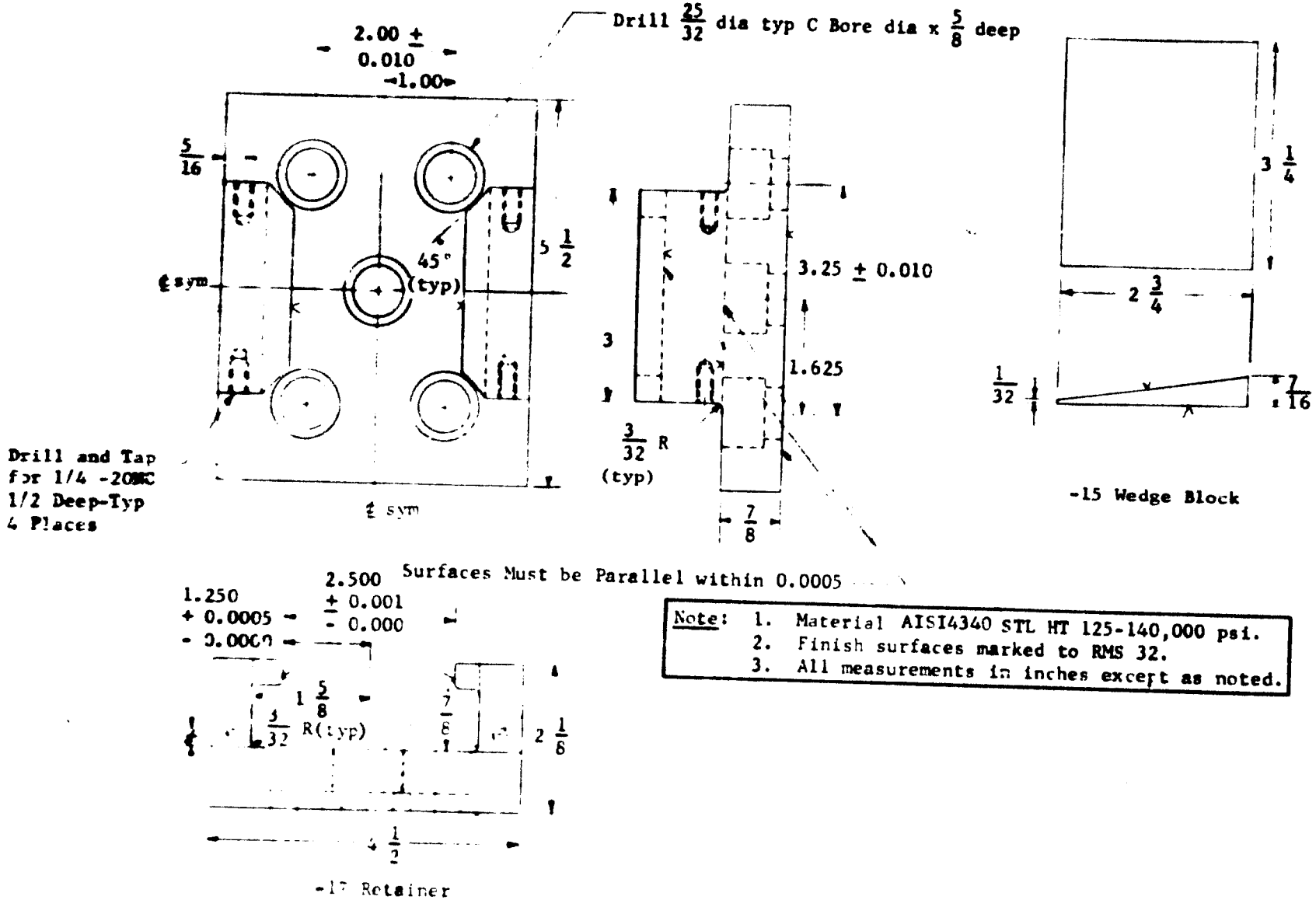

Note:
1. Material AISI4340 STL HT 125-140,000 psi.
2. Finish surfaces marked to RMS 32.
3. All measurements in inches except as noted.

Fig. A-5 Upper Retainer Plate and Wedge Block

Note:
1. Material 304/321 S/STL condition A.
2. Break all sharp edges.
3. Parts to be mated plus brazed to form rough block for -19 assembly.
4. All measurements in inches except as noted.

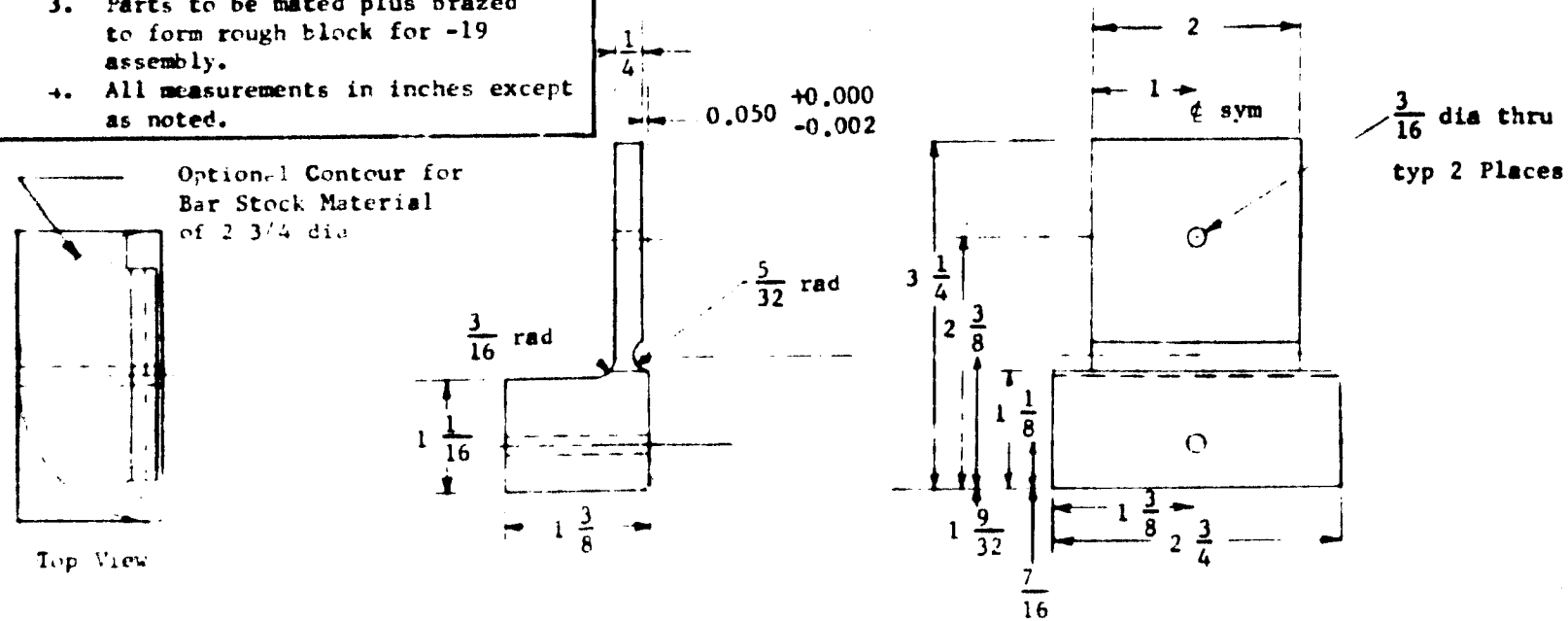

Fig. A-6 (a) Grip Block Half

Note:
1. Material 304/321 S/STL, condition A
2. Rough blank for -19 assembly shown.
3. Use of slit for initial alignment of part axis.
4. Braze joint location.
5. All measurements in inches except as noted.

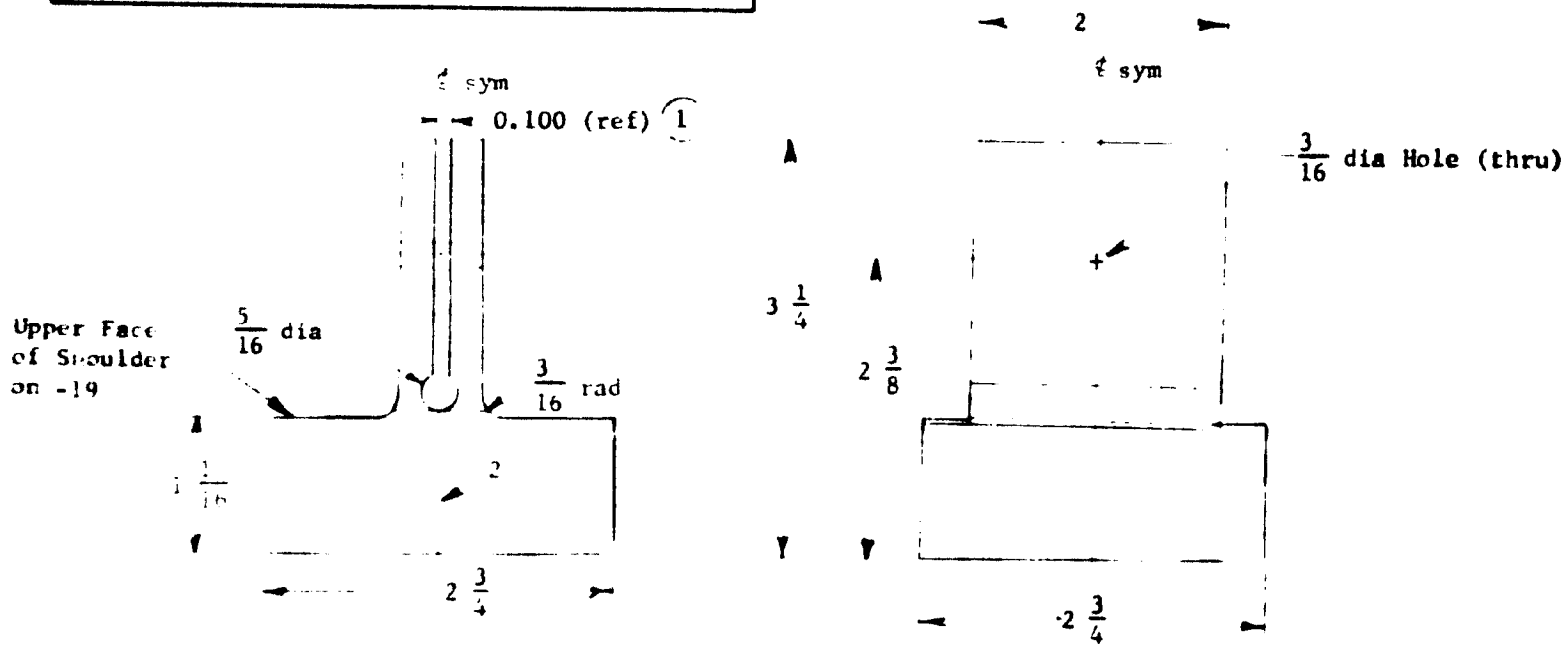

Fig. A-6 (b) Grip Block Assembly Rough Blank

Note:
1. Material AISI 321S/STL.
2. Parts to be finished machined from -7 halves after brazing.
3. Alignment determined initially from slot in stock blank.
4. All measurements in inches except as noted.

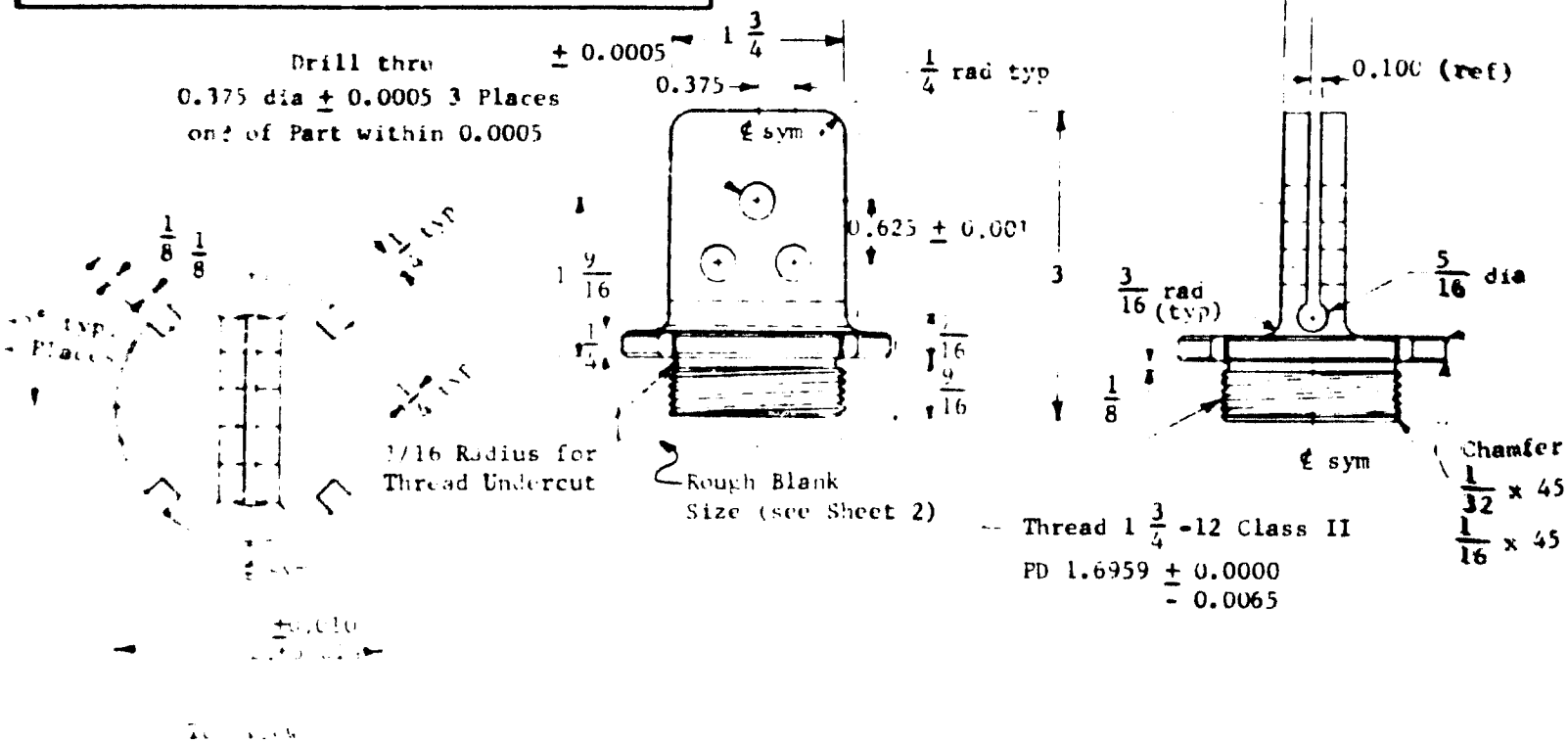

Fig. A-6 (c) Grip Block Assembly

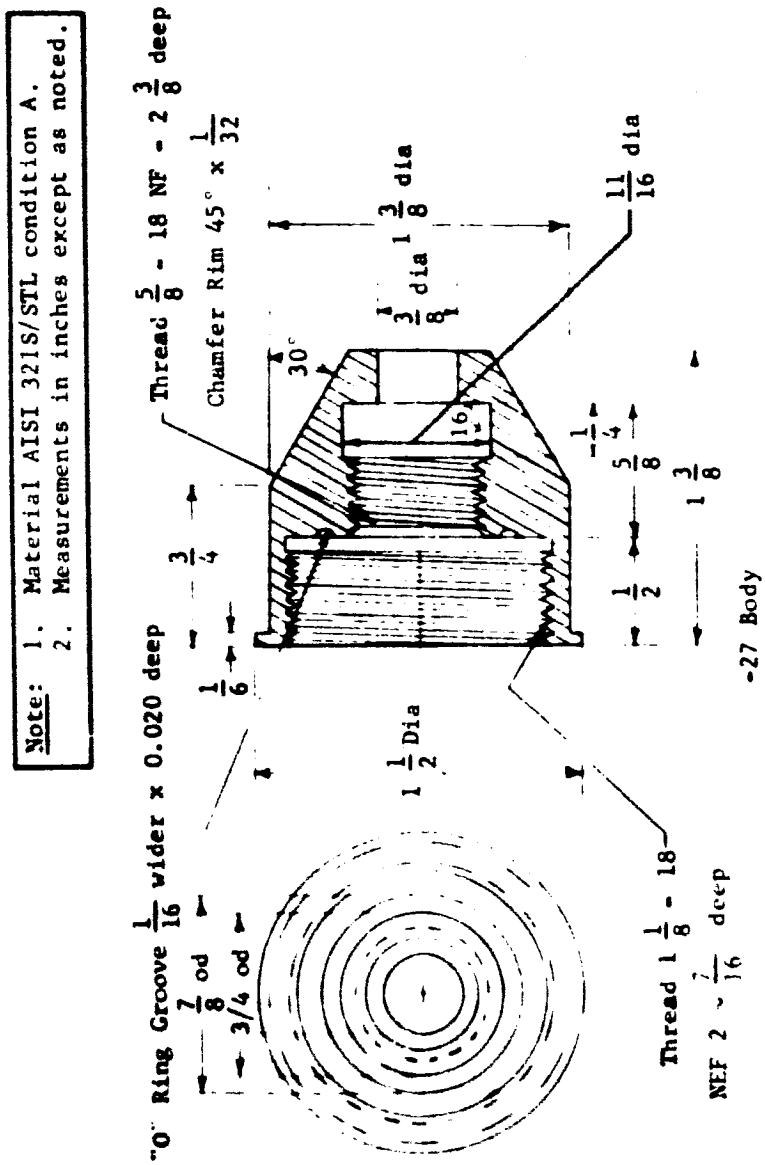

Fig. A-7 Vacuum Fitting-Cryostat Stem

APPENDIX B

TENSILE DATA

Table B-1 Tensile Properties of 2014-T6 Aluminum Alloy at Cryogenic Temperatures

Temperature (°F)	Ultimate Strength (ksi)	Yield Strength, 0.2% Offset (ksi)	Elongation in 2-in. (%)	Modulus of Elasticity, (psi x 10^6)	Weld Strength (ksi)	Notch Strength* (ksi)	Notch Strength Ratio
70	71.8 70.4 70.9 71.0 avg	67.3 66.3 65.9 66.5 avg	10.5 10.0 9.5 10.0 avg	10.6	55.1 55.3 59.0 56.5 avg	77.0 77.7 77.8 77.5 avg	1.09
-320	85.3 84.9 85.9 85.4 avg	76.4 75.8 75.8 76.0 avg	11.5 12.0 12.0 11.8 avg	11.7	66.2 64.6 67.0 65.9 avg	91.2 91.2 90.4 90.9 avg	1.06
-423	100.0 99.0 96.3 98.4 avg	83.0 82.8 80.7 82.2 avg	14.0 13.5 13.5 13.7 avg	12.3	74.3 72.2 69.5 68.5 71.2 70.5 71.1 avg	102.0 102.5 101.0 101.9 avg	1.04

*K_t = 3.5.

Table B-2 Tensile Properties of 2219-T87 Aluminum Alloy at Cryogenic Temperatures

Temperature (°F)	Ultimate Strength (ksi)	Yield Strength 0.2% Offset (ksi)	Elongation, in 2-in. (%)	Modulus of Elasticity, (psi x 10^6)	Weld Strength (ksi)	Notch Strength* (ksi)	Notch Strength Ratio
70	66.6 66.9 66.5 66.7 avg	55.2 55.7 55.2 55.4 avg	11.0 11.0 10.5 10.8 avg	10.5	45.2 50.4 50.6 48.7 avg	69.5 69.1 69.1 69.2 avg	1.04
-320	85.4 85.0 85.0 85.1 avg	65.3 66.0 66.0 65.8 avg	12.5 13.0 12.5 12.7 avg	11.6	63.2 61.0 63.0 62.4 avg	87.2 85.6 86.6 86.5 avg	1.02
-423	100.4 101.0 96.1 99.2 avg	71.0 70.6 68.5 70.0 avg	15.0 15.0 13.5 14.5 avg	12.5	72.2 65.9 70.0 65.5 68.7 64.2 67.7 avg	98.4 99.2 94.2 97.3 avg	0.98

*K_t = 3.5.

Table B-3 Tensile Properties of 2219-T62 Aluminum Alloy at Cryogenic Temperatures

Temperature (°F)	Ultimate Strength (ksi)	Yield Strength 0.2% Offset (ksi)	Elongation, in 2-in. (%)	Modulus of Elasticity, (psi x 10^6)	Weld Strength (ksi)	Notch Strength* (ksi)	Notch Strength Ratio
70	59.0 58.8 59.0 58.9 avg	41.5 41.2 42.2 41.6 avg	11.0 11.5 11.0 11.2 avg	10.2	45.0 45.7 46.7 45.8 avg	63.6 62.6 63.7 63.3 avg	1.07
-32°	76.6 79.9 76.9 [illegible] avg	51.9 59.3 54.0 55.3 avg	14.5 13.0 13.5 13.7 avg	11.1	54.7 53.4 53.5 53.9 avg	81.0 75.9 77.8 78.2 avg	1.01
-423	96.0 96.0 96.0 96.0 avg	[illegible] [illegible] [illegible] [illegible] avg	28.0 29.0 27.5 28.2 avg	11.7	63.6 61.0 64.1 62.9 avg	90.8 91.4 —— 91.1 avg	0.95

*K_t = 3.0

Table B-4. Tensile Properties of 70[illegible] Aluminum Alloy at Cryogenic Temperatures

Temperature (°F)	Ultimate Strength (ksi)	Yield Strength 0.2% Offset (ksi)	Elongation, in 2-in. (%)	Modulus of Elasticity, (psi × 10^6)	Weld Strength (ksi)	Notch Strength* (ksi)	Notch Strength Ratio
70	64.4	55.8	12.0	10.0	47.9	69.9	1.09
	64.5	58.4	12.5		45.2	70.0	
	63.4	58.7	13.0		46.6	69.6	
	64.0	58.6	12.5		46.8		
	64.5	59.0	12.0		49.5		
	64.0	58.2	12.5		44.5		
	64.1 avg	58.1 avg	12.4 avg		46.8 avg	69.8 avg	
-320	79.2	67.9	18.0	11.6	50.3	86.9	1.10
	79.9	68.2	20.0		48.0	87.3	
	80.0	68.5	19.0		56.7	87.3	
	77.7	64.7	18.5		55.8		
	78.0	64.7	20.0		57.3		
	79.0	67.5	19.5		53.6		
	78.9 avg	66.9 avg	19.1 avg		52.8 avg	87.2 avg	
-423	95.4	74.3	23.0	11.9	54.2		0.98
	95.3	74.0	25.1		56.3	94.0	
	95.1	73.1	23.5		51.1	93.6	
	94.5	74.7	23.0		54.2	93.0	
	97.4	73.7	24.0		55.0		
	94.7	74.0	23.5		51.9		
	95.4 avg	74.0 avg	23.7 avg		53.8 avg	93.5 avg	

*K_t = 3.5.

Table B-5 Tensile Properties of 5456-H343 Aluminum Alloy at Cryogenic Temperatures

Temperature (°F)	Ultimate Strength (ksi)	Yield Strength 0.2% Offset (ksi)	Elongation, in 2-in. (%)	Modulus of Elasticity, (psi x 10^6)	Weld Strength (ksi)	Notch Strength* (ksi)	Notch Strength Ratio
70	56.4 56.8 56.5 56.6 avg	43.2 43.6 43.7 43.5 avg	9.5 9.5 9.5 9.5 avg	10.3	52.0 52.3 50.0 51.4 avg	58.3 58.7 59.3 58.8 avg	1.04
-320	72.8 70.8 73.4 72.3 avg	50.7 50.7 50.5 50.6 avg	9.5 7.0 11.0 9.2 avg	11.4	58.5 61.9 57.8 59.4 avg	71.0 71.3 70.4 70.9 avg	0.98
-423	80.4 82.6 80.8 — 81.3 avg	53.9 54.1 54.0 — 54.0 avg	8.5 11.5 9.5 — 9.8 avg	11.7	54.8 58.0 55.9 52.8 53.5 57.3 55.4 avg	78.8 79.4 77.6 — 78.6 avg	0.97

*K_t = 3.5.

Table B-6 Tensile Properties of 7075-T6 Aluminum Alloy at Cryogenic Temperatures

Temperature (°F)	Ultimate Strength (ksi)	Yield Strength 0.2% Offset (ksi)	Elongation, in 2-in. (%)	Modulus of Elasticity, (psi x 10^6)	Notch Strength* (ksi)	Notch Strength Ratio
70	78.6 79.2 78.5 78.8 avg	71.4 72.5 70.8 71.6 avg	10.5 10.5 10.5 10.5 avg	10.2	96.0 95.8 96.2 96.0 avg	1.22
-320	98.2 99.1 99.5 98.9 avg	85.3 83.7 84.6 84.5 avg	12.5 11.5 10.0 11.3 avg	11.4	94.0 100.9 94.4 96.4 avg	0.97
-423	100.2 95.5 105.9 100.5 avg	88.4 82.1 87.8 86.1 avg	11.5 2.5† 10.5 11.0 avg of 2	11.9	92.7 91.9 83.0 89.2 avg	0.89

*K_t = 3.5.

†Failed through gage mark.

Table B-7 Tensile Properties of 2020-T6 Aluminum Alloy at Cryogenic Temperatures

Temperature (°F)	Ultimate Strength (ksi)	Yield Strength 0.2% Offset (ksi)	Elongation, in 2-in. (%)	Modulus of Elasticity, (psi x 10^6)
70	82.7 82.3 82.7 82.6 avg	78.9 77.7 79.1 78.6 avg	8.0 8.0 8.0 8.0 avg	11.1
-320	97.5 97.1 98.0 97.5 avg	87.0 87.2 87.6 87.3 avg	7.0 7.0 7.5 7.2 avg	12.3
-423	110.3 110.0 128.0 116.1 avg	94.8 94.6 100.9 96.8 avg	10.0 10.0 12.5 10.8 avg	13.6

Table B-8 Tensile Properties of 5Al-2.5Sn Titanium Alloy at Cryogenic Temperatures

Temperature (°F)	Ultimate Strength (ksi)	Yield Strength 0.2% Offset (ksi)	Elongation, in 2-in. (%)	Modulus of Elasticity, (psi x 10^6)	Weld Strength (ksi)	Notch Strength* (ksi)	Notch Strength Ratio
70	114.5 116.3 115.9 115.6 avg	106.7 106.9 108.9 107.5 avg	16.5 16.0 16.5 16.3 avg	15.8	113.1 111.7 112.8 112.5 avg	157.5 157.6 158.5 157.9 avg	1.37
-320	185.5 185.7 185.9 185.7 avg	173.4 173.2 173.4 173.3 avg	19.5 18.8 19.3 19.2 avg	17.4	183.7 181.9 181.6 182.4 avg	239.0 225.0 238.4 234.1 avg	1.26
-423	226.9 237.4 236.7 233.6 avg	--† 211.3 --† 211.3 avg	2.0 2.0 2.0 2.0 avg	--	245.2 216.9 220.1 227.4 avg	273.2 226.7 269.8 256.6 avg	1.10

*K_t = 3.5.

†Strain gage failed.

Table B-9 Tensile Properties of Solution Treated and Aged 6Al-4V Titanium Alloy at Cryogenic Temperatures

Temperature (°F)	Ultimate Strength (ksi)	Yield Strength 0.2% Offset (ksi)	Elongation, in 2-in. (%)	Modulus of Elasticity, (psi x 10^6)	Weld Strength (ksi)	Notch Strength* (ksi)	Notch Strength Ratio
70	165.4 165.4 165.0 165.3 avg	154.3 154.4 153.2 154.0 avg	17.5 16.0 16.5 16.7 avg	16.1	150.7 148.0 ——— 149.4 avg	190.8 190.8 190.7 190.8 avg	1.15
-320	242.7 242.7 243.2 243.0 avg	--† 228.2 230.1 229.2 avg	8.3 10.5 9.8 9.5 avg	17.5	236.0 235.2 231.8 234.3 avg	277.3 276.9 244.0 266.1 avg	1.09
-423	297.7 295.7 296.5 296.6 avg	282.1 --† 284.9 283.5 avg	2.5 2.5 2.5 2.5 avg	--	277.5 280.4 268.3 275.4 avg	290.4 276.3 257.1 274.6 avg	0.93

*K_t = 3.5.

†Strain gage failed.

Table B-10 Tensile Properties of Solution Treated and Aged 13V-11Cr-3Al Titanium Alloy at Cryogenic Temperatures

Temperature (°F)	Ultimate Strength (ksi)	Yield Strength 0.2% Offset (ksi)	Elongation, in 2-in. (%)	Modulus of Elongation (psi x 10^6)	Weld Strength (ksi)
70	206.0 197.2 195.2 199.5 avg	-- 184.3 181.3 182.8 avg of 2	5.5 7.0 7.0 6.5 avg	16.1	143.8 143.5 145.9 144.4 avg
-320	218.0 185.0 201.0	-- -- --	--* --* --†	16.8	125.6 (95.7) 129.8 127.7 avg of 2
-423	--	--	--	--	81.3 88.3 (49.5) 84.8 avg of 2

*Failed through pinhole.

†Failed outside gage mark.

Table B-11 Tensile Properties of 321 Stainless Steel Alloy at Cryogenic Temperatures

Temperature (°F)	Ultimate Strength (ksi)	Yield Strength 0.2% Offset (ksi)	Elongation, in 2-in. (%)	Modulus of Elasticity, (psi x 10^6)	Weld Strength (ksi)	Notch Strength* (ksi)	Notch Strength Ratio
70	85.5 86.6 86.3 86.1 avg	37.4 38.4 38.3 38.0 avg	53.0 55.0 58.0 55.3 avg	26.0	86.8 86.8 86.6 86.7 avg	90.1 90.2 90.8 90.4 avg	1.05
-320	205.3 206.4 206.1 205.9 avg	44.8 45.2 43.0 44.3 avg	46.5 47.5 46.0 46.7 avg	29.5	208.0 208.8 198.3 205.0 avg	225.4 217.1 219.3 220.6 avg	1.07
-423	253.5 235.2 --‡ 244.5 avg	52.5 --† 52.8 52.6 avg	44.0 29.0 --‡ 36.0 avg	30.7	115.0 118.7 155.0 129.6 avg	212.1 153.4 180.9 182.1 avg	0.77

*K_t = 3.5.

†Strain gage failed.

‡Failed in bearing.

APPENDIX C

FATIGUE DATA

Table C-1 Fatigue Properties[a] of Parent Metal 2014-T6 Aluminum Alloy

Temperature					
70°F		-320°F		-423°F	
Maximum Tension Stress (1000 psi)	Cycles to Failure	Maximum Tension Stress (1000 psi)	Cycles to Failure	Maximum Tension Stress (1000 psi)	Cycles to Failure
50.0	3.00×10^3	65.0	1.80×10^3	65.0	1.00×10^3
50.0	4.00×10^3	65.0	2.00×10^3	65.0	1.00×10^3
50.0	5.00×10^3	65.0	2.60×10^3	65.0	8.00×10^3 [b]
40.0	2.00×10^4	50.0	3.33×10^4	62.5	1.50×10^4
40.0	2.50×10^4	50.0	4.17×10^4	62.5	2.60×10^4
40.0	3.30×10^4	50.0	6.96×10^4	62.5	3.50×10^4
30.0	1.30×10^5	40.0	8.89×10^4	50.0	2.76×10^5
30.0	1.57×10^5	40.0	9.50×10^4	50.0	3.70×10^5
30.0	3.45×10^5	40.0	1.10×10^5	50.0	4.17×10^5
[illegible]	1.25×10^5	30.0	2.00×10^5	45.0	1.22×10^6
[illegible]	1.76×10^5	30.0	2.58×10^5	45.0	1.12×10^6 (disc)
[illegible]	5.62×10^5	30.0	2.73×10^5	45.0	1.00×10^6 (disc)
[illegible]	1.20×10^7 (disc)	25.0	1.07×10^6		
20.0	1.19×10^7 (disc)	25.0	2.54×10^6		
17.5	6.62×10^5	25.0	5.02×10^6 (disc)		
17.5	1.03×10^6				
[illegible]	5.41×10^5				
[illegible]	1.28×10^6				
[illegible]	2.00×10^6 (disc)				
[illegible]	8.70×10^6 (disc)				

a. Axial load R = -1.
b. Specimen previously run at 45,000 psi for 1.12×10^6 cylces without failure.

Table C-2 Fatigue Properties[a] of Notched[b] 2014-T6 Aluminum Alloy

Temperature					
70°F		-320°F		-423°F	
Maximum Tension Stress (1000 psi)	Cycles to failure	Maximum Tension Stress (1000 psi)	Cycles to Failure	Maximum Tension Stress (1000 psi)	Cycles to Failure
32.0	1.00×10^3	25.0	4.90×10^3 [c]	40.0	1.00×10^3 [f]
30.0	2.00×10^3	25.0	6.20×10^3	35.0	2.00×10^3
28.0	3.00×10^3	25.0	6.30×10^3	30.0	5.00×10^3 [g]
25.0	5.00×10^3	25.0	6.60×10^3 [d]	27.5	9.00×10^3 [h]
25.0	8.00×10^3	25.0	7.20×10^3 [e]	25.0	1.70×10^4
20.0	1.30×10^4	20.0	1.33×10^4	20.0	3.00×10^4
20.0	2.50×10^4	15.0	3.57×10^4	17.5	2.10×10^4
18.0	2.10×10^4	15.0	6.11×10^4	17.5	5.40×10^4
15.0	6.60×10^4	10.0	9.78×10^4	15.0	9.70×10^4
12.0	1.13×10^5	10.0	1.74×10^5	12.5	2.40×10^5
11.0	1.34×10^5	10.0	1.79×10^5	10.0	6.60×10^5
10.0	5.09×10^5	10.0	4.16×10^5	7.5	6.10×10^5
7.0	1.25×10^6 (disc)	10.0	2.04×10^6 (disc)	5.0	1.00×10^6 (disc)
6.0	1.24×10^6 (disc)	10.0	2.13×10^6 (disc)	5.0	1.02×10^6 (disc)
5.0	1.14×10^6 (disc)	8.0	4.05×10^5	5.0	1.07×10^6 (disc)
		6.0	1.12×10^6 (disc)		

a. Stress ratio (R) = -1.
b. Stress concentation (K_t) = 3.5.
c. thru h. Specimen previously run at indicated stress for number of cycles shown without failure.

Footnote	Stress (psi)	Cycles
c.	10,000	2.04×10^6
d.	6,000	1.12×10^6
e.	10,000	2.13×10^6
f.	5,000	1.00×10^6
g.	5,000	1.07×10^6
h.	5,000	1.02×10^6

Table C-3 Fatigue Properties[a] of Welded 2014-T6 Aluminum Alloy

Temperature					
70°F		-320°F		-423°F	
Maximum Tension Stress (1000 psi)	Cycles to Failure	Maximum Tension Stress (1000 psi)	Cycles to Failure	Maximum Tension Stress (1000 psi)	Cycles to Failure
30.0	2.00×10^3	35.0	1.00×10^2	50.0	5.00×10^2
35.0	7.00×10^3	32.0	2.00×10^3	40.0	2.00×10^3
30.0	1.00×10^4	30.0	1.05×10^4	40.0	3.00×10^3
22.0	1.50×10^4	30.0	2.74×10^4	40.0	6.00×10^3
22.0	2.10×10^4	30.0	2.75×10^4	40.0	6.00×10^3[b]
22.0	6.90×10^4	20.0	2.51×10^5	35.0	1.80×10^4
15.0	1.70×10^5	20.0	3.42×10^5	35.0	6.80×10^4
15.0	3.29×10^5	20.0	5.51×10^5	35.0	8.40×10^4
15.0	5.14×10^5	10.0	1.59×10^6 (disc)	30.0	1.82×10^5
9.0	1.02×10^6 (disc)	10.0	3.30×10^6 (disc)	30.0	2.65×10^5
9.0	1.03×10^6 (disc)	10.0	5.29×10^6 (disc)	30.0	3.18×10^5
9.0	1.03×10^6 (disc)			25.0	3.44×10^5
				17.5	1.01×10^6 (disc)
				17.5	1.03×10^6
				17.5	1.06×10^6

a. Axial load R = -1.
b. Specimen previously run at 17,500 psi for 1.01×10^6 cycles without failure.

Table C-4 Fatigue Properties[a] of Parent Metal 2219-T87 Aluminum Alloy

Temperature					
70°F		-320°F		-423°F	
Maximum Tension Stress (1000 psi)	Cycles to Failure	Maximum Tension Stress (1000 psi)	Cycles to Failure	Maximum Tension Stress (1000 psi)	Cycles to Failure
50.0	9.00×10^2	55.0	6.00×10^2	62.5	1.50×10^3
40.0	3.00×10^3	55.0	1.70×10^3	62.5	3.00×10^3
40.0	3.00×10^3	55.0	1.90×10^3	62.5	4.00×10^3[c]
40.0	4.00×10^3	35.0	4.51×10^4	62.5	7.00×10^3
40.0	9.90×10^3	35.0	6.46×10^4	62.5	7.50×10^3
40.0	1.49×10^4	35.0	8.02×10^4	55.0	4.40×10^4
40.0	2.27×10^4	35.0	1.16×10^5	55.0	6.60×10^4
35.0	2.43×10^4	30.0	1.01×10^5	55.0	8.90×10^4
35.0	2.82×10^4	25.0	1.05×10^6[b]	50.0	1.24×10^5
35.0	3.19×10^4	25.0	2.05×10^6[b]	47.5	1.73×10^5
30.0	4.86×10^4	20.0	5.21×10^6 (disc)	47.5	1.74×10^5
30.0	1.40×10^5	15.0	1.05×10^6	47.5	3.05×10^5
30.0	1.66×10^5	15.0	2.21×10^6	40.0	7.95×10^5
25.0	1.80×10^5	15.0	2.31×10^6	40.0	1.46×10^6 (disc)
25.0	3.08×10^5			40.0	1.46×10^6 (disc)
25.0	6.76×10^5				
22.5	3.56×10^5				
22.5	9.52×10^5				
22.5	3.40×10^6				
20.0	4.45×10^6				
20.0	1.24×10^7 (disc)				

a. Axial load R = -1.
b. Failed through pinholes.
c. Specimen previously run at 40,000 psi for 1.46×10^6 cycles without failure.

Table C-5 Fatigue Properties[a] of Notched[b] 2219-T87 Aluminum Alloy

Temperature					
70°F		-320°F		-423°F	
Maximum Tension Stress (1000 psi)	Cycles to Failure	Maximum Tension Stress (1000 psi)	Cycles to Failure	Maximum Tension Stress (1000 psi)	Cycles to Failure
32.0	1.00×10^3	27.5	2.10×10^3	35.0	1.00×10^3
30.0	1.50×10^3	25.0	3.50×10^3	30.0	2.00×10^3[f]
30.0	1.60×10^4[c]	25.0	4.30×10^3[e]	29.0	5.00×10^3[g]
25.0	4.00×10^3	22.5	7.8×10^3	27.5	8.00×10^3[h]
25.0	4.00×10^3[d]	20.0	1.95×10^4	25.0	1.20×10^4
20.0	1.00×10^4	15.0	4.90×10^4	22.5	1.00×10^4
15.0	3.30×10^4	10.0	7.63×10^4	22.5	1.50×10^4
12.0	9.70×10^4	10.0	8.89×10^4	20.0	2.80×10^4
10.0	1.60×10^5	10.0	7.61×10^5	17.5	3.90×10^4
9.0	5.63×10^5	7.5	3.09×10^5	15.0	1.04×10^5
8.0	7.30×10^5	7.0	3.98×10^5	12.5	1.72×10^5
8.0	1.10×10^6 (disc)	7.0	4.66×10^5	10.0	4.34×10^5
7.0	1.15×10^6 (disc)	5.0	1.07×10^6	7.0	1.00×10^6 (disc)
7.0	7.32×10^6	6.0	6.94×10^6 (disc)	7.0	1.01×10^6 (disc)
				7.0	1.02×10^6 (disc)

a. Stress ratio (R) = -1.
b. Stress concentration (K_t) = 3.5.
c. thru h. Specimen previously run at indicated stress for number of cycles shown without failure.

Footnote	Stress (psi)	Cycles
c.	8,000	1.10×10^6
d.	7,000	1.15×10^6
e.	6,000	6.94×10^6
f.	7,000	1.01×10^6
g.	7,000	1.02×10^6
h.	7,000	1.00×10^6

Table C-6 Fatigue Properties[a] of Welded 2219-T87 Aluminum Alloy

Temperature					
70°F		-320°F		-423°F	
Maximum Tension Stress (1000 psi)	Cycles to Failure	Maximum Tension Stress (1000 psi)	Cycles to Failure	Maximum Tension Stress (1000 psi)	Cycles to Failure
30.0	1.00×10^3	32.0	3.10×10^3	45.0	1.00×10^3
30.0	6.00×10^3	32.0	5.50×10^3	45.0	1.00×10^3
30.0	9.00×10^3	32.0	5.70×10^3	45.0	2.00×10^3
20.0	2.40×10^4	25.0	4.10×10^4	45.0	2.00×10^3[b]
20.0	3.30×10^4	25.0	4.74×10^4	45.0	5.00×10^3[c]
20.0	5.30×10^4	25.0	5.14×10^4	42.5	1.70×10^4
15.0	7.90×10^4	17.5	1.89×10^5	40.0	3.50×10^4
15.0	1.94×10^5	17.5	3.19×10^5	35.0	5.50×10^4
15.0	2.09×10^5	17.5	5.41×10^5	35.0	7.40×10^4
10.0	2.04×10^6	12.5	9.93×10^5	35.0	1.17×10^5
10.0	1.22×10^6	12.5	3.27×10^6	30.0	2.15×10^5
10.0	1.04×10^7 (disc)	12.5	4.57×10^6	30.0	2.36×10^5
				30.0	4.22×10^5
				22.5	7.78×10^6
				22.5	1.04×10^6 (disc)
				22.5	1.13×10^6 (disc)

a. Axial load R = -1.

b. Specimen previously run at 22,500 psi for 1.04×10^6 cycles without failure.

c. Specimen previously run at 22,500 psi for 1.13×10^6 cycles without failure.

Table C-7 Fatigue Properties[a] of Parent Metal 2219-T62 Aluminum Alloy

Temperature					
70°F		320°F		-423°F	
Maximum Tension Stress (1000 psi)	Cycles to Failure	Maximum Tension Stress (1000 psi)	Cycles to Failure	Maximum Tension Stress (1000 psi)	Cycles to Failure
36.0	4.00×10^3	45.0	7.00×10^2[d]	65.0	1.00×10^3
35.0	5.00×10^3	45.0	1.30×10^3	62.0	2.00×10^3[g]
34.0	5.00×10^3	43.0	1.50×10^3[e]	60.0	4.00×10^3[h]
32.0	1.00×10^3	43.0	1.90×10^3	60.0	8.00×10^3
30.0	1.50×10^4	43.0	2.60×10^3	57.0	7.00×10^3[i]
30.0	1.50×10^4[b]	40.0	5.50×10^3[f]	55.0	1.20×10^4
30.0	3.20×10^4[c]	40.0	9.90×10^3	50.0	3.80×10^4
25.0	6.30×10^4	40.0	1.23×10^4	50.0	9.00×10^4
22.0	3.32×10^5	35.0	2.37×10^4	45.0	5.70×10^4
20.0	2.70×10^5	35.0	3.85×10^4	45.0	8.50×10^4
19.0	7.27×10^5	30.0	1.35×10^5	40.0	$3.93 \quad 10^5$
18.5	1.43×10^6	30.0	1.58×10^5	40.0	4.42×10^5
18.0	3.45×10^6 (disc)	25.0	2.75×10^5	35.0	1.02×10^6 (disc)
15.0	3.14×10^5 (disc)	25.0	8.68×10^5	35.0	1.04×10^6 (disc)
		20.0	7.68×10^5	35.0	1.12×10^6 (disc)
		20.0	1.33×10^6		
		18.0	1.68×10^6 (disc)		
		18.0	2.02×10^6 (disc)		
		18.0	2.23×10^6 (disc)		

a. Stress ratio (R) = -1.
b. thru i. Specimen previously run at indicated stress for number of cycles shown without failure.

Footnote	Stress (psi)	Cycles
b.	15,000	3.14×10^6
c.	18,000	3.45×10^6
d.	18,000	2.02×10^6
e.	18,000	2.23×10^6
f.	18,000	1.68×10^6
g.	35,000	1.12×10^6
h.	35,000	1.04×10^6
i.	35,000	1.02×10^6

Table C-8 Fatigue Properties[a] of Notched[b] 2219-T62 Aluminum Alloy

Temperature					
70°F		-320°F		-423°F	
Maximum Tension Stress (1000 psi)	Cycles to Failure	Maximum Tension Stress (1000 psi)	Cycles to Failure	Maximum Tension Stress (1000 psi)	Cycles to Failure
25.0	2.00×10^3 [c]	30.0	1.20×10^3	40.0	1.00×10^3
20.0	4.00×10^3 [d]	30.0	2.30×10^3 [f]	35.0	2.00×10^3
20.0	5.00×10^3 [e]	20.0	1.20×10^4 [g]	30.0	4.00×10^3 [i]
20.0	6.00×10^3	20.0	1.29×10^4 [h]	25.0	5.00×10^3
20.0	7.00×10^3	10.0	7.43×10^4	22.5	7.00×10^3
15.0	2.20×10^4	10.0	1.05×10^5	20.0	1.70×10^4
15.0	2.80×10^4	10.0	3.70×10^5	17.0	2.20×10^4
15.0	3.00×10^4	7.0	3.45×10^5	16.5	2.80×10^4 [j]
10.0	1.06×10^5	7.0	5.55×10^5	15.0	7.40×10^4
10.0	1.14×10^5	5.0	1.11×10^6 (disc)	12.5	1.37×10^5
[illegible]	3.45×10^5	5.0	1.13×10^6 (disc)	10.0	3.85×10^5
[illegible]	8.78×10^5	5.0	1.20×10^6 (disc)	7.5	1.03×10^6 (disc)
[illegible]	1.15×10^6 (disc)			7.0	9.20×10^5
[illegible]	1.26×10^6 (disc)			6.0	1.03×10^6 (disc)
6.0	1.52×10^6 (disc)				

a. Stress ratio (R) = -1.
b. Stress concentration $(K_t) = 3.5$.
c. thru j. Specimen previously run at indicated stress for number of cycles shown without failure.

Footnote	Stress (psi)	Cycles
c.	6,000	1.52×10^6
d.	7,500	1.26×10^6
e.	7,500	1.15×10^6
f.	5,000	1.70×10^6
g.	5,000	1.11×10^6
h.	5,000	1.13×10^6
i.	6,000	1.03×10^6
j.	7,500	1.03×10^6

Table C-9 Fatigue Properties[a] of Welded 2219-T62 Aluminum Alloy

Temperature					
70°F		-320 F		-423°F	
Maximum Tension Stress (1000 psi)	Cycles to Failure	Maximum Tension Stress (1000 psi)	Cycles to Failure	Maximum Tension Stress (1000 psi)	Cycles to Failure
30.0	1.00×10^3	40.0	1.4×10^3 [d]	50.0	1.00×10^3
30.0	1.00×10^3 [b]	40.0	1.7×10^3 [e]	50.0	2.00×10^3
30.0	2.00×10^3 [c]	40.0	3.5×10^3	50.0	3.00×10^3 [g]
27.0	8.00×10^3	40.0	4.1×10^3	47.5	4.00×10^3 [h]
27.0	1.10×10^4	30.0	1.15×10^4 [f]	45.0	9.00×10^3
20.0	5.70×10^4	30.0	2.21×10^4	42.5	1.20×10^4 [i]
20.0	7.60×10^4	30.0	4.28×10^4	41.0	2.00×10^4
20.0	7.80×10^4	30.0	5.14×10^4	40.0	3.60×10^4
15.0	1.54×10^5	20.0	2.10×10^5	35.0	1.00×10^5
15.0	3.03×10^5	20.0	4.83×10^5	30.0	3.60×10^4
15.0	3.20×10^5	17.0	3.40×10^5	30.0	2.55×10^5
12.0	1.19×10^6	15.0	1.11×10^6	28.5	6.57×10^5
12.0	1.50×10^6 (disc)	15.0	1.81×10^6	25.0	4.62×10^5
10.0	1.30×10^6 (disc)	15.0	1.20×10^6	25.0	1.02×10^6 (disc)
10.0	1.46×10^6			22.5	1.00×10^6 (disc)
				22.5	1.08×10^6 (disc)

a. Stress ratio (R) = -1.
b. thru i. Specimen previously run at indicated stress for number of cycles shown without failure.

Footnote	Stress (psi)	Cycles
b.	12,000	1.50×10^6
c.	10,000	1.30×10^6
d.	15,000	1.11×10^6
e.	15,000	1.81×10^6
f.	15,000	1.20×10^6
g.	22,500	1.00×10^6
h.	25,000	1.02×10^6
i.	22,500	1.08×10^6

Table C-10 Fatigue Properties[a] of Parent Metal 7039-T6 Aluminum Alloy

Temperature					
70 F		-320°F		-423°F	
Maximum Tension Stress (1000 psi)	Cycles to Failure	Maximum Tension Stress (1000 psi)	Cycles to Failure	Maximum Tension Stress (1000 psi)	Cycles to Failure
80.0	4.00×10^3 [b]	75.0	1.00×10^3	75.0	1.00×10^3 [i]
70.0	9.00×10^3 [c]	70.0	2.00×10^3	70.0	4.00×10^3 [j]
60.0	1.10×10^4 [d]	65.0	4.00×10^3 [f]	65.0	7.00×10^3
50.0	1.40×10^4	60.0	7.00×10^3 [g]	60.0	1.60×10^4
45.0	2.20×10^4	55.0	1.00×10^4	55.0	1.40×10^4 [k]
35.0	2.40×10^4	52.0	1.20×10^4 [h]	50.0	3.60×10^4
30.0	3.30×10^4	50.0	2.90×10^4	47.5	5.50×10^4
30.0	6.30×10^4	45.0	3.90×10^4	45.0	1.97×10^5
[illegible]	$.60 \times 10^4$	42.5	6.70×10^4	40.0	1.01×10^5
20.0	2.04×10^5	40.0	1.31×10^5	40.0	4.31×10^5
[illegible]	1.27×10^6 (disc)	[illegible]	3.77×10^5	40.0	1.02×10^6 (disc)
[illegible]	1.21×10^6 (disc)	22.5	9.28×10^5	37.5	1.00×10^6 (disc)
17.0	1.26×10^6 (disc)	30.0	1.00×10^6 (disc)	37	1.02×10^6 (disc)
17.0	1.29×10^6 (disc)	30.0	1.02×10^6 (disc)		
	-	30.0	1.78×10^6 (disc)		

a. Stress ratio (R) = -1.

b. thru k. Specimen previously run at indicated stress for number of cycles shown without failure.

Footnote	Stress (psi)	Cycles
b.	17,000	1.29×10^6
c.	17,000	1.26×10^6
d.	18,000	1.21×10^6
e.	20,000	1.27×10^6
f.	30,000	1.02×10^6
g.	30,000	1.00×10^6
h.	[illegible],000	1.78×10^6
i.	37,000	1.02×10^6
j.	37,000	1.00×10^6
k.	40,000	1.02×10^6

Table C-11 Fatigue Properties[a] of Notched[b] 7039 T6 Aluminum Alloy

Temperature					
70°F		-320°F		-423°F	
Maximum Tension Stress (1000 psi)	Cycles to Failure	Maximum Tension Stress (1000 psi)	Cycles to Failure	Maximum Tension Stress (1000 psi)	Cycles to Failure
25.0	3.0×10^3	40.0	1.00×10^3	35.0	1.00×10^3[h]
[illegible]	4.0×10^3[c]	35.0	2.00×10^3[e]	30.0	3.00×10^3
25.0	5.0×10^3[d]	30.0	3.00×10^3[f]	25.0	4.00×10^3[i]
20.0	7.0×10^3	25.0	6.00×10^3	22.5	7.00×10^3[j]
20.0	7.0×10^3	22.5	8.00×10^3[g]	19.6	1.30×10^4
15.0	1.3×10^4	20.0	1.90×10^4	18.5	2.30×10^4
10.0	6.8×10^4	15.0	4.00×10^4	17.5	3.20×10^4
10.0	9.3×10^4	12.5	$6.[illegible] \times 10^4$	15.0	6.30×10^4
8.0	1.15×10^5	10.0	$1.6[illegible] \times 10^5$	12.5	8.60×10^4
8.0	3.68×10^5	8.5	2.04×10^5	11.0	2.65×10^5
7.0	8.84×10^5	7.5	7.05×10^5	9.0	2.61×10^5
6.0	1.481×10^6 (disc)	6.5	5.07×10^5	9.0	3.04×10^5
6.0	1.646×10^6 (disc)	6.5	1.00×10^6 (disc)	7.5	1.01×10^6 (disc)
6.0	3.397×10^6	6.0	1.00×10^6 (disc)	7.5	1.01×10^6 (disc)
		6.0	1.03×10^6 (disc)	7.5	1.03×10^6 (disc)

a. Stress ratio (R) = -1.
b. Stress concentration (K_t) = 3.5.
c. thru j. Specimen previously run at indicated stress for number for cycles whown without failure.

Footnote	Stress (psi)	Cycles
c.	6,000	1.481×10^6
d.	6,000	1.646×10^6
e.	6,000	1.00×10^6
f.	6,000	1.03×10^6
g.	6,000	1.00×10^6
h.	7,000	1.03×10^6
i.	7,500	1.01×10^6
j.	7,500	1.01×10^6

Table C-12 Fatigue Properties[a] Welded 2014-T6 Aluminum Alloy

Temperature					
70°F		-320°F		-423°F	
Maximum Tension Stress (1000 psi)	Cycles to Failure	Maximum Tension Stress (1000 psi)	Cycles to Failure	Maximum Tension Stress (1000 psi)	Cycles to Failure
30.0	4.0×10^3	40.0	1.00×10^3[e]	40.0	1.00×10^3
25.0	3.0×10^3[b]	35.0	1.00×10^3	40.0	2.00×10^3
25.0	8.0×10^3[c]	32.5	1.00×10^4	37.5	3.00×10^3[f]
25.0	8.0×10^3	30.0	1.40×10^4	36.0	5.00×10^3
20.0	9.0×10^3	27.5	4.00×10^4	36.0	8.00×10^3[g]
20.0	2.2×10^4[d]	25.0	2.10×10^4	35.0	2.30×10^4
15.0	3.05×10^4[b]	24.0	1.58×10^5	30.0	1.63×10^5
15.0	4.45×10^5[b]	22.5	3.36×10^5	25.0	2.90×10^5
15.0	7.65×10^4	20.0	5.08×10^5	25.0	7.10×10^5
12.0	2.48×10^5	18.0	8.86×10^5	22.5	5.62×10^5
10.0	1.46×10^5[b]	16.5	1.59×10^6	20.0	8.61×10^5
10.0	4.82×10^5	16.0	1.46×10^6	18.0	1.00×10^6 (disc)
9.0	1.135×10^6 (disc)	16.0	1.75×10^6 (disc)	18.0	1.04×10^6 (disc)
8.0	1.480×10^6 (disc)				
8.0	1.553×10^6 (disc)				

a. Stress ratio (R) = -1.
b. thru g. Specimen previously run at indicated stress for number of cycles shown without failure.

Footnote	Stress (psi)	Cycles
b.	8,000	1.135×10^6
c.	8,000	1.553×10^6
d.	8,000	1.480×10^6
e.	16,000	1.75×10^6
f.	[illegible]	1.00×10^6
g.	16,000	1.04×10^6

h. Specimen tested without wedges to preload ends.

Table C-13 Fatigue Properties[a] of Parent Metal 5456-H343 Aluminum Alloy

Temperature					
70°F		-320°F		-423°F	
Maximum Tension Stress (1000 psi)	Cycles to Failure	Maximum Tension Stress (1000 psi)	Cycles to Failure	Maximum Tension Stress (1000 psi)	Cycles to Failure
[illegible]	1.50×10^3	52.0	1.50×10^3	55.0	7.00×10^3
[illegible]	4.00×10^3	52.0	4.50×10^3	55.0	8.00×10^3
38.5	5.00×10^3	52.0	4.60×10^3	55.0	1.00×10^4
38.5	5.00×10^3	50.0	9.10×10^3	50.0	1.60×10^4
35.0	8.00×10^3	50.0	1.64×10^4	50.0	3.20×10^4
35.0	$1.[illegible] \times 10^4$	50.0	1.65×10^4	50.0	3.30×10^4
35.0	1.40×10^4	40.0	34.2×10^4	45.0	8.90×10^4
[illegible]	2.83×10^4	40.0	4.37×10^4	42.5	3.05×10^5
[illegible]	4.30×10^4	40.0	6.21×10^4	42.5	3.20×10^5
30.0	5.25×10^4	30.0	6.87×10^4	42.5	5.19×10^5
[illegible]	$[illegible].25 \times 10^4$	30.0	1.32×10^5	40.0	8.86×10^5 (disc)
[illegible]	1.70×10^5	30.0	2.38×10^5	40.0	9.07×10^5
[illegible]	4.59×10^5	25.0	7.94×10^5	40.0	1.52×10^6 (disc)
[illegible]	5.33×10^5	25.0	1.10×10^6		
[illegible]	1.00×10^6	25.0	4.43×10^6 (disc)		
[illegible]	1.69×10^6				
[illegible]	4.96×10^6 (disc)				

[a] Axial load R = -1.

Table C-14 Fatigue Properties[a] of Notched[b] 5456-H343 Aluminum Alloy

Temperature					
70°F		-320°F		-423°F	
Maximum Tension Stress (1000 psi)	Cycles to Failure	Maximum Tension Stress (1000 psi)	Cycles to Failure	Maximum Tension Stress (1000 psi)	Cycles to Failure
25.0	1.00×10^3	25.0	1.00×10^3 [c]	30.0	1.00×10^3
20.0	6.00×10^3	20.0	1.60×10^3 [d]	25.0	3.00×10^3
20.0	7.00×10^3	20.0	2.30×10^3	22.5	3.00×10^3 [f]
15.0	2.80×10^4	20.0	3.80×10^3	22.5	3.00×10^3
15.0	3.20×10^4	20.0	6.10×10^3 [e]	22.5	2.00×10^3 [g]
15.0	3.60×10^4	15.0	4.59×10^3	20.0	1.30×10^4
10.0	2.09×10^5	10.0	3.71×10^4	18.5	6.00×10^3 [h]
10.0	3.83×10^5	10.0	8.15×10^4	17.5	2.90×10^4
9.0	3.04×10^5	10.0	3.44×10^5	16.0	5.90×10^4
7.5	1.18×10^6	7.5	1.50×10^5	15.0	9.70×10^4
7.5	1.51×10^6 (disc)	7.5	2.24×10^5	14.0	1.09×10^5
6.0	7.23×10^6 (disc)	5.0	6.88×10^5	12.5	3.06×10^5
		4.0	1.66×10^6 (disc)	9.0	1.02×10^6 (disc)
		4.0	1.96×10^6 (disc)	9.0	1.05×10^6 (disc)
		3.0	1.70×10^6 (disc)	9.0	1.05×10^6 (disc)

a. Stress ratio (R) = -1.
b. Stress concentration (K_t) = 3.5.
c. thru h. Specimen previously run at indicated stress for number of cycles shown without failure.

Footnote	Stress (psi)	Cycles
c.	4,000	1.66×10^6
d.	4,000	1.96×10^6
e.	5,000	1.70×10^6
f.	9,000	1.02×10^6
g.	9,000	1.05×10^6
h.	9,000	1.05×10^6

Table C-15 Fatigue Properties[a] of Welded 5456-H343 Aluminum Alloy

Temperature					
70°F		-320°F		-423°F	
Maximum Tension Stress (1000 psi)	Cycles to Failure	Maximum Tension Stress (1000 psi)	Cycles to Failure	Maximum Tension Stress (1000 psi)	Cycles to Failure
[illegible]	2.00×10^3	32.0	2.60×10^3	40.0	1.20×10^4
30.0	2.00×10^3	32.0	4.80×10^3	35.0	3.00×10^3
30.0	3.00×10^3	32.0	8.40×10^3	35.0	6.00×10^3
20.0	1.60×10^4	25.0	1.44×10^4	35.0	2.70×10^4
20.0	2.20×10^4	25.0	2.54×10^4	30.0	2.40×10^4
20.0	4.50×10^4	25.0	4.94×10^4	30.0	8.70×10^4
[illegible]	2.45×10^5	17.0	2.04×10^5	30.0	9.90×10^4
13.8	3.33×10^5	17.0	2.62×10^5	25.0	3.30×10^5
13.8	3.90×10^5	17.0	4.21×10^5	25.0	4.12×10^5
10.0	5.35×10^5	12.0	1.41×10^6	17.5	1.00×10^6 (disc)
10.0	2.44×10^6	12.0	2.58×10^6	17.5	1.07×10^6 (disc)
10.0	3.71×10^6	12.0	5.23×10^6 (disc)	17.5	1.19×10^6

a. Axial load R = -1.

Table C-16 Fatigue Properties[a] of Parent Metal 7075-T6 Aluminum Alloy

Temperature					
70°F		-320°F		-423°F	
Maximum Tension Stress (1000 psi)	Cycles to Failure	Maximum Tension Stress (1000 psi)	Cycles to Failure	Maximum Tension Stress (1000 psi)	Cycles to Failure
63.0	1.50×10^3	60.0	2.20×10^3	80.0	1.00×10^3
63.0	1.80×10^3	60.0	5.50×10^3	80.0	1.00×10^3
63.0	2.00×10^3	60.0	6.70×10^3	80.0	1.00×10^3[b]
40.0	1.40×10^4	40.0	7.12×10^4	80.0	2.00×10^3
40.0	1.80×10^4	40.0	7.98×10^4	65.0	4.20×10^4
40.0	1.90×10^4	40.0	[illegible]	60.0	4.20×10^4
30.0	2.80×10^4	30.0	[illegible]	60.0	7.10×10^4
30.0	3.20×10^4	30.0	2.67×10^5	60.0	8.80×10^4
30.0	4.10×10^4	30.0	6.58×10^5	50.0	1.42×10^5
17.5	3.06×10^5	20.0	1.32×10^6	50.0	4.35×10^5
17.5	3.44×10^5	20.0	3.44×10^6	50.0	4.35×10^5
17.5	4.20×10^5	20.0	4.30×10^6	42.5	4.63×10^5
12.5	2.07×10^6	17.5	5.12×10^6 (disc)	37.5	4.05×10^6
12.5	2.57×10^6	17.5	5.35×10^6 (disc)	35.0	1.08×10^6
12.5	1.03×10^7 (disc)			35.0	1.11×10^6 (disc)
				35.0	1.20×10^6 (disc)

a. Axial load R = -1.
b. Specimen previously run at 35,000 psi for 1.11×10^6 cycles without failure.

Table C-1. Fatigue Properties[a] of Notched[b] 7075-T6 Aluminum Alloy

Temperature					
70°F		-320°F		-423°F	
Maximum Tension Stress (1000 psi)	Cycles to Failure	Maximum Tension Stress (1000 psi)	Cycles to Failure	Maximum Tension Stress (1000 psi)	Cycles to Failure
[illegible]	1.00×10^3	25.0	1.00×10^3 [f]	30.0	1.00×10^3
[illegible]	6.00×10^3	22.5	2.00×10^3 [g]	25.0	5.00×10^3
[illegible]	4.00×10^3 [c]	20.0	4.00×10^3 [h]	22.5	1.30×10^4 [i]
[illegible]	4.00×10^3 [d]	20.0	1.10×10^4	20.0	1.20×10^4
20.0	1.60×10^4	17.5	1.20×10^4	17.5	1.60×10^4
20.0	2.70×10^4	15.0	1.00×10^4	15.0	2.10×10^4
20.0	9.00×10^4 [e]	13.5	2.30×10^4	14.0	7.40×10^4
[illegible]	4.40×10^4	12.0	5.20×10^4	13.5	[illegible]
[illegible]	5.52×10^5	11.0	5.50×10^4	12.5	4.07×10^5
[illegible]	2.22×10^5	10.0	8.80×10^4	11.0	2.72×10^5
[illegible]	5.37×10^5	9.0	1.38×10^5	10.0	5.13×10^5
[illegible]	1.78×10^6 (disc)	7.5	2.32×10^5	10.0	1.02×10^6 (disc)
[illegible]	1.46×10^6 (disc)	5.0	9.70×10^5	10.0	1.07×10^6 (disc)
[illegible]	5.03×10^6 (disc)	[illegible]	1.35×10^6 (disc)		
		5.0	1.72×10^6 (disc)		

a. Stress ratio (R) = -1.
b. Stress concentration (K_t) = 3.5.
c. thru i. Specimen previously run at indicated stress for number of cycles shown without failure.

Footnote	Stress (psi)	Cycles
c.	7,500	5.03×10^6
d.	7,500	1.46×10^6
e.	7,500	5.37×10^6
f.	5,000	1.72×10^6
g.	5,000	1.88×10^6
h.	5,000	1.35×10^6
i.	10,000	1.07×10^6

Table C-18 Fatigue Properties[a] of Parent Metal 2020-T6 Aluminum Alloy

Temperature					
70°F		-320°F			-423°F
Maximum Tension Stress (1000 psi)	Cycles to Failure	Maximum Tension Stress (1000 psi)	Cycles to Failure	Maximum Tension Stress (1000 psi)	Cycles to Failure
50.0	2.00×10^3	70.0	1.00×10^3	70.0	3.00×10^3 [b]
50.0	2.00×10^3	70.0	1.20×10^3	67.5	4.00×10^3
50.0	4.00×10^3	70.0	2.30×10^3	67.5	1.50×10^4
40.0	8.00×10^3	50.0	2.90×10^4	60.0	1.70×10^4
40.0	9.00×10^3	50.0	4.31×10^4	60.0	2.10×10^4 [c]
40.0	1.00×10^4	50.0	9.23×10^4	60.0	2.90×10^4
30.0	4.80×10^4	40.0	7.42×10^4	60.0	4.30×10^4
30.0	8.50×10^4	40.0	7.70×10^4	57.3	8.60×10^4
30.0	9.30×10^4	40.0	1.22×10^5	50.0	1.16×10^5
20.0	1.25×10^5	40.0	1.97×10^5	50.0	1.53×10^5
20.0	1.49×10^5	30.0	1.16×10^5	50.0	1.99×10^5
20.0	1.60×10^5	30.0	2.49×10^5	42.5	7.75×10^5
18.0	1.76×10^6	30.0	3.27×10^5	40.0	1.09×10^6
18.0	3.90×10^6	30.0	1.22×10^6	40.0	1.41×10^6 (disc)
18.0	1.03×10^7 (disc)	22.5	1.37×10^6	40.0	1.50×10^6 (disc)
		22.5	2.13×10^6		
		22.5	4.16×10^6		

a. Axial load R = -1.
b. and c. Specimen previously run at indicated stress for number of cycles shown without failure.

Footnote	Stress (psi)	Cycles
b.	40,000	1.50×10^6
c.	40,000	1.41×10^6

Table C-19 Fatigue Properties[1] of Annealed Parent Metal 5Al-2.5Sn Titanium Alloy

Temperature					
70°F		-320°F		-423°F	
Maximum Tension Stress (1000 psi)	Cycles of Failure	Maximum Tension Stress (1000 psi)	Cycles to Failure	Maximum Tension Stress (1000 psi)	Cycles to Failure
125.0	6.00×10^2	180.0	1.00×10^2	220.0	1.00×10^{3}
[illegible]	1.00×10^3	180.0	3.10×10^3	220.0	1.00×10^{3}
[illegible]	6.00×10^3	180.0	4.80×10^3	220.0	1.00×10^{3}
[illegible]	8.00×10^3	175.0	3.00×10^3	220.0	3.00×10^{3}
135.0	1.30×10^4	160.0	6.90×10^3	220.0	3.00×10^{3}
125.0	2.00×10^4	160.0	4.53×10^4	200.0	1.30×10^{4}
100.0	5.30×10^4	150.0	1.35×10^4	180.0	3.00×10^{4}
100.0	8.10×10^4	150.0	2.35×10^4	170.0	4.00×10^{4}
75.0	1.88×10^5	150.0	9.11×10^4	160.0	2.30×10^{4}
75.0	2.04×10^5	120.0	6.46×10^4	140.0	9.00×10^{4}
75.0	2.71×10^5	120.0	7.40×10^4	130.0	1.15×10^{5}
70.0	1.36×10^6 (disc)	120.0	1.34×10^5	130.0	1.01×10^{5}
70.0	2.00×10^6 (disc)	119.5	6.75×10^4	130.0	2.85×10^5
[illegible]	2.00×10^6 (disc)	119.0	2.03×10^6	115.0	1.08×10^5
				105.0	3.79×10^5
				105.0	1.11×10^6 (disc)
				105.0	1.12×10^6 (disc)
				105.0	1.13×10^6 (disc)

[1] Axial load R = 0.02.

[illegible] Specimen previously run at indicated stress for number of cycles shown without failure.

Footnote	Stress (psi)	Cycles
b.	105,000	1.11×10^6
c.	105,000	1.12×10^6
d.	105,000	1.13×10^6

Table [illegible] Fatigue Properties[a] of Notched[b] 5Al-2.5Sn Titanium Alloy

Temperature					
70°F		-320°F		-423°F	
Maximum Tension Stress (1000 psi)	Cycles to Failure	Maximum Tension Stress (1000 psi)	Cycles to Failure	Maximum Tension Stress (1000 psi)	Cycles to Failure
70.0	4.00×10^3	110.0	1.00×10^3	100.0	2.00×10^3
70.0	5.00×10^3	90.0	4.00×10^3	90.0	2.00×10^3
70.0	5.00×10^3 [c]	80.0	4.00×10^3 [f]	80.0	3.00×10^3 [i]
60.0	7.00×10^3 [d]	70.0	7.00×10^3	70.0	7.00×10^3 [j]
60.0	9.00×10^3	65.0	1.03×10^4	60.0	9.00×10^3
60.0	1.10×10^4	60.0	2.80×10^4 [g]	55.0	1.50×10^4 [k]
60.0	2.10×10^4 [e]	55.0	2.70×10^4	50.0	6.10×10^4
50.0	2.60×10^4	50.0	5.70×10^4	45.0	6.30×10^4
50.0	3.20×10^4	45.0	6.10×10^4 [h]	40.0	1.07×10^5
50.0	2.14×10^5	40.0	2.81×10^5	35.0	1.14×10^5
45.0	2.29×10^5	35.0	2.11×10^5	30.0	2.13×10^5
40.0	1.14×10^6 (disc)	30.0	2.62×10^5	25.0	5.52×10^5
40.0	1.35×10^6 (disc)	28.0	2.43×10^6 (disc)	20.0	1.02×10^6 (disc)
35.0	1.47×10^6 (disc)	25.0	1.03×10^6 (disc)	20.0	1.06×10^6 (disc)
		25.0	2.61×10^6 (disc)	20.0	1.07×10^6 (disc)

a. Stress ratio (R) = 0.01.
b. Stress concentration (K_t) = 3.5.
c. thru k. Specimen previously run at indicated stress for number of cycles shown without failure.

Footnote	Stress (psi)	Cycles
c.	30,000	1.14×10^6
d.	30,000	1.47×10^6
e.	30,000	1.35×10^6
f.	25,000	1.03×10^6
g.	25,000	2.61×10^6
h.	28,000	2.43×10^6
i.	20,000	1.02×10^6
j.	20,000	1.06×10^6
k.	20,000	1.07×10^6

Table C-21 Fatigue Properties[a] of Annealed Welded 5Al-2.5Sn Titanium Alloy

Temperature					
70°F		-320°F		-423°F	
Maximum Tension Stress (1000 psi)	Cycles to Failure	Maximum Tension Stress (1000 psi)	Cycles to Failure	Maximum Tension Stress (1000 psi)	Cycles to Failure
105.0	5.00×10^3	155.0	5.00×10^3	144.0	9.00×10^3
105.0	1.00×10^4	150.0	6.00×10^3 [b]	130.0	8.00×10^3 [d]
105.0	1.20×10^4	125.0	1.80×10^4	120.0	5.00×10^3
90.0	1.10×10^4	110.0	2.60×10^4 [c]	100.0	1.90×10^4
90.0	2.30×10^4	95.0	2.60×10^4	90.0	2.60×10^4
90.0	3.00×10^4	85.0	1.24×10^4	85.0	5.40×10^4
72.0	6.40×10^4	82.5	5.90×10^4	75.0	6.80×10^4
70.0	4.79×10^5	82.5	6.70×10^4	70.0	4.60×10^4
70.0	1.15×10^6	80.0	6.90×10^4	70.0	1.71×10^5
70.0	2.30×10^6	80.0	1.15×10^6 (disc)	60.0	1.141×10^5
		77.5	1.09×10^5	60.0	1.12×10^6 (disc)
		77.5	1.10×10^6 (disc)		
		75.0	4.30×10^4		

a. Axial load, R = 0.01.
b. thru d. Specimen previously run at indicated stress for number of cycles shown without failure.

Footnote	Stress (psi)	Cycles
b.	77,500	1.10×10^6
c.	80,000	1.15×10^6
d.	60,000	1.12×10^6

Table C-22 Fatigue Properties[a] of Solution Treated and Aged Parent Metal 6Al-4V Titanium Alloy

Temperature					
70°F		-320°F		-423°F	
Maximum Tension Stress (1000 psi)	Cycles to Failure	Maximum Tension Stress (1000 psi)	Cycles to Failure	Maximum Tension Stress (1000 psi)	Cycles to Failure
150.0	7.50×10^3	182.0	2.50×10^3	180.0	1.00×10^3
150.0	9.50×10^3	182.0	4.80×10^3	180.0	8.00×10^3 [b]
150.0	1.40×10^4	182.0	1.02×10^4	180.0	1.30×10^4 [c]
135.0	1.70×10^4	160.0	1.22×10^4	180.0	1.90×10^4 [d]
135.0	1.90×10^4	160.0	1.86×10^4	170.0	2.30×10^4 [e]
135.0	2.00×10^4	160.0	2.44×10^4	160.0	1.60×10^4
85.0	1.00×10^5	118.0	2.79×10^4	160.0	2.20×10^4
85.0	1.32×10^5	100.0	5.19×10^4	160.0	3.10×10^4
85.0	3.24×10^5	100.0	8.01×10^4	143.0	3.40×10^4
70.0	2.59×10^5	100.0	8.31×10^5	140.0	3.90×10^4
70.0	1.97×10^6 (disc)	98.0	7.32×10^4	135.0	3.30×10^4
70.0	2.04×10^6 (disc)	96.0	6.29×10^4	135.0	3.40×10^4
		90.0	1.60×10^5	130.0	2.70×10^4
		90.0	3.60×10^5 (disc)	130.0	2.34×10^5
				130.0	1.02×10^6 (disc)
				125.0	1.21×10^6 (disc)
				110.0	1.12×10^6 (disc)
				110.0	1.13×10^6

a. Axial load R = 0.01.
b. thru e. Specimen previously run at indicated stress for number of cycles shown without failure.

Footnote	Stress (psi)	Cycles
b.	110,000	1.12×10^6
c.	110,000	1.13×10^6
d	130,000	1.02×10^6
e.	125,000	1.21×10^6

Table C-23 Fatigue Properties[a] of Notched[b] 6Al-4V Titanium Alloy

Temperature					
70°F		-320°F		-423°F	
Maximum Tension Stress (1000 psi)	Cycles to Failure	Maximum Tension Stress (1000 psi)	Cycles to Failure	Maximum Tension Stress (1000 psi)	Cycles to Failure
70.0	4.00×10^3	60.0	1.25×10^4 [f]	90.0	2.00×10^3 [g]
70.0	5.00×10^3 [c]	60.0	1.97×10^4	80.0	4.00×10^3 [h]
70.0	5.00×10^3 [d]	60.0	2.15×10^4	70.0	7.00×10^3 [i]
60.0	6.00×10^3	60.0	3.00×10^4	65.0	1.10×10^4
60.0	1.00×10^3 [e]	50.0	1.31×10^4	60.0	3.00×10^4
50.0	8.00×10^3	50.0	3.39×10^4	54.3	1.90×10^4
50.0	1.10×10^4	45.0	1.55×10^6	50.0	2.40×10^4
45.0	4.80×10^4	45.0	2.51×10^4 [j]	50.0	3.40×10^4
45.0	6.60×10^4	45.0	4.25×10^4	50.0	4.00×10^4
42.0	9.20×10^4	40.0	2.54×10^4 [j]	45.0	1.52×10^5
40.0	1.33×10^6 (disc)	40.0	1.16×10^5 [j]	32.5	1.05×10^6 (disc)
40.0	1.42×10^6 (disc)	40.0	2.45×10^5 [j]	30.0	8.9×10^4 [j]
40.0	4.73×10^6 (disc)	40.0	1.87×10^6 (disc)	28.0	1.00×10^6 (disc)
				28.0	1.00×10^6 (disc)

a. Stress ratio (R) = 0.01.
b. Stress concentration (K_t) = 3.5.
c. thru i. Specimen previously run at indicated stress for number of cycles shown without failure.

Footnote	Stress (psi)	Cycles
c.	40,000	4.73×10^6
d.	40,000	1.42×10^6
e.	40,000	1.33×10^6
f.	40,000	1.87×10^6
g.	28,000	1.00×10^6
h.	28,000	1.00×10^6
i.	32,500	1.05×10^6

j. The machine hydraulic load controller failed.

Table C-24 Fatigue Properties[a] of Solution Treated and Aged Welded 6Al-4V Titanium Alloy

Temperature					
70°F		-320°F		-423°F	
Maximum Tension Stress (1000 psi)	Cycles to Failure	Maximum Tension Stress (1000 psi)	Cycles to Failure	Maximum Tension Stress (1000 psi)	Cycles to Failure
150.0	3.00×10^3	160.0	7.00×10^3	130.0	7.00×10^3
140.0	4.00×10^3	150.0	5.00×10^3	130.0	1.10×10^4
140.0	4.00×10^3	145.0	5.00×10^3[b]	120.0	2.00×10^3[e]
100.0	2.30×10^4	140.0	1.00×10^3	125.0	8.00×10^3[f]
100.0	3.60×10^4	140.0	1.90×10^4[c]	120.0	7.00×10^3[g]
100.0	4.50×10^4	135.0	1.70×10^4	110.0	1.30×10^4
97.0	6.00×10^4	130.0	7.00×10^3	105.0	1.70×10^4
90.0	8.30×10^4	120.0	2.70×10^4[d]	100.0	5.90×10^4
90.0	1.29×10^5	115.0	2.80×10^4	95.0	2.20×10^4
85.0	5.04×10^4	110.0	3.40×10^4	90.0	9.00×10^4
85.0	1.10×10^5	100.0	2.10×10^4	85.0	1.79×10^5
85.0	1.82×10^6	95.0	1.80×10^4	82.5	1.22×10^5
		90.0	4.70×10^4	80.0	1.03×10^6 (disc)
		90.0	6.00×10^4	80.0	1.15×10^6 (disc)
		87.5	2.04×10^5	80.0	1.50×10^6 (disc)
		85.0	1.10×10^6 (disc)		
		80.0	1.03×10^6 (disc)		
		80.0	1.12×10^6 (disc)		

a. Axial load R = 0.01.

b. thru g. Specimen previously run at indicated stress for number of cycles shown without failure.

Footnote	Stress (psi)	Cycles
b.	85,000	1.10×10^6
c.	80,000	1.03×10^6
d.	80,000	1.12×10^6
e.	80,000	1.03×10^6
f.	80,000	1.50×10^6
g.	80,000	1.15×10^6

Table C-25 Fatigue Properties[a] of Solution Treated and Aged Parent Metal 13V-11Cr-3Al Titanium Alloy

Temperature					
70°F		-320°F		-423°F	
Maximum Tension Stress (1000 psi)	Cycles to Failure	Maximum Tension Stress (1000 psi)	Cycles to Failure	Maximum Tension Stress (1000 psi)	Cycles to Failure
175.0	4.50×10^3	175.0	2.00×10^3	160.0	1.00×10^3
175.0	7.00×10^3	160.0	7.00×10^3	160.0	2.00×10^3
175.0	7.80×10^3	140.0	9.00×10^3	160.0	6.00×10^3
120.0	1.70×10^4	137.5	1.30×10^4	145.0	2.00×10^3
120.0	2.10×10^4	135.0	2.10×10^4	125.0	5.00×10^3
120.0	2.50×10^4	130.0	1.10×10^4	125.0	1.00×10^4
79.3	1.04×10^5	125.0	8.17×10^3	125.0	1.10×10^4
79.3	1.19×10^5	122.0	5.98×10^5	110.0	1.39×10^5
79.3	4.95×10^6 (disc)	120.0	1.60×10^6	105.0	[illegible]
79.3	5.14×10^6 (disc)	120.0	3.96×10^5	105.0	[illegible]
77.5	1.00×10^6 (disc)	115.0	6.00×10^4	100.0	[illegible]
		115.0	9.80×10^4	100.0	[illegible]
		105.0	[illegible]		
		97.5	[illegible]		

a. Axial load R = 0.01.

b. Specimen previously [illegible]

Table C-26 Fatigue Properties[a] of Welded 13V-11Cr-3Al Titanium Alloy

Temperature					
70°F		-320°F		-423°F	
Maximum Tension Stress (1000 psi)	Cycles to Failure	Maximum Tension Stress (1000 psi)	Cycles to Failure	Maximum Tension Stress (1000 psi)	Cycles to Failure
175.0	1.00×10^3	90.0	1.30×10^3	100.0	1.00×10^3
100.0	3.50×10^3	80.0	1.00×10^2[d]	80.0	1.00×10^3[g]
100.0	5.00×10^3	80.0	3.70×10^3	75.0	2.00×10^3
90.0	6.00×10^3[b]	75.0	3.50×10^3[e]	65.0	2.00×10^3[h]
80.0	1.40×10^4[c]	70.0	6.10×10^3[f]	65.0	3.00×10^3[i]
70.0	3.70×10^4	60.0	1.47×10^4	60.0	1.10×10^4
60.0	2.40×10^4	50.0	9.50×10^3	50.0	2.00×10^4
55.0	4.60×10^4	40.0	2.40×10^4	45.0	4.60×10^4
50.0	1.60×10^5	30.0	3.60×10^4	42.0	2.13×10^5
45.0	2.83×10^5	20.0	8.59×10^4	40.0	2.60×10^4
42.0	1.31×10^5	12.0	1.18×10^6 (disc)	40.0	4.40×10^4
40.0	4.00×10^6 (disc)	10.0	1.15×10^6 (disc)	40.0	1.01×10^4 (disc)
40.0	1.03×10^7 (disc)	8.0	1.10×10^6 (disc)	35.0	9.70×10^4
				35.0	1.82×10^5
				35.0	1.03×10^6 (disc)
				30.0	1.60×10^6 (disc)

a. Stress ratio (R) = 0.01.
b. thru i. Specimen previously run at indicated stress for number of cycles shown without failure.

Footnote	Stress (psi)	Cycles
b.	40,000	4.00×10^6
c.	40,000	1.03×10^7
d.	12,000	1.18×10^6
e.	8,000	1.10×10^6
f.	10,000	1.15×10^6
g.	40,000	1.01×10^6
h.	65,000	$1.[illegible] \times 10^6$
i.	30,000	1.60×10^6

Table C-27 Fatigue Properties[a] of Parent Metal AISI 321 Stainless Steel

Temperature					
70°F		-320°F		-423°F	
Maximum Tension Stress (1000 psi)	Cycles to Failure	Maximum Tension Stress (1000 psi)	Cycles to Failure	Maximum Tension Stress (1000 psi)	Cycles to Failure
60.0	5.00×10^{2} [b]	90.0	9.00×10^{2} [e]	120	1.0×10^{3} [i]
50.0	1.00×10^{3}	80.0	1.92×10^{4}	120	1.0×10^{3} [j]
45.0	1.00×10^{3}	75.0	4.33×10^{4} [f]	115	1.0×10^{3} [k]
45.0	2.00×10^{3} [c]	70.0	4.50×10^{4}	110	1.2×10^{4}
42.0	5.00×10^{3}	70.0	6.02×10^{4} [g]	110	1.7×10^{4}
40.0	6.00×10^{3} [d]	60.0	1.09×10^{5}	100	3.6×10^{4}
40.0	8.00×10^{3}	55.0	1.82×10^{5}	90	3.4×10^{4}
40.0	1.20×10^{4}	55.0	1.84×10^{5} [h]	80	4.6×10^{4}
35.0	7.20×10^{4}	50.0	3.70×10^{5}	80	1.31×10^{5}
33.0	9.80×10^{4}	45.0	1.99×10^{6} (disc)	70	1.69×10^{5}
33.0	2.98×10^{5}	44.0	8.38×10^{4}	60	2.7×10^{4}
32.0	1.09×10^{5}	42.0	1.81×10^{6} (disc)	60	4.86×10^{5}
32.0	4.74×10^{5}	40.0	2.28×10^{6} (disc)	50	1.00×10^{6} (disc)
31.0	1.14×10^{6} (disc)	40.0	2.32×10^{6} (disc)	50	1.01×10^{6} (disc)
30.0	1.25×10^{6} (disc)			50	1.00×10^{6} (disc)
30.0	1.31×10^{6} (disc)				

a. Stress ratio (R) = -1.

b. thru k. Specimen previously run at indicated stress for number of cycles shown without failure.

Footnote	Stress (psi)	Cycles
b.	30,000	1.31×10^{6}
c.	31,000	1.14×10^{6}
d.	30,000	1.25×10^{6}
e.	42,000	1.81×10^{6}
f.	45,000	1.99×10^{6}
g.	40,000	2.28×10^{6}
h.	40,000	2.32×10^{6}
i.	50,000	1.00×10^{6}
j.	50,000	1.00×10^{6}
k.	50,000	1.01×10^{6}

Table C-28 Fatigue Properties[a] of Notched[b] AISI 321 Stainless Steel

Temperature					
70°F		-320°F		-423°F	
Maximum Tension Stress (1000 psi)	Cycles to Failure	Maximum Tension Stress (1000 psi)	Cycles to Failure	Maximum Tension Stress (1000 psi)	Cycles to Failure
40.0	1.00×10^3	65.0	8.20×10^3	80.0	1.00×10^3[j]
35.0	2.00×10^3[c]	60.0	1.50×10^3[f]	75.0	2.00×10^3[k]
35.0	4.00×10^3[d]	60.0	6.40×10^3	70.0	1.00×10^3[l]
35.0	6.00×10^3	60.0	6.79×10^3[g]	70.0	5.00×10^3
30.0	2.80×10^4[e]	60.0	8.10×10^3	65.1	7.00×10^3
30.0	3.40×10^4	50.0	1.48×10^4[h]	60.0	9.00×10^3
30.0	5.20×10^4	40.0	2.89×10^4[i]	55.0	1.80×10^4
25.0	1.22×10^5	40.0	3.91×10^4	50.0	1.50×10^4
23.0	1.17×10^5	40.0	4.12×10^4	50.0	3.10×10^4
21.0	3.42×10^5	35.0	3.97×10^4	45.0	6.60×10^4
20.0	6.59×10^5	30.0	1.57×10^5	40.0	9.70×10^4
20.0	1.12×10^6 (disc)	30.0	1.12×10^5	35.0	1.76×10^5
18.0	7.44×10^5	25.0	3.82×10^5	30.0	4.43×10^5
17.0	1.56×10^6 (disc)	23.0	1.37×10^6 (disc)	27.0	1.19×10^5
16.0	1.49×10^6 (disc)	22.0	1.10×10^6 (disc)	25.0	8.12×10^5
		22.0	1.12×10^6 (disc)	25.0	1.02×10^6 (disc)
		20.0	6.94×10^6 (disc)	23.5	1.00×10^6 (disc)
				23.5	1.03×10^6[r] (disc)

a. Stress ratio (R) = -1.
b. Stress concentration (K_t) = 3.5.
c. thru l. Specimen previously run at indicated stress for number of cycles shown without failure.

Footnote	Stress (psi)	Cycles
c.	20,000	1.12×10^6
d.	16,000	1.49×10^6
e.	17,000	1.56×10^6
f.	22,000	1.12×10^6
g.	23,000	1.37×10^6
h.	22,000	1.10×10^6
i.	20,000	6.94×10^6
j.	23,500	1.00×10^6
k.	23,500	1.03×10^6
l.	25,000	1.02×10^6

Table C-29 Fatigue Properties[a] of Welded AISI 321 Stainless Steel

Temperature					
70°F		-320°F		-423°F	
Maximum Tension Stress (1000 psi)	Cycles to Failure	Maximum Tension Stress (1000 psi)	Cycles to Failure	Maximum Tension Stress (1000 psi)	Cycles to Failure
40.0	1.00×10^3 [b]	80.0	1.10×10^3 [e]	100.0	2.00×10^3 [g]
40.0	2.00×10^3	80.0	3.60×10^3	100.0	6.00×10^3 [h]
40.0	3.00×10^3	80.0	5.70×10^3 [f]	90.0	4.00×10^3 [i]
40.0	4.00×10^3 [c]	80.0	7.90×10^3	90.0	2.90×10^4
40.0	5.00×10^3	60.0	5.06×10^4	80.0	9.00×10^3
40.0	6.00×10^3 [d]	50.0	5.49×10^4	70.0	5.20×10^4
30.0	2.30×10^4	40.0	1.58×10^5	70.0	5.20×10^4
30.0	6.60×10^4	35.0	8.61×10^4	60.0	3.40×10^4
25.0	7.20×10^4	35.0	2.01×10^5	50.0	1.33×10^5
25.0	1.90×10^5	35.0	1.30×10^6	45.0	2.45×10^5
[illegible]	1.53×10^6 (disc)	30.0	4.10×10^5	40.0	3.61×10^5
[illegible]	7.89×10^5	30.0	1.12×10^6 (disc)	30.0	8.22×10^5
[illegible]	1.07×10^6	30.0	1.90×10^6 (disc)	27.5	1.0×10^6 (disc)
[illegible]	$1.[illegible] \times 10^6$	28.0	2.24×10^6	27.5	1.005×10^6 (disc)
[illegible]	1.20×10^6 (disc)			27.5	1.103×10^6 (disc)
[illegible]	4.50×10^6 (disc)				

a. Stress ratio (R) = -1.
b. thru i. Specimen previously run at indicated stress for number of cycles shown without failure.

Footnote	Stress (psi)	Cycles
b.	22,000	1.53×10^6
c.	18,000	1.20×10^6
d.	18,000	4.50×10^6
e.	30,000	1.90×10^6
f.	30,000	1.12×10^6
g.	27,500	1.01×10^6
h.	27,500	1.00×10^6
i.	27,500	1.10×10^6